

## Review

# Global approaches to understanding ubiquitination

Peter Kaiser\* and Lan Huang†‡

Addresses: \*Department of Biological Chemistry, School of Medicine, †Department of Physiology and Biophysics, and ‡Department of Developmental and Cell Biology, University of California, Irvine, CA 92697-1700, USA.

Correspondence: Peter Kaiser. E-mail: pkaiser@uci.edu

Published: 29 September 2005

Genome Biology 2005, 6:233 (doi:10.1186/gb-2005-6-10-233)

The electronic version of this article is the complete one and can be found online at <http://genomebiology.com/2005/6/10/233>

© 2005 BioMed Central Ltd

## Abstract

Ubiquitination - the linkage of one or more molecules of the protein ubiquitin to another protein - regulates a wide range of biological processes in all eukaryotes. We review the proteome-wide strategies that are being used to study aspects of ubiquitin biology, including substrates, components of the proteasome and ubiquitin ligases, and deubiquitination.

Ubiquitin, a small protein of 76 amino acids, is highly conserved in all eukaryotes. In a multi-step process, ubiquitin is covalently linked to lysine residues of substrate proteins. If a single molecule of ubiquitin is linked to a protein, this is referred to as mono-ubiquitination, a process that is of particular importance for protein trafficking but has also been shown to regulate retrovirus budding and to modulate protein function directly [1]. A lysine residue of a ubiquitin molecule attached to a substrate can itself serve as an acceptor for an additional ubiquitin molecule, and this process can be repeated so that poly-ubiquitinated proteins form. Poly-ubiquitin chains serve as recognition signals for the 26S proteasome, the major regulator of protein abundance in cells, and poly-ubiquitination thus often initiates proteolysis of the substrate. But poly-ubiquitination can also regulate protein function directly without affecting stability, in ways similar to mono-ubiquitination and other post-translational modifications. The mechanisms underlying proteolysis-independent regulation by poly-ubiquitination are only poorly understood but might function by changing conformation or adding or obscuring a binding site (Figure 1; for reviews see [1-3]).

The transfer of ubiquitin is a multi-step process that involves at least three classes of enzymes: ubiquitin-activating enzymes, generally called E1 enzymes; ubiquitin-conjugating enzymes or E2s; and ubiquitin ligases, E3s (Figure 1). E3 ubiquitin ligases are of particular importance because they

confer substrate specificity to the system by interacting directly with substrate proteins and thereby directing the transfer of ubiquitin. The human genome encodes an estimated 500-600 ubiquitin ligases, a number comparable to the 518 predicted kinases [4,5]. If you consider that each ubiquitin ligase is active on several substrates, you can get some impression of the complexity and importance of the ubiquitin system.

Ubiquitination is a highly dynamic process and is balanced by deconjugation of ubiquitin by deubiquitinating enzymes (DUBs). The more than 70 DUBs that are estimated to be encoded in the human genome are responsible for the reversible nature of ubiquitin modifications and have important roles in recycling ubiquitin from proteasome substrates, in stabilizing proteins by counteracting their poly-ubiquitination, and in opposing the proteolysis-independent regulatory roles of ubiquitin modifications (for reviews see [6,7]). DUBs together with E1, E2 and E3 enzymes and the proteasome make up the ubiquitin-proteasome system.

The large number of proteins that constitute the ubiquitin-proteasome system and the enormous number of ubiquitination substrates mean that global approaches are required if we are to understand fully the role of ubiquitination in cell biology, development, and disease. Large-scale studies of the entire system are still in their early stages, but they have

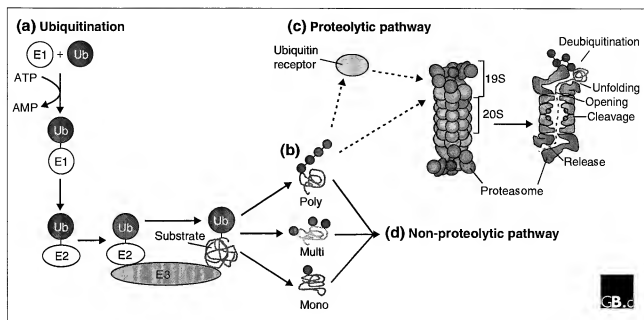


**Figure 1**

The ubiquitin proteasome system. (a) Ubiquitin is activated by a ubiquitin-activating enzyme (E1) and transferred onto substrate proteins by ubiquitin-conjugating enzymes (E2) and ubiquitin ligases (E3), resulting in (b) either attachment of a single ubiquitin molecule (mono-ubiquitination), attachment of multiple ubiquitin units to several substrate lysine residues on the same protein (multi-ubiquitination) or synthesis of ubiquitin chains (poly-ubiquitination). (c) Many poly-ubiquitinated proteins are subsequently degraded by the 26S proteasome, which consists of the catalytic 20S complex and the regulatory 19S particles. Degradation substrates are either delivered to the proteasome by soluble ubiquitin receptors or recognized by the intrinsic ubiquitin-binding activity of the 19S particle. At the 19S proteasome the ubiquitin chain is disassembled, and the substrate is unfolded before it can enter the cavity of the 20S subunit where proteolysis takes place. Finally, proteolytic fragments exit the proteasome in a poorly understood way. (d) Ubiquitination can also directly regulate protein function in a proteolysis-independent manner, via mono-, multi- or poly-ubiquitinated proteins.

already made important contributions to the field. Here, we review the approaches taken in some of these studies and their findings.

### Proteomic approaches to characterizing the ubiquitin-proteasome system

Multi-protein complexes and protein-protein interactions have important roles in the ubiquitin-proteasome system. Both the 26S proteasome (see Figure 1c) and E3 ubiquitin ligases have been studied extensively using protein-complex purification coupled with mass-spectrometric protein identification [8-11]. Studies of the subunit composition of proteasomes from various organisms have revealed that the 26S proteasome complex consists of the 20S complex (made up of seven  $\alpha$  and seven  $\beta$  subunits) and the 19S complex (made up of six ATPase and twelve non-ATPase subunits) [12]. The 20S complex is well characterized as forming the catalytic core; the 19S regulatory complex is believed to be responsible for substrate recognition and unfolding (Figure 1c), but the specific functions of most of the 19S subunit components are still not well understood. There is accumulating evidence for a non-proteolytic role for the proteasome in processes such as transcription, chromatin packaging, and DNA repair

[13,14]. Additional subunits found in the majority of proteasome complexes have been identified following the development of new protein-purification and protein-identification techniques [8,15]. Recently, hybrid 26S proteasome complexes have been characterized, in which one copy of the 19S is present at one end of the 20S core and the other end is capped by Bml10, a newly characterized HEAT repeat protein in yeast. Bml10 and its mammalian ortholog PA28 function as 20S activators [16,17]. These complexes seem to have labile structures that cannot be preserved during the purification steps. Although the hybrid complexes reconstituted *in vitro* have higher peptidase activity than the classic versions, their roles in the degradation of ubiquitinated substrates *in vivo* are unclear [16,17]. Given the heterogeneous population and functional diversity of the various proteasome complexes, it remains a challenging task to purify and identify the subpopulations of proteasome complexes and to correlate the differences in their composition with their distinct functions *in vivo*.

A diverse groups of proteasome-interacting proteins, including ubiquitin ligases, DUBs, heat-shock proteins and many other proteins have been identified by affinity purification and mass spectrometry as well as from genome-wide two-hybrid

screens for protein-protein interactions [8,15,18-21]. Many of the identified interactions seem to be labile under conditions of active ATP hydrolysis by the 19S regulatory complex because addition of ATP coincides with the release of the interacting proteins [8]. This modulation has been suggested to be a part of the mechanism of protein degradation [22]. New methodologies are needed if we are to identify and characterize proteasome-interacting proteins fully, to understand how the different interacting proteins influence the catalytic cycle, and to clarify how they link the ubiquitin-proteasome system to other biological processes.

Mass-spectrometric approaches have also contributed much to our current understanding of the complex composition of E3 ubiquitin ligases. Two types of ubiquitin ligase that play important roles in cell-cycle regulation have been extensively investigated: SCFs and the anaphase-promoting complex/cyclosome (APC/C). SCF ubiquitin ligases are named after three of their four subunits - Skp1, Cdc53 (also known as Cul1) and one member of the F-box protein family - and they also include the Ring-H2 protein Hrt1 (also known as Roc1 or Rbx1) [23]. The substrate specificity of SCFs depends on the different F-box proteins that are tethered to the Cdc53-Hrt1 ubiquitin-ligase module by Skp1. Using sequential rounds of epitope tagging, affinity purification and mass spectrometry (a procedure called SEAM), Skp1 was found to form a variety of complexes, including some that are most likely to have functions other than ubiquitination [9,24,25].

In comparison, proteomic approaches have shown that the APC/C, which regulates mitosis, has a more complex structure than SCFs with at least 13 components [26]. Despite some success in identifying the subunits and also the modifications of APC/C, the molecular functions of the individual subunits are largely unknown. Exceptions are the RING-finger subunit Apc11 and the cullin-like subunit Apc2, which are believed to have a direct role in ubiquitin transfer [27].

Perhaps because of the large number of ubiquitin ligases present in the genome, ubiquitin-ligase proteomics is still in its infancy. Affinity purification coupled with mass spectrometry has promised great advances in the study of the composition of protein complexes and the identification of their interacting partners. But further advancements in proteomic research are expected to provide more information on the protein complexes involved in the ubiquitin-proteasome system, including their post-translational modifications, the stoichiometry of their subunits and how they are assembled.

### Identification of ubiquitination substrates *in vitro*

The large number of putative E3 ubiquitin ligases makes systematic characterization of their substrates a formidable task, but it is one that will be important if we are to gain a global view of the dynamics of the ubiquitin system. E3-substrate

interactions are generally only transient, and substrates are usually either degraded by the proteasome and/or released from the E3 ligase after the transfer of ubiquitin. This makes detection of E3-ligase-substrate interactions difficult. Two-hybrid assays have successfully identified some substrates of ubiquitin ligases [28], but identification of proteins that can interact with E3 ligases does not necessarily pinpoint substrates. A more effective strategy is to identify E3 substrates by their ubiquitination or degradation by the 26S proteasome.

One of the first effective large-scale attempts used *Xenopus* oocyte extracts to identify substrates of the APC/C, a ubiquitin ligase that regulates mitosis [29-32]. The approach exploited the unique regulation of APC/C activity: it is inactive during interphase but active during mitosis. When added to mitotic extracts, APC/C substrates are ubiquitinated and rapidly degraded by the proteasome, but the same substrates are unchanged in interphase lysates. In a large-scale approach *Xenopus* cDNA clones that had been *in vitro* translated and labeled were divided into small pools and incubated with interphase and mitotic oocyte extracts. Proteins that disappeared specifically from mitotic extracts were isolated, and this led to the identification of several important APC/C substrates, including cyclin B, the DNA-replication inhibitor geminin, and the anaphase inhibitor securin [29-32].

A different *in vitro* approach was applied to identifying the potential substrates of the ubiquitin ligase that is formed by a heterodimer of BRCA1 and BARD1 [33,34]: the BRCA1/BARD1 heterodimer functions as a tumor suppressor that is important for protection from breast and ovarian cancer, and its ubiquitin-ligase activity has been linked to its protective function [35]. Sato and colleagues [33] immunoprecipitated BRCA1/BARD1 complexes, which were added to a ubiquitination reaction *in vitro*, that used ubiquitin tagged with the FLAG epitope. The rationale behind the approach was that substrates of ubiquitination by BRCA1 should be bound to the immunoprecipitated BRCA1 and subsequently ubiquitinated with FLAG-ubiquitin *in vitro*. Proteins conjugated to FLAG-ubiquitin were purified and identified by mass spectrometry [33]. A more directed strategy restricted the hunt for BRCA1-BARD1 substrates to components of the centrosome [34], because BRCA1 has been implicated in the regulation of centrosome duplication [36]. Starita and colleagues [34] incubated mammalian centrosome-containing cell fractions with recombinant BRCA1-BARD1 ligase complexes and biotinylated ubiquitin. Ubiquitinated proteins were detected through the biotin tag on ubiquitin and subsequently identified by mass spectrometry [34]. Both of these strategies [33,34] identified promising candidate BRCA1-BARD1 substrates - nucleoplasm/B23 [33] and  $\gamma$ -tubulin [34] - that might be connected to the tumor-suppressor function of BRCA1. A high-throughput strategy has also been used to identify substrates of the yeast ubiquitin ligase Rsp5 *in vitro*. A luminescent assay involving biotinylated ubiquitin was used to screen several hundred purified yeast

proteins for Rsp5-dependent ubiquitination *in vitro*. Previously known, as well as new, candidate substrates of Rsp5 were identified [37].

A more general *in vitro* approach [38] used total HeLa cell lysates for large-scale identification of ubiquitinated proteins. Cell lysates were incubated with ubiquitin tagged with six histidines (6xHis-ubiquitin) and an ATP-regenerating system to sustain ubiquitination *in vitro*. The 6xHis-ubiquitin was covalently attached to proteins by the E1, E2, and E3 enzymes present in the cell lysates, and this allowed purification of ubiquitinated proteins on the basis of the affinity of 6xHis-ubiquitin to  $\text{Ni}^{2+}$  ions (Ni-chelate chromatography) [38]. Over 100 ubiquitin-linked proteins were identified by mass spectrometry, of which a relatively high proportion was already implicated in the ubiquitin proteasome pathway, such as E2 and E3 enzymes and proteasome subunits. Because relatively mild purification conditions were chosen, both ubiquitinated proteins and proteins associated with them were identified. This is illustrated by the identification of 16 out of 18 subunits of the 19S proteasome; covalent modification of 19S proteasome subunits with ubiquitin has so far not been reported, but an intrinsic affinity of the 19S proteasome for poly-ubiquitin chains is well known [39] and is most likely to be responsible for the identification of these proteins in the study [38]. *Bona fide* ubiquitinated proteins can be distinguished from associated, copurifying proteins by fractionation strategies that use highly denaturing conditions and break non-covalent interactions. Such stringent purification conditions have been widely used to demonstrate covalent attachment of ubiquitin to specific proteins [40], as well as in proteome-wide approaches to identifying ubiquitinated proteins, as discussed below.

### Ubiquitination substrates *in vivo*

Identification of all ubiquitinated proteins in a cell under a given growth condition or developmental state is an ambitious aim, but it no longer seems impossible given the tremendous pace at which mass-spectrometry-based proteomics is developing (reviewed in [41]). Ubiquitin profiling was pioneered by Peng and colleagues [42] and usually involves expression of 6xHis-tagged ubiquitin in cells (Figure 2). The cellular ubiquitin system conjugates 6xHis-ubiquitin to target proteins and allows their purification by Ni-chelate chromatography. Because Ni-chelate purification is compatible with fully denaturing conditions, proteins that are associated with ubiquitinated proteins but are not ubiquitination substrates themselves can efficiently be removed. The purified ubiquitinated proteins are fragmented by trypsin (or similar proteases) to generate peptides, which can be used for mass-spectrometric identification of the proteins present in the purified fraction. More than 1,000 candidate ubiquitination substrates were identified using this method in the relatively simple eukaryote *Saccharomyces cerevisiae* [42], whose genome

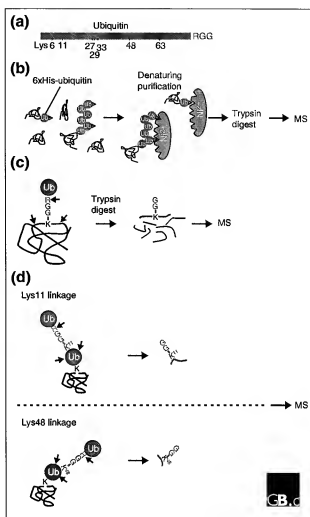


**Figure 2**

Global strategies that use mass spectrometry (MS) to study ubiquitination.

(a) Diagram of the lysine residues in ubiquitin; the carboxy-terminal Arg-Gly-Gly (RGG) motif is also indicated. (b) In ubiquitin profiling, 6xHis-tagged ubiquitin expressed in cells is conjugated to substrate proteins, and this facilitates purification of ubiquitinated proteins under denaturing conditions by Ni-chelate chromatography, in which histidine-tagged proteins bind specifically to immobilized  $\text{Ni}^{2+}$  ions. Purified ubiquitinated proteins are digested with trypsin and the resulting peptides are analyzed by mass spectrometry to identify the proteins present in the sample. (c) Precise ubiquitination sites can be determined by mass spectrometry because of a characteristic mass shift caused by diglycine that is retained on ubiquitinated lysine residues within peptides after trypsin digestion. (d) A similar strategy allows differentiation between the various types of ubiquitin chain linkages that can lead to diverse ubiquitin-chain topologies. Depending on the lysine residue in ubiquitin that was used for the ubiquitin-ubiquitin linkage, different linkage-specific signature peptides with characteristic masses are produced by trypsin digestion. These signature peptides can be detected and distinguished by mass spectrometry.

encodes roughly 5,800 proteins. Surprisingly, most of the well-studied (and less abundant) ubiquitinated proteins were absent from the list, suggesting that many more yeast

proteins than the identified 1,000 candidates are ubiquitination substrates.

At first glance, it seems that a surprisingly large fraction of the proteome is ubiquitinated. But misfolded proteins, which can be generated by translation inaccuracy, folding problems or oxidative damage, are ubiquitinated and degraded as part of the protein quality-control pathway [43]. One can therefore expect that at least a small fraction of any protein will be ubiquitinated, and that sufficiently sensitive analytical methods might find that all proteins can be ubiquitination substrates. It is important to bear in mind that current ubiquitin-profiling experiments can indicate only whether any of a given protein is ubiquitinated but cannot give any estimate of what fraction of the protein is ubiquitinated. This imposes some limitations on how the results of large-scale studies can be interpreted.

To find more specific substrates of the ubiquitin-proteasome system, recent proteomic approaches have focused on specific parts of the system. Ubiquitin profiling has been used successfully to study the endoplasmic reticulum associated degradation pathway (ERAD) [44]. Membrane-enriched fractions from yeast cells expressing 6xHis-ubiquitin were used as a starting material for purification of ubiquitinated proteins and their subsequent identification by mass spectrometry. More than 80 candidate ERAD substrates were identified [44].

Mayor and colleagues [45] enriched for proteasome substrates on a poly-ubiquitin-binding protein resin and followed this with denaturing Ni-chelate chromatography in order to purify ubiquitinated proteins from yeast cells expressing 6xHis-ubiquitin. Remarkably, by profiling a yeast strain with a mutation in the proteasomal ubiquitin receptor Rpn10, they could identify 54 candidate ubiquitination substrates that require Rpn10 for degradation [45]. Among them were the transcription factor Gen4 and the cell cycle regulator Sic1, two known proteasome substrates whose abundance is low. This study [45] demonstrates how subtractive ubiquitin profiling can help to define substrates of particular pathways of the ubiquitin-proteasome system. It is not hard to imagine that a similar strategy, in which cells defective in a particular E3 ligase are compared with wild-type cells, could be used for large-scale identification of the specific substrates of individual ubiquitin ligases. Furthermore, the introduction to proteomic analyses of various mass-spectrometric strategies that use stable isotope labeling promises to transform ubiquitin-profiling experiments by enabling detection of quantitative changes in ubiquitin profiles [46-48].

### Ubiquitination sites and ubiquitin-chain topology

The pioneering ubiquitin-profiling experiments of Peng and colleagues [42] demonstrated the feasibility of large-scale identification of ubiquitin-attachment sites in substrate proteins. This is possible because, after trypsin digestion, the

two carboxy-terminal residues of ubiquitin remain attached to the lysine residue of the substrate protein (Figure 2c). These two additional glycine residues lead to a characteristic 114 Da increase in the mass of the ubiquitinated substrate peptide, which is diagnostic for the ubiquitinated residue and can be monitored by mass spectrometry [42]. Over 100 precise ubiquitin attachment sites have been identified by analyzing peptide-mass data from global ubiquitin-profiling experiments [42,44]. Bioinformatic analyses of these data sets showed that ubiquitination sites are almost exclusively exposed on the protein surface, and located preferentially in a sequence environment that is predicted to form a loop structure [49]. No conserved ubiquitination motif could be defined, however.

A related strategy allowed detection of different ubiquitin chain topologies *in vivo* [42,50]. Formation of a poly-ubiquitin chain requires isopeptide linkages between the terminal carboxyl group of a free ubiquitin molecule and one of seven lysine residues present in a substrate-attached ubiquitin (Figure 2a,d). The most important chain topology is formed through the lysine in position 48 of ubiquitin [51]. Chains linked through Lys48 are the principal recognition signals for the proteasome and generally induce substrate degradation [52]. Chains linked through Lys63 do not induce substrate degradation but have direct effects on protein activity [53,54]; the biological role of other ubiquitin chain topologies is unclear. From the analytical perspective, the ubiquitin chain linkage can be regarded as a specific example of a ubiquitination site in a substrate: the substrate in this case is ubiquitin itself. Chain linkage can therefore be determined by the characteristic 114 Da mass shift, as described above (Figure 2c,d) [41].

Rather surprisingly, analysis of mass data from large-scale ubiquitin-profiling experiments [42] has revealed that all seven lysine residues in ubiquitin are used to form ubiquitin chains *in vivo*. The abundance of the different chain-linkage types was ranked and suggested that linkage through Lys48 is the most abundant topology, followed by Lys63 and Lys11 chains and the less frequent linkages through Lys33, Lys27, Lys6, and Lys29 (the latter is detected only in combination with Lys33 linkage) [42]. These results emphasize the complexity of ubiquitin biology. At the same time, interpretation of these experiments [42] is somewhat limited because they can describe only the linkage between two ubiquitins and cannot determine to which protein the chain was attached or whether the chain was attached to a substrate at all (Figure 2d). Similarly, it is unclear whether ubiquitin chains are homogenous or can contain mixed linkage types. The only rigorously studied example so far of a substrate-attached ubiquitin chain *in vivo* demonstrated the presence of a homogenous ubiquitin chain [50]. Many more studies are necessary, however, before we can decide whether mixed chains exist *in vivo* and whether they encode biologically important information.

### Chemistry-based and global *in vivo* approaches to deubiquitination

DUBs are an important component of the ubiquitin-proteasome system. They are proteases and can therefore be targeted by activity-dependent probes, which form covalent bonds with their active sites and have been successfully applied to other classes of proteases [55,56]. An elegant strategy using an activity-based approach to target DUBs has led to the identification of numerous deubiquitinating activities in cell lysates and the discovery of the new class of DUBs that contain an OTU domain (a domain characteristic of the ovarian tumor superfamily of proteins) [57]. Briefly, ubiquitin fused to a hemagglutinin (HA) epitope tag at its amino terminus and to one of various cysteine-reactive probes (which react with cysteine proteases) at the carboxyl terminus is incubated with total cell lysates. The active site of each DUB forms a covalent bond with the cysteine-reactive group on the HA-ubiquitin probe (Figure 3a) and can therefore be immunopurified using the HA tag and subsequently identified by mass spectrometry (Figure 3b) [58]. Activity-based ubiquitin probes have also been used to generate profiles of DUB activity in different cell lines and tissues and to identify proteins that interact with DUBs (Figure 3b) [58,59].

The problem of identifying DUBs that react with a specific ubiquitinated protein has been elegantly addressed using a collection of RNA-interference (RNAi) vectors that knock down the expression of more than 50 DUBs in mammalian cells [60]. Because the steady-state level of ubiquitin conjugates reflects the balance between ubiquitination and deubiquitination, knockdown of the activity of a specific DUB increases the fraction of the ubiquitinated form of its substrates. This strategy helped to identify the DUB USP1 as the deubiquitinating activity that acts on the mono-ubiquitinated version of FANCD2 (a protein defective in the Fanconi anemia complementation group D2) [60]. A similar collection of small interfering RNAs (siRNAs) has enabled the identification of the familial cylindromatosis tumor suppressor gene (*CYLD*) as a DUB involved in regulation of the NF $\kappa$ B transcriptional control pathway [61].

More than 25 years have passed since the initial discovery of the ubiquitin system. Ubiquitin has since extended its role from a protein-degradation signal to a regulatory protein modification that affects all areas of biology. The importance of the ubiquitin-proteasome system in biology was acknowledged with the 2004 Chemistry Nobel Prize to Aaron Ciechanover, Avram Herschko, and Irwin Rose, who first established its main features. The complexity and significance of the ubiquitin-proteasome system has started to attract global approaches that are beginning to make important contributions to our understanding of the system. Chemistry-based approaches to deubiquitination have demonstrated the effectiveness of these strategies, and analogous activity-based probes for studying the ubiquitin transfer will be of similar

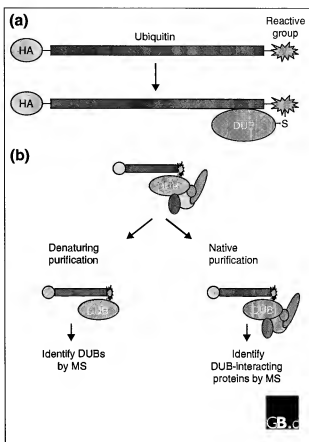


**Figure 3**  
Activity-based profiling of deubiquitinating enzymes and interacting proteins. (a) Ubiquitin fused to an amino-terminal epitope tag (for example hemagglutinin, HA) and a carboxy-terminal reactive group forms a covalent conjugate with deubiquitinating enzymes (DUBs; for details of the generation of these ubiquitin probes, see [57]). (b) The DUB-ubiquitin conjugates can be immunopurified using the HA epitope. Immunopurification under native conditions allows identification of DUBs and their interacting proteins by mass spectrometry (MS). The immunopurified fractions can be further separated by gel electrophoresis, and DUB-ubiquitin conjugates can be detected by anti-HA immunoblotting. Proteins corresponding to HA-reactive bands can be eluted from silver-stained gels (not shown) and the DUBs can be identified by mass spectrometry.

importance. Proteomics using mass spectrometry has had a tremendous impact on the field, as it has helped to describe the nature and regulation of multi-protein complexes that themselves regulate the ubiquitin-proteasome system. Large-scale ubiquitin-profiling experiments have highlighted the involvement of the system in a wide range of processes and demonstrated the complexity of ubiquitin-chain topology. Mass-spectrometric approaches promise to be particularly powerful in the future because one of the previous limitations - the inherent non-quantitative nature of these experiments - has been overcome by stable-isotope-based quantification strategies [48-50].

Some of the global approaches described here for the study of the ubiquitin system have also been applied to the study of other ubiquitin-like proteins, such as SUMO, ISG15, and Nedd8 [62,63]. The strategies that have been proven to be effective for studying ubiquitin biology will be just as important for rapidly advancing our understanding of the role of the growing family of ubiquitin-like modifiers.

## Acknowledgements

We thank K. Rick for critically reading the manuscript. Work in the laboratory of P.K. is supported by grants from NIH (GM-66164) and the California Breast Cancer Research Program (11NB-0177). L.H. acknowledges support from NIH (GM074830) and the DOD (PC-041126).

## References

- Hicke L: Protein regulation by monoubiquitin. *Nat Rev Mol Cell Biol* 2001, 2:195-201.
- Hershiko A, Ciechanover A: The ubiquitin system. *Annu Rev Biochem* 1998, 67:425-479.
- Pickart CM: Back to the future with ubiquitin. *Cell* 2004, 116:181-190.
- Wilkinson KD, Venturi KH, Friedrich KL, Mullaly JE: The ubiquitin signal: assembly, recognition and termination. *EMBO Rep* 2005, 6:815-820.
- Johnson SA, Hunter T: Kinomics: methods for deciphering the kinome. *Nat Methods* 2005, 2:17-25.
- Wilkinson KD: Regulation of ubiquitin-dependent processes by deubiquitinating enzymes. *FASEB J* 1997, 11:1245-1256.
- Wilkinson KD: Ubiquitination and deubiquitination: targeting of proteins for degradation by the proteasome. *Semin Cell Dev Biol* 2000, 11:141-148.
- Verma R, Chen S, Feldman R, Schietz D, Yates J, Dohmen J, Deshaies RJ: Proteasomal proteomics: identification of nucleotide-sensitive proteasome-interacting proteins by mass spectrometric analysis of affinity-purified proteasomes. *Mol Biol Cell* 2000, 11:3425-3439.
- Seol JH, Shevchenko A, Deshaies RJ: Skp1 forms multiple protein complexes, including RAVE, a regulator of V-ATPase assembly. *Nat Cell Biol* 2001, 3:384-391.
- Toon HJ, Feoktistova A, Wolfe BA, Jennings JL, Link AJ, Gould KL: Proteomics analysis identifies new components of the fission and budding yeast anaphase-promoting complexes. *Curr Biol* 2002, 12:2048-2054.
- Zacharias W, Shevchenko A, Andrews PD, Ciosk R, Galova M, Stark MJ, Mann M, Nasmyth K: Mass spectrometric analysis of the anaphase-promoting complex from yeast: identification of a subunit related to cullins. *Science* 1998, 279:1216-1219.
- Pickart CM, Cohen RE: Proteasomes and their kin: proteases in the machine age. *Nat Rev Mol Cell Biol* 2004, 5:177-187.
- Russell SJ, Reed SH, Huang W, Friedberg EC, Johnston SA: The 19S regulatory complex of the proteasome functions independently of proteolysis in nucleotide excision repair. *Mol Cell* 1999, 3:687-695.
- Muranian M, Tansey WP: How the ubiquitin-proteasome system controls transcription. *Nat Rev Mol Cell Biol* 2003, 4:192-201.
- Leggett DS, Hanna J, Borodovsky A, Crossas B, Schmidt M, Baker RT, Walz T, Ploegh H, Finley D: Multiple associated proteins regulate proteasome structure and function. *Mol Cell* 2002, 10:495-507.
- Cascio P, Call M, Pierre BM, Walz T, Goldberg AL: Properties of the hybrid form of the 26S proteasome containing both 19S and PA28 complexes. *EMBO J* 2002, 21:2636-2645.
- Schmidt M, Haas W, Crossas B, Santamaria PG, Gyll S, Walz T, Finley D: The HEAT repeat protein Blm10 regulates the yeast proteasome by capping the core particle. *Nat Struct Mol Biol* 2005, 12:294-303.
- Ho Y, Grubler A, Heilbut A, Bader GD, Moore L, Adams SL, Millar A, Taylor P, Bennett K, Boulikier K, et al: Systematic identification of protein complexes in *Saccharomyces cerevisiae* by mass spectrometry. *Nature* 2002, 415:180-183.
- Gavin AC, Bosche M, Krause R, Grandi P, Marzioch M, Bauer A, Schultz J, Rick JM, Michon AM, Cruciat CM, et al: Functional organization of the yeast proteome by systematic analysis of protein complexes. *Nature* 2002, 415:141-147.
- Davy A, Bello P, Thierry-Mieg N, Vaglio P, Hlti J, Doucette-Stamm L, Thierry-Mieg D, Reboul J, Boulton S, Walhout AJ, et al: A protein-protein interaction map of the *Connarabitis elegans* 26S proteasome. *EMBO J* 2001, 20:21-28.
- Cagney G, Uetz P, Fields S: Two-hybrid analysis of the *Saccharomyces cerevisiae* 26S proteasome. *Physiol Genomics* 2001, 7:27-34.
- Babbitt SE, Kiss A, Deffenbaugh AE, Chang YH, Bailly E, Erdjument-Bromage H, Tempst P, Buranda T, Shter L, Baumer J, et al: ATP hydrolysis-dependent disassembly of the 26S proteasome is part of the catalytic cycle. *Cell* 2005, 121:553-565.
- Petrocki MD, Deshaies RJ: Function and regulation of cullin-RING ubiquitin ligases. *Nat Rev Mol Cell Biol* 2005, 6:9-20.
- Kaplan KB, Hyman AA, Sorger PK: Regulating the yeast kinetochore by ubiquitin-dependent degradation and Skp1p-mediated phosphorylation. *Cell* 1997, 91:491-500.
- Galan JM, Wiederkehr A, Seol JH, Haguenauer-Trapais R, Deshaies RJ, Riezman H, Peter M: Skp1p and the F-box protein Rcy1p form a non-SCF complex involved in recycling of the SNARE Snclp in yeast. *Mol Biol Cell* 2001, 21:3105-3117.
- Harper JW, Burton JL, Solomon MJ: The anaphase-promoting complex: it's not just for mitosis any more. *Genes Dev* 2002, 16:2179-2206.
- Zacharias W, Nasmyth K: Whose end is destruction: cell division and the anaphase-promoting complex. *Genes Dev* 1999, 13:2039-2058.
- Uetz P, Giot L, Cagney G, Mandfield TA, Judson RS, Knight JR, Lockshon D, Narayan V, Srinivasan M, Pochart P, et al: A comprehensive analysis of protein-protein interactions in *Saccharomyces cerevisiae*. *Nature* 2000, 403:623-627.
- Lustig KD, Stukenberg PT, McGarry TJ, King RW, Cryns VL, Mead PE, Zou L, Yuan J, Kirschner MW: Small pool expression screening: identification of genes involved in cell cycle control, apoptosis, and early development. *Methods Enzymol* 1997, 283:83-99.
- Zou H, McGarry TJ, Bernal T, Kirschner MW: Identification of a vertebrate sister-chromatid separation inhibitor involved in transformation and tumorigenesis. *Science* 1999, 285:18-22.
- McGarry TJ, Kirschner MW: Geminin, an inhibitor of DNA replication, is degraded during mitosis. *Cell* 1998, 93:1043-1053.
- King RW, Lustig KD, Stukenberg PT, McGarry TJ, Kirschner MW: Expression cloning in the test tube. *Science* 1997, 277:973-974.
- Sato K, Hayami R, Wu W, Nishikawa T, Nishikawa H, Okuda Y, Ogata H, Fukuda M, Ohta T: Nucleophosmin/B23 is a candidate substrate for the BRCA1-BARD1 ubiquitin ligase. *J Biol Chem* 2004, 279:30919-30922.
- Starita LM, Machida Y, Sankaran S, Elias JE, Griffin K, Schlegel BP, Gygi SP, Parvin JD: BRCA1-dependent ubiquitination of gamma-tubulin regulates centrosome number. *Mol Cell Biol* 2004, 24:8457-8466.
- Narod SA, Foulkes WD: BRCA1 and BRCA2: 1994 and beyond. *Nat Rev Cancer* 2004, 4:65-676.
- Deng CX: Roles of BRCA1 in centrosome duplication. *Oncogene* 2002, 21:6222-6227.
- Kus BM, Gajadhar A, Stanger K, Cho R, Sun W, Rouleau N, Lee T, Chan D, Wolting C, Edwards AM, et al: A high throughput screen to identify substrates for the ubiquitin ligase Rsp5. *J Biol Chem* 2005, 280:29470-29478.
- Gururaj T, Li W, Noble VYS, Payan DG, Anderson DC: Multiple functional categories of proteins identified in an *in vitro* cellular ubiquitin affinity extract using shotgun peptide sequencing. *J Proteome Res* 2003, 2:394-404.
- Ebasser S, Finley D: Delivery of ubiquitinated substrates to protein-unfolding machines. *Nat Cell Biol* 2005, 7:142-149.
- Kaiser P, Fick K, Wittenberg C, Reed SC: Regulation of transcription by ubiquitination without proteolysis: Cdc40SCF(Med30)-mediated inactivation of the transcription factor Met4. *Cell* 2000, 102:303-314.
- Kirkpatrick DS, Denison C, Gyll S: Weighing in on ubiquitin: the expanding role of mass-spectrometry-based proteomics. *Nat Cell Biol* 2005, 7:750-757.
- Peng J, Schwarz D, Elias JE, Thoresen CC, Cheng D, Marschik G, Roelofs J, Finley D, Gygi SP: A proteomics approach to understanding protein ubiquitination. *Nat Biotechnol* 2003, 21:921-926.

43. McClellan AJ, Tam S, Kaganovich D, Frydman J: **Protein quality control: chaperones culling corrupt conformations.** *Nat Cell Biol* 2005, 7:736-741.
44. Hitchcock AL, Auld K, Gygi SP, Silver PA: **A subset of membrane-associated proteins is ubiquitinated in response to mutations in the endoplasmic reticulum degradation machinery.** *Proc Natl Acad Sci USA* 2003, 100:12735-12740.
45. Mayor T, Lipford JR, Graumann J, Smith GT, Dushalesh RJ: **Analysis of polyubiquitin conjugates reveals that the Rpn10 substrate receptor contributes to the turnover of multiple proteasome targets.** *Mol Cell Proteomics* 2005, 4:741-751.
46. Ong SE, Foster LJ, Mann M: **Mass spectrometric-based approaches in quantitative proteomics.** *Methods* 2003, 29:124-130.
47. Ong SE, Blagoev B, Kratchmarova I, Kristensen DB, Steen H, Pandey A, Mann M: **Stable isotope labeling by amino acids in cell culture, SILAC, as a simple and accurate approach to expression proteomics.** *Mol Cell Proteomics* 2002, 1:376-386.
48. Gygi SP, Rist B, Gerber SA, Turecek F, Gelb MH, Aebersold R: **Quantitative analysis of complex protein mixtures using isotope-coded affinity tags.** *Nat Biotechnol* 1999, 17:994-999.
49. Catic A, Collins C, Church GM, Ploegh HL: **Preferred in vivo ubiquitination sites.** *Bioinformatics* 2004, 20:3302-3307.
50. Flick K, Ouni I, Wohlschlegel JA, Capati C, McDonald VH, Yates JR, Kaiser P: **Proteolysis-independent regulation of the transcription factor Met4 by a single Lys 48-linked ubiquitin chain.** *Nat Cell Biol* 2004, 6:634-641.
51. Finley D, Sadis S, Monia BP, Boucher P, Ecker DJ, Crooke ST, Chau V: **Inhibition of proteolysis and cell cycle progression in a multiubiquitination-deficient yeast mutant.** *Mol Cell Biol* 1994, 14:5501-5509.
52. Pickart CM: **Targeting of substrates to the 26S proteasome.** *FASEB J* 1997, 11:1055-1066.
53. Spence J, Sadis S, Haas AL, Finley D: **A ubiquitin mutant with specific defects in DNA repair and multiubiquitination.** *Mol Cell Biol* 1995, 15:1265-1273.
54. Wang C, Deng L, Hong M, Akkaraju GR, Inoue J, Chen ZJ: **TAK1 is a ubiquitin-dependent kinase of MKK and IKK.** *Nature* 2001, 412:346-351.
55. Liu Y, Patriocelli MP, Cravatt BF: **Activity-based protein profiling: the serine hydrolases.** *Proc Natl Acad Sci USA* 1999, 96:14694-14699.
56. Greenbaum D, Medzhitzky KF, Burlingame A, Bogoy M: **Epoxide electrophiles as activity-dependent cysteine protease profiling and discovery tools.** *Chem Biol* 2000, 7:569-581.
57. Hemelaar J, Galardy PJ, Borodovsky A, Kessler BM, Ploegh HL, Ova H: **Chemistry-based functional proteomics: mechanism-based activity-profiling tools for ubiquitin and ubiquitin-like specific proteases.** *J Proteome Res* 2004, 3:268-276.
58. Borodovsky A, Ova H, Kolli N, Gan-Erdene T, Wilkinson KD, Ploegh HL, Kessler BM: **Chemistry-based functional proteomics reveals novel members of the deubiquitinating enzyme family.** *Chem Biol* 2002, 9:1149-1159.
59. Ova H, Kessler BM, Rolan U, Galardy PJ, Ploegh HL, Masucci MG: **Activity-based ubiquitin-specific protease (USP) profiling of virus-infected and malignant human cells.** *Proc Natl Acad Sci USA* 2004, 101:2253-2258.
60. Nijman SM, Huang TT, Dirac AM, Brummelkamp TR, Kerkhoven RM, D'Andrea AD, Bernards R: **The deubiquitinating enzyme USP1 regulates the Fanconi anemia pathway.** *Mol Cell* 2005, 17:331-339.
61. Brummelkamp TR, Nijman SM, Dirac AM, Bernards R: **Loss of the cylindromatosis tumour suppressor inhibits apoptosis by activating NF-kappaB.** *Nature* 2003, 424:797-801.
62. Denison C, Kirkpatrick DS, Gygi SP: **Proteomic insights into ubiquitin and ubiquitin-like proteins.** *Curr Opin Chem Biol* 2005, 9:69-75.
63. Weichman RL, Gordon C, Mayer RJ: **Ubiquitin and ubiquitin-like proteins as multifunctional signals.** *Nat Rev Mol Cell Biol* 2005, 6:599-609.

# Candidates for Peptide Receptor Radiotherapy Today and in the Future

Jean Claude Reubi, MD<sup>1</sup>; Helmut R. Mäcke, PhD<sup>2</sup>; and Eric P. Krenning, MD<sup>3</sup>

<sup>1</sup>Division of Cell Biology and Experimental Cancer Research, Institute of Pathology, University of Berne, Berne, Switzerland;

<sup>2</sup>Radiopharmacy, Department of Nuclear Medicine, University Hospital Basel, Basel, Switzerland; and <sup>3</sup>Department of Nuclear Medicine, Erasmus Medical Center, Rotterdam, The Netherlands

Regulatory peptide receptors are overexpressed in numerous human cancers. These receptors have been used as molecular targets by which radiolabeled peptides can localize cancers in vivo and, more recently, to treat cancers with peptide receptor radiation therapy (PRRT). This review describes the candidate tumors eligible for such radiotherapy on the basis of their peptide receptor content and discusses factors in PRRT eligibility. At the present time, PRRT is performed primarily with somatostatin receptor- and cholecystokinin-2 (CCK2)-receptor-expressing neuroendocrine tumors with radiolabeled octreotide analogs or with radiolabeled CCK2-selective analogs. In the future, PRRT may be extended to many other tumor types, including breast, prostate, gut, pancreas, and brain tumors; that have recently been shown to overexpress several other peptide receptors, such as gastrin-releasing peptide-, neurotensin-, substance P-, glucagon-like peptide 1-, neuropeptide Y-, or corticotropin-releasing factor-receptors. A wide range of radiolabeled peptides is being developed for clinical use. Improved somatostatin or CCK<sub>2</sub> analogs as well as newly designed bombesin, neurotensin, substance P, neuropeptide Y, and glucagon-like peptide-1 analogs offer promise for future PRRT.

**Key Words:** tumor targeting; radiopeptides; receptors; peptide receptor radiation therapy; tumor selection

J Nucl Med 2005; 46:675-755

In the past decade, there has been increasing evidence of peptide receptor expression on various human cancers (1). This observation has permitted the development of in vivo peptide receptor targeting of these tumors for diagnostic or therapeutic purposes (2,3). Because of the success of peptide receptor radiation therapy (PRRT) in somatostatin receptor-positive cancers, it is appropriate to review the various peptide receptors and corresponding tumors that are or may become candidates for PRRT and discuss eligibility criteria for patients with cancer. With the recent development of other "intelligent drug molecules" (e.g., imatinib,

trastuzumab, and epidermal growth factor-receptor inhibitors) targeted to specific entities, it is increasingly important to select the right patient candidate for the right drug (4). If we do not systematically preselect PRRT patients on the basis of rational molecular biologic grounds, then clinical applications may yield poorly reproducible therapeutic results for these drugs and lead to false conclusions about the efficacy of targeted drug therapy in general (4).

## GENERAL CRITERIA FOR PRRT ELIGIBILITY

Two types of criteria should guide decisions on eligibility of cancer patients for PRRT: clinical and molecular biologic criteria (Table 1).

### Clinical Criteria

Patients eligible for PRRT are those with cancer and multiple inoperable metastases. Most of these patients have been pretreated. Often, established adjuvant palliative therapies (chemotherapy, radiotherapy) have been tried in these patients with little or no success before PRRT (3). Patients with a single brain tumor are also eligible when a surgical approach or nonsurgical treatments (chemo- and radiotherapy) have failed (5).

### Molecular Biologic Criteria

An absolute prerequisite for PRRT inclusion of a cancer patient from the categories cited in the previous paragraph is that the cancer expresses the corresponding peptide receptor in the primary tumor and in metastases. It is a further prerequisite that receptor density is high. Finally, knowing that peptide receptor expression in cancers may be heterogeneous (i.e., that some tumor areas can express a high receptor density whereas others lack the receptors), it is obvious that the more homogeneously a peptide receptor is expressed in a tumor, the better candidate target it is for PRRT (1,6).

Because many peptides act through multiple peptide receptor subtypes, it is crucial that the peptide receptor subtype expressed by a given tumor correspond to the subtype to which the radioligand used for PRRT binds with high affinity.

Although tumor location is in most cases not a crucial criterion for PRRT eligibility, it should be remembered that

Received Apr. 23, 2004; revision accepted Sep. 30, 2004.

For correspondence or reprints contact: Jean Claude Reubi, MD, Division of Cell Biology and Experimental Cancer Research, Institute of Pathology, University of Berne, P.O. Box 82, Münstertstrasse 31, CH-3010 Berne, Switzerland.

E-mail: reubi@pathology.unibe.ch

**TABLE 1**  
General Criteria for Peptide Receptor Radiation  
Therapy Eligibility

Clinical
Cancer with inoperable multiple metastases; single brain tumors.
No success with established therapies.
Molecular biological
Tumor expressing adequate peptide receptors.
Expressed subtype corresponds to affinity profile of radioligand.
Tumor expressing a high density of receptors.
Preferably homogenous distribution.
Tumor localization preferably outside the blood-brain barrier (alternative application for central nervous system tumors).
Preferably high radiosensitivity.

peptides usually cross the blood-brain barrier with difficulty. Therefore, brain tumors, including glioblastomas with partially perturbed blood-brain barrier, will be less accessible to intravenously injected peptides than are peripheral tumors. This does not mean that patients with brain tumors are ineligible for PRRT. Indeed, brachytherapy may be used as a PRRT alternative for brain tumor patients, based on the use of radiolabeled peptides applied locally to the tumor (5).

Although tumor size was shown to play an important role in the efficacy of PRRT in animal tumor models, similar studies have not been published for humans (7).

Tumor radiosensitivity is of clear importance in the success of targeted radiotherapy, but the radiosensitivity of a specific tumor ranks behind peptide receptor expression in

eligibility criteria for PRRT. However, when 2 tumors have similar levels of peptide receptors, the one that is more radiosensitive is a better candidate for PRRT. It is not clear whether a radiosensitive tumor that usually has only a low density of somatostatin receptors (e.g., lymphomas) will be a good PRRT candidate.

#### TUMORS AND RECEPTORS ELIGIBLE FOR PRRT TODAY

The choice of the right tumor patients as PRRT candidates today is based on the following knowledge: (a) Previous information from in vitro receptor studies in cancer (1). These studies have provided data about incidence and receptor density in various human cancers. This allows the physician to make a first selection of types of tumors with high incidence of peptide receptor expression that may be eligible for PRRT. (b) Results of in vivo receptor scintigraphy with the relevant radioligand in the patient of interest. Such data should not only allow detection or confirmation of the site of the primary tumor and metastases but also permit evaluation of receptor density in the targeted tumor. To achieve the latter, the nuclear physician can calculate a tumor-to-liver ratio as a relative measure of receptor number (3). This ratio must be high for PRRT eligibility (3).

PRRT has been established for 2 peptide receptor systems: somatostatin receptors and, to a lesser extent, for cholecystokinin-2 (CCK2) receptors (Table 2). For both systems, clinical studies have reported efficacy in a significant number of patients (8-11).

**TABLE 2**  
Current Tumor and Peptide Receptor Candidates for PRRT

Administration route	Tumors	In vitro evidence	In vivo evidence	
			Diagnostic	PRRT (ref.)
Intravenous	Somatostatin receptor sst2-expressing tumors			
	GEP NET*	+	+	+ (3,8,10,11)
	Paragangliomas*	+	+	+ (43)
	Pheochromocytomas*	+	+	+ (43)
	Small-cell lung cancer	+	+	
	Medullary thyroid cancer	+	+	+ (43)
	Breast cancer	+	+	
	Renal cell cancer	+	+	
	Thyroid cancer	+	+	+
	Malignant lymphomas	+	+	
	CCK2 receptor expressing tumors			
	Medullary thyroid cancer*	+	+	+ (9)
	GIST*	+		
	Small-cell lung cancer	+	+	
	GEP NET	+	+	
Topical	Sex cord stromal ovarian tumor	+		
	sst2-expressing central nervous system tumors			
	Medulloblastomas*	+	+	+
	Gliomas	+	+	+ (5,12)

\*Most eligible for PRRT, on the basis of high incidence and density of receptors.

### Somatostatin Receptors

Several groups have shown that cancers with a high somatostatin receptor density, in particular sst2 subtype (Table 2), are eligible for somatostatin receptor radiotherapy (3,8,10,11). This is predominantly the case for gastroenteropancreatic (GEP) neuroendocrine tumors (NETs), especially carcinoids and gastrinomas, which frequently have a high sst2 receptor density. Other NETs, such as pheochromocytomas, paragangliomas, and bronchial carcinoids, are also strong candidates (1). Small-cell lung cancers and medullary thyroid carcinomas, in selected cases, also have a receptor density sufficiently high to be included in this list. In practice, the pituitary adenomas (growth hormone, thyroid-stimulating hormone, and inactive adenomas) are not considered PRRT candidates, although they usually have very high sst2 density. The reason they are not considered for PRRT is the therapeutic success of established alternative methods. Finally, a small percentage of non-NETs at times may be selected for PRRT, including inoperable meningiomas, neuroblastomas, a subgroup of metastatic breast tumors characterized by high receptor density, metastatic renal cell carcinomas, and thyroid cancers (1).

All these tumors are usually reached adequately by intravenous application of the radioligand. However, as mentioned previously, a few tumor types, such as brain tumors, are less accessible by the intravenous route. These tumors (gliomas and medulloblastomas) may be targeted by a topical application of  $^{90}\text{Y}$ - or  $^{177}\text{Lu}$ -labeled octreotide derivatives. PRRT using octreotide derivatives has been shown to be successful for peripheral as well as central nervous system tumors (3,5,12).

### CCK2 Receptors

Only a few reports have shown cancers with a high density of CCK2 receptors to be eligible for CCK2 receptor radiotherapy. On the basis of previous in vitro receptor studies, Behr et al. (9) selected as a first choice medullary thyroid carcinomas for in vivo targeting, because these express CCK<sub>2</sub> receptors in virtually all cases and have shown encouraging preliminary PRRT data (13). The main limiting problem for the development of PRRT using CCK2 receptors may be the high and therefore problematic kidney uptake with current CCK analogs (9). Fortunately, a new generation of CCK analogs has been designed with much less kidney uptake (14). CCK2 receptors have been shown to be overexpressed in several other cancers, including some GEP NETs, small-cell lung cancers, ovarian tumors, and, most interesting, also in gastrointestinal stromal tumors (GISTs), where they can be expressed in extremely high density (13,15,16).

### Other Peptide Receptors

Proof of principle of in vivo targeting has been obtained recently with other peptide receptors. These include gastrin-releasing peptide (GRP) receptors, neurotensin (NT) receptors, and vasoactive intestinal peptide (VIP) receptors (17–19). However, no PRRT data on clinical use of these

peptides are available, so these candidates will be discussed more thoroughly in the section on PRRT for the future.

### In Vivo Versus In Vitro Receptor Evaluation

Extensive studies have been performed to assess the specificity of somatostatin receptor scintigraphy by comparing it directly with in vitro somatostatin receptor status (20). In most of the PRRT studies, however, patient eligibility was based only on  $^{111}\text{In}$ -diethylenetriaminepentaacetic acid<sup>D</sup> (DTPA)-octreotide (Octreoscan; Mallinckrodt, Inc.) or CCK2 receptor scintigraphy in vitro rather than on an in vitro evaluation of receptor expression in surgically resected tumor samples. In vivo peptide receptor scanning is preferred because  $^{111}\text{In}$ -DTPA-octreotide or CCK2 receptor scintigraphy has the advantage of being noninvasive with no requirement for tumor sampling. Moreover, these scanning methods can provide information about whole-body distribution of receptor-positive tumors and give a relative approximation of their density using the tumor-to-liver ratio. However, in vivo scintigraphy cannot give a clear assessment of the homogeneity or heterogeneity of receptor distribution within the tumors. This information and precise quantification can be obtained by in vitro receptor autoradiography, with the limitation that usually only a portion of the tumor is assessed. Figure 1 depicts homogeneously distributed somatostatin receptors in a GEP NET compared with heterogeneously distributed somatostatin receptors in a breast cancer, as measured by in vitro receptor autoradiography.

### TUMOR AND RECEPTOR PRRT CANDIDATES FOR THE FUTURE

Table 3 lists several peptide receptors and tumor types that may become eligible for PRRT in the near future. This list is based primarily on current in vitro receptor data from surgical samples. In vitro receptor data have been consid-



**FIGURE 1.** Homogeneous distribution of somatostatin receptors in a GEP NET (A–C) and nonhomogeneous distribution in a breast cancer (D–F). (A and D) Hematoxylin-eosin stained sections. Bars = 1 mm. (B and E) Total binding of  $^{125}\text{I}$ -Tyr<sup>3</sup>-octreotide with homogeneous distribution in B but not in E. (C and F) Nonspecific binding.

**TABLE 3**  
Tumor and Peptide Receptor Candidates for Peptide Receptor Radiation Therapy in Future

Administration route	Tumor	In vitro evidence	In vivo evidence	
			Diagnostic (ref)	PRRT
Intravenous	GRP-R-expressing tumors			
	Prostate cancer*	+	+ (44)	
	Breast cancer*	+	+ (17)	
	GIST*	+		
	Small-cell lung cancer	+		
	NT <sub>1</sub> -R-expressing tumors			
	Exocrine pancreatic cancer*	+	+ (18)	
	Meningiomas	+		
	Ewing sarcomas	+		
	VIP-R-expressing tumors			
	VPAC <sub>1</sub> *†	+	+ (19)	
	VPAC <sub>2</sub> ; GIST*, other stromal tumors	+		
	NPY-R-expressing tumors			
	Y <sub>1</sub> ; breast Ca*	+		
	Y <sub>1</sub> /Y <sub>2</sub> ; sex cord stromal ovarian tumors	+		
	Y <sub>1</sub> /Y <sub>2</sub> ; adrenal tumors	+		
	GLP1-R-expressing tumors			
	Insulinomas*	+		
	Gastrinomas	+		
	CRF-R-expressing tumors			
	CRF <sub>1</sub> ; ACTH-prod. pituitary adenomas	+		
	paragangliomas	+		
	CRF <sub>2</sub> ; growth hormone-prod. pituitary adenomas	+		
	nonfunctioning pituitary adenomas	+		
	Tumors expressing multiple sst subtypes			
	Medullary thyroid cancer	+		
	Pituitary adenomas	+		
	Prostate cancers	+		
	Gastric cancers	+		
Topical	SP-R (NK1)-expressing central nervous system tumors			
	Gliomas*	+	+	+ (31)

\*Most eligible for PRRT, on the basis of high incidence and density of receptors.

†Gastrointestinal cancers; many other VPAC<sub>1</sub>-R-expressing tumors may be inadequate because of high VPAC<sub>1</sub> expression in normal tissues.

ered to be largely predictive for in vivo conditions, based on the excellent correlation between in vitro and in vivo receptor evaluation (20). The list is further supported by a limited number of reports on in vivo targeting for diagnostic purposes. PRRT studies are still largely absent in this group.

**GRPs.** Of great potential interest for PRRT are GRP receptors, because they are abundant in most breast and prostate cancers. Samples tested in vitro have originated only from surgically operable tumors. The investigated sample collection, therefore, has consisted predominantly of primaries rather than of metastatic tissues and rarely has contained advanced undifferentiated cancers or hormone-insensitive cancers (21,22). This means that the GRP receptor status of the latter tumor group remains largely unknown, having not been investigated for technical reasons. GRP receptor heterogeneity is frequent in breast cancer and could pose a potential problem for GRP receptor radiotherapy (21). One target that may be extremely attractive for

PRRT is GISTs, because of the extraordinarily high GRP receptor density found in these tumors (16).

**NT Receptors.** A subgroup of ductal pancreatic carcinoma expresses a high density of NT receptors (23). A preliminary in vivo NT receptor scanning study visualized a faint signal from a tumor with a high density of these receptors (18). These tumors may be attractive for PRRT, despite the low cellularity of the type of cancer, often consisting of few but strongly receptor-positive neoplastic ducts embedded within a receptor-negative surrounding fibrosis (as in chronic pancreatitis) (23). This low cellularity may explain in part the weakness of the in vivo signal. Other tumors expressing NT receptors are meningiomas and Ewing sarcomas.

**VIP Receptors.** Although a majority of human cancers express VIP receptors of the VIP-pituitary adenylate cyclase-activating polypeptide 1 (VPAC<sub>1</sub>) subtype, the targeting of VPAC<sub>1</sub>-receptors for PRRT is unlikely to be have

great potential because of the ubiquitous distribution of VPAC1 in most organs (24). Conversely, VPAC2, which is only rarely expressed in normal tissues, may be a target for PRRT in VPAC2-expressing cancers. GISTs, with high VPAC2 receptor density, may be most attractive examples (16). In vivo data using  $^{125}\text{I}$ -VIP as a universal ligand targeting VPAC1 and VPAC2 are available as proof of concept that VIP receptor-positive tumors, specifically gastrointestinal cancers, can be targeted in vivo in selected patients (19,25).

**Neuropeptide-Y (NPY) Receptors.** NPY receptors have been found to be highly expressed in breast cancer, predominantly as Y1 subtype, as well as in a subgroup of ovarian tumors (sex cord stromal tumors) and adrenal tumors (26–28). This is a new family of peptide receptors for which in vivo scanning studies in human tumors should be performed.

**Glucagon-Like-Peptide 1 (GLP1) Receptors.** A very high density of GLP1 receptors was reported in virtually all insulinomas and, at lower density, in gastrinomas, suggesting the use of GLP1 analogs for PRRT of these tumors (15). Whereas rat insulinomas were reported to be targeted in vivo by GLP1 analogs, such evidence is still missing for human insulinomas.

**Corticotropin-Releasing Factor (CRF) Receptors.** CRF receptors are expressed in selected human cancers (29). Those with a high density include adrenocorticotrophic hormone-producing pituitary adenomas and paragangliomas (CRF1) as well as GH-producing and nonfunctioning pituitary adenomas (CRF2). These may be attractive PRRT candidates.

**Neurokinin 1 (NK1) receptors.** Because gliomas have a density of NK1 receptors that is considerably higher than that of somatostatin receptors, the same topical approach for somatostatin receptors has been proposed and a pilot study was started to evaluate the effect of PRRT in glioblastomas (12,30). The study is still in progress, but encouraging preliminary data have been reported (31).

## MULTIRECEPTOR TARGETING

The presence of multiple peptide receptors in selected cancers may be the basis for multireceptor radiotherapy using 2 or more radiotracers concomitantly. This strategy would have 2 main advantages. First, 2 or more radioligands administered concomitantly could considerably increase the therapeutic dose to the tumor. Second, some of the problems related to receptor heterogeneity in tumors may be overcome, because it is likely that more tumor cells would be targeted with 2 or more radioligands than would be possible with only a single ligand. Figure 2 illustrates this with the example of CCK and somatostatin receptors. Most of the CCK receptors are distributed on the right part of the sample, whereas most of the somatostatin receptors are on the left. It is expected that PRRT with radiolabeled CCK and somatostatin analogs administered together would be

HE CCK-R SS-R

**FIGURE 2.** Concomitant but complementary distribution of CCK and somatostatin receptors in adjacent sections of GEP NET. (A) Hematoxylin-eosin stained section. Bar = 1 mm. (B) Autoradiograph showing CCK receptors predominantly expressed in right part of tumor. (C) Autoradiograph showing somatostatin receptors predominantly found in left part of tumor.

more successful than PRRT using either tracer alone, because the tumor would be targeted much more homogeneously. Such multireceptor targeting could possibly prevent or reduce resistance or escape from radiotherapy. Tumors of interest for multireceptor targeting include breast cancers (expressing concomitantly GRP and NPY receptors) and GISTs (with GRP, CCK2, and VPAC2 receptors) (16,32).

## PEPTIDE RADIOLIGAND CANDIDATES

A prerequisite for successful PRRT is the availability of adequate peptide tracers. The best developed tracers at present are usually characterized by binding affinities in the low nanomolar range. So far, these small peptides have not been found to be immunogenic, unlike antibodies used in radiolabeled therapy. Peptide radioligands include those used for somatostatin receptor targeting, which are mostly derived from octreotide (2). Moreover, the development of adequate peptide radioligands for other receptors is also rapidly progressing (Table 4). Although many groups are working to develop GRP, CCK2, and NT radioligands, little information is available on adequate NPY, GLP-1, and VIP ligands to be used for PRRT (1).

## Radioligands in Human Use Today

**Somatostatin.** Prototypical in targeted radiotherapy are radioligands based on somatostatin analogs. Four of these ligands are in clinical use. They are depicted in Figure 3. The oldest agent is  $^{111}\text{In}$ -DTPA-octreotide. This peptide radioligand was designed for scintigraphy and, because of the Auger and conversion electrons emitted by  $^{111}\text{In}$ , has been suggested to be useful for therapy as well. One of the drawbacks of this radioligand is its only moderate binding affinity to sst2 and almost negligible affinity to sst1, 3, 4, and 5. In addition, DTPA is not a suitable chelator for commercially available  $\beta$ -emitters such as  $^{90}\text{Y}$  and  $^{177}\text{Lu}$ . For these radiometals, it is better to use the macrocyclic chelator 1,4,7,10-tetraazacyclododecane- $N,N',N'',N'''$ -tetraacetic acid (DOTA). It forms very stable (thermodynamically and kinetically) metal complexes. The DOTA-coupled

**TABLE 4**  
**Peptide Radioligands for In Vivo Targeting of Tumors Expressing Peptide Receptors**

Peptide receptor	Radioligands in use in humans	Radioligands in development	Reference
Somatostatin			
sst2	DTPAOC DOTATOC DOTATATE	Carbohydrated derivatives and other biodistribution modifiers	8,10,38,39,45
sst2,5	DOTA-lanreotide		46
sst2,3,5		DOTANOC DOTABOC DOTANOCate DOTABOCate KE 108 and derivatives	35,36
sst1,2,3,4,5			37
Bombesin			
GRF-R	Demobesin; RP527		17,34
NMB-R	—	—	
BB <sub>3</sub>	—	—	
CCK			
CCK <sub>2</sub>	Minigastrin; CCK analog	MG-11	9,14,47
Neurotensin			
NT-1	—	Neurotensin XI	18
NPY			
Y <sub>2</sub>	—	Ac-[Ahx <sup>6-24</sup> ,K <sup>69m</sup> Tc(Co) <sub>3</sub> ]-PADA]-NPY	41
GLP1	—	Exendin-3 or -4	42
NK1	DOTAGA-substance P		31

somatostatin-based radiopeptides are <sup>90</sup>Y-DOTA<sup>0</sup>-Tyr<sup>3</sup>-oct-reotide (<sup>90</sup>Y-DOTATOC, <sup>90</sup>Y-SMT-487), <sup>90</sup>Y-DOTA-lan-reotide (MAURITIUS), and <sup>177</sup>Lu-DOTA-Tyr<sup>3</sup>-The<sup>8</sup>-oct-reotide (<sup>177</sup>Lu-DOTATATE). They differ with regard to the sst receptor subtype affinity profile (33). The DOTATATE derivative has the highest sst2 receptor affinity, whereas DOTA-lanreotide has lower affinity to sst2 but shows sst5 affinity (33).

**CCK/Gastrin.** As indicated previously, CCK2 receptors may be attractive targets for internal radiotherapy. The ligand used for the first clinical trial was a DTPA-D-Glu chelator-modified minigastrin (Fig. 4) labeled with <sup>90</sup>Y. Because of kidney and hemotoxicity, the trial was stopped (9). New gastrin-derived ligands with much lower kidney toxicity but excellent target affinity are being developed (14). In these, 4 glutamic acid residues have been deleted from the minigastrin derivative. This truncated radiopeptide showed an improved binding affinity to the CCK2-receptor (0.2 vs. 1.0 nmol/L) and retained tumor uptake in the rat CA 20948 tumor model but showed a kidney uptake that was lower by a factor of 25 (14).

**Substance P.** Another peptide candidate used in PRRT for brain tumors is <sup>90</sup>Y-DOTAGA-substance P, shown in Figure 5. This tracer is given as brachytherapy intratumorally or into the tumor cavity (31). It is directed against the NK1 receptor, overexpressed in human glioblastoma (30). The peptide is metabolically unstable, and the efficacy of PRRT in glioblastoma (targeting the NK1 receptors) could probably be increased if radiopeptides resistant to proteases were introduced into the clinic.

**Bombesin.** Two <sup>99m</sup>Tc-based bombesin ligands with high affinity for GRP receptors are being used clinically. One is

called demobesin, a tetraamine-derivatized bombesin antagonist [D-Phe<sup>6</sup>,Leu-NHEt<sup>13</sup>,desMet<sup>14</sup>] bombesin (6–14) (34). Preliminary results show good tumor delineation in prostate cancer patients.

The other <sup>99m</sup>Tc-based ligand is a N<sub>3</sub>S chelator coupled to bombesin (7–14) via a gly-5-aminovaleric acid spacer. It can be labeled with high specific activity and radiochemical yield and has been shown to identify breast and prostate primary cancer and metastases (17). This agent should also be suitable for labeling with <sup>188</sup>Re, the therapeutic congener of <sup>99m</sup>Tc.

**NT.** Little activity has been reported on the development of NT-based radioligands. Buchegger et al. (18) published a study of 4 patients using a metabolically stabilized (8–13) neurotensin analog, (NT-XI) modified with N-carboxy-methyl-histidine for labeling with a Tc(CO)<sub>3</sub><sup>+</sup> unit. Research is being pursued by this group using the carbonyl approach, with the therapeutic goal of labeling with the β-emitter <sup>188</sup>Re.

#### Radioligands in Development

**Somatostatin.** There are still potential improvements in the field of somatostatin receptor targeting. One step being pursued is the development of somatostatin-based radioligands with a broader receptor subtype affinity profile. This may not only extend the range of targeted cancer candidates but also increase the tumor uptake, because of the presence of several receptor subtypes on the same tumor cell.

Several new compounds have been developed that show high affinity to sst2, 3, and 5 (35,36). These were modified at position 3 of the octapeptide. The best radiopeptides were

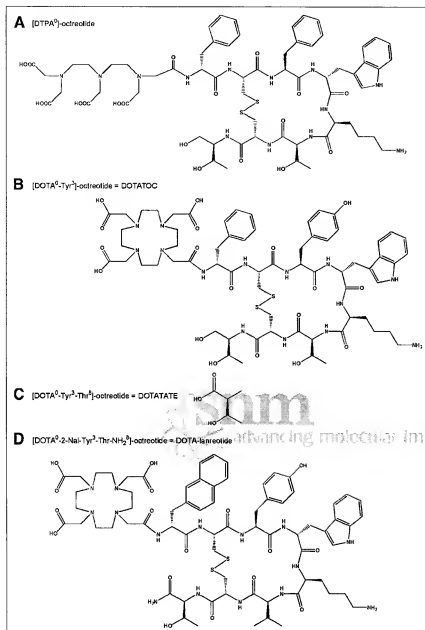


**FIGURE 3.** Chemical structures of DTPA- and DOTA-modified somatostatin-based peptides for targeted radiotherapy. (A) DTPA<sup>3</sup>-octreotide. (B) DOTA<sup>2</sup>-Tyr<sup>3</sup>-octreotide (DOTATOC). (C) DOTA<sup>2</sup>-Tyr<sup>3</sup>-Thr<sup>4</sup>-octreotide (DOTATATE). (D) DOTA<sup>2</sup>-2-Nal-Tyr<sup>3</sup>-Thr-NH<sub>2</sub>-octreotide (DOTA-lanreotide).

those with unnatural amino acids 1-naphthyl-alanine (1-Nal) and benzothienyl-alanine (BzThi).

Attempts are also being made to develop pansomatostatin radioligands. Data on the first peptide, KE 108, which has

higher potency than somatostatin-28 to all receptor subtypes and can be radioiodinated, were published recently (37).

This peptide was also modified by coupling DOTA to the *N*-terminus (Fig. 6). It was still able to bind with high

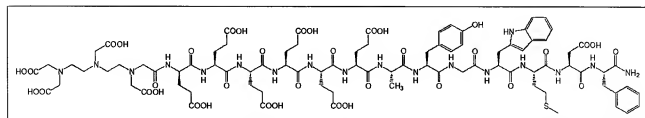
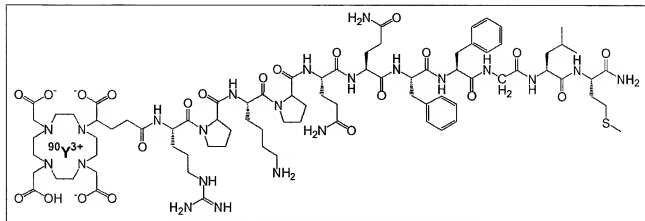


**FIGURE 4.** Structural formula of the CCK2-selective analog DTPA-D-Glu<sub>5</sub>-Ala-Tyr-Gly-Trp-Met-Asp-PheNH<sub>2</sub> (minigastrin).



affinity to all 5 somatostatin receptor subtypes (Reubi and Mäcke, unpublished data).

Another recent strategy has been to couple octreotide or octreotate derivatives to carbohydrates to improve tracer pharmacokinetics (38,39).

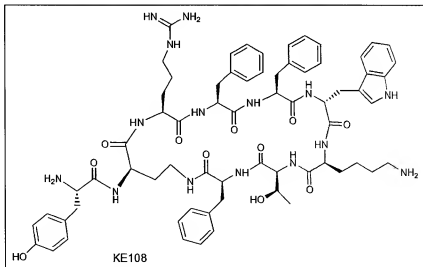
**Bombesin.** A promising group of peptides was developed by Hoffman et al. (40) for targeted radiotherapy of GRP receptor-positive tumors. These are based on the bombesin (7-14) sequence and coupled to DOTA via aminocarboxyl spacer groups. These peptides were successfully labeled with  $^{177}\text{Lu}$ ,  $^{166}\text{Ho}$ , and other radiolanthanides. They are especially promising candidates for PRRT of prostate and breast cancer patients.

**NPY.** A new radioligand was described by Langer et al. (41). This research group has used the  $\text{Tc}(\text{CO})_3^+$  approach and developed a highly selective high-affinity  $Y_2$ -receptor ligand  $\text{Ac}[\text{Ahx}^{5-24}, \text{K}^+ (^{99m}\text{Tc}(\text{CO})_3\text{-2-picolylamine } N,N\text{-diacetic acid (PADA)})\text{-NPY}$ . This radioligand has about 1.5 nmol/L  $Y_2$ -affinity if complexed to cold  $\text{Re}(\text{CO})_3^+$ . An

other NPY radioligand in development is the  $Y_1/Y_2$ -selective [ $K^{nat}Re(CO)_3$ -PADA, A<sup>26</sup>]-NPY derivative, found to bind with 16 nmol/L affinity to  $Y_1$  and 8.5 nmol/L to  $Y_2$  (41).

**GLP-1.** GLP-1 is an intestinal hormone that stimulates insulin secretion. Its action is mediated by a receptor expressed in islet cells. These receptors are massively overexpressed in insulinoma (15). Therefore, radiolabeled versions of GLP-1 and its metabolically more stable congener exendin 3 or 4 have been developed and studied in mouse models.  $^{111}\text{In}$  was coupled to these peptides via DTPA-complexation, and  $^{125}\text{I}$  labeling was performed via the IODO-GEN method (42).

**Conclusion.** In general one may conclude that those peptides that will perform adequately in diagnostic imaging eventually will be coupled to DOTA and DOTAGA for labeling with the  $\beta$ -emitters suitable for PRRT or with technology enabling  $^{188}\text{Re}$  labeling. Research in this direction is ongoing in academia and industry.



## REFERENCES

- Reubi JC. Peptide receptors as molecular targets for cancer diagnosis and therapy. *Endocr Rev*. 2003;24:389–427.
- Heppeler A, Froldevaux S, Eberle AN, Maacke HR. Receptor targeting for tumor localization and therapy with radiolabeled peptides. *Curr Med Chem*. 2000;7:971–994.
- Kwekkeboom DJ, Krenning EP, de Jong M. Peptide receptor imaging and therapy. *J Nucl Med*. 2000;41:1704–1713.
- Tollfson PJ, Saxman S, Coleman CN. Molecular targets for radiation therapy: bringing preclinical data into clinical trials. *Clin Cancer Res*. 2003;9:3518–3520.
- Merlo A, Hausman O, Wasner M, et al. Locoregional regulatory peptide receptor targeting with the diffusible somatostatin analogue <sup>90</sup>Y-labeled DOTAT<sup>10</sup>-D-Phe-Tyr<sup>3</sup>-octreotide (DOTATOC): a pilot study in human gliomas. *Clin Cancer Res*. 1999;5:1025–1033.
- Reubi JC, Waser B, Foekens JA, Klijn JGM, Lamberts SWJ, Laisius J. Somatostatin receptor incidence and distribution in breast cancer using receptor autoradiography: relationship to EGFR receptors. *Int J Cancer*. 1990;46:416–420.
- de Jong M, Broeman WA, Remond-Buffin E, et al. Tumor response after <sup>90</sup>Y-DOTATOC/Tyr<sup>3</sup>octreotide radionuclide therapy in a transplantable rat tumor model is dependent on tumor size. *J Nucl Med*. 2001;42:1841–1846.
- Kwekkeboom DJ, Bakker WH, Kam BL, et al. Treatment of patients with gastro-entero-pancreatic (GEP) tumors with the novel radiolabelled somatostatin analogue [<sup>111</sup>In-DOTA<sup>1</sup>-Tyr<sup>3</sup>-octreotide]. *Eur J Nucl Med*. 2003;30:417–422.
- Behr TM, Behr TM. Cholecystokinin-B/Gastrin receptor-targeting peptides for staging and therapy of medullary thyroid cancer and other cholecystokinin-B receptor-expressing malignancies. *Semin Nucl Med*. 2002;32:97–109.
- Waltherer C, Pless M, Maacke HR, Haldemann A, Mueller-Brand J. The clinical value of [<sup>90</sup>Y-DOTA<sup>1</sup>-D-Phe-Tyr<sup>3</sup>-octreotide (<sup>90</sup>Y-DOTATOC)] in the treatment of neuroendocrine tumours: a clinical phase II study. *Ann Oncol*. 2001;12:941–945.
- Pignatelli G, Zobil S, Crenesini M, et al. Receptor-mediated radiotherapy with <sup>90</sup>Y-DOTA<sup>1</sup>-D-Phe-Tyr<sup>3</sup>-octreotide. *Eur J Nucl Med*. 2001;28:426–434.
- Schumacher T, Hofer S, Eichhorn K, et al. Local injection of the <sup>90</sup>Y-labelled peptide vector DOTATOC to control gliomas of WHO grades II and III: an extended pilot study. *Eur J Nucl Med*. 2002;29:486–493.
- Reubi JC, Schaer JC, Waser B. Cholecystokinin (CCK)-A and CCK-B/gastrin receptors in human tumors. *Cancer Res*. 1997;57:1377–1386.
- Bernard BF, Böhle M, Broeman WA, et al. Preclinical evaluation of munitin analogs for CCK-B receptor targeting. *Cancer Biother & Radiopharm*. 2003;18:281.
- Reubi JC, Waser B. Coexistent expression of several peptide receptors in neuroendocrine tumors as molecular basis for in vivo multireceptor tumor targeting. *Eur J Nucl Med*. 2003;30:781–793.
- Reubi JC, Korner M, Waser B, Mazzocchielli L, Guillou L. High expression of peptide receptors as a novel target in gastrointestinal stromal tumours. *Eur J Nucl Med Mol Imaging*. 2004;31:803–810.
- Van de Wiele C, Dumont F, Vanden Broecke R, et al. Technetium-99m PS27, a GRP analogue for visualisation of GRP receptor-expressing malignancies: a feasibility study. *Eur J Nucl Med*. 2000;27:1694–1699.
- Buchegger F, Bonvin F, Kotsinski M, et al. Radiolabelled neurotensin analog, <sup>99m</sup>Tc-NI-XI, evaluated in ductal pancreatic adenocarcinoma patients. *J Nucl Med*. 2003;44:1649–1654.
- Virgolini I, Radler M, Körtner A, et al. 123-I-vasoactive intestinal peptide (VIP) receptor scanning: update of imaging results in patients with adenocarcinomas and endocrine tumors of the gastrointestinal tract. *Nucl Med Biol*. 1996;23:685–692.
- Krenning EP, Kwekkeboom DJ, Pauwels S, Kroes LK, Reubi JC. *Somatostatin Receptor Scintigraphy*. New York, NY: Raven Press; 1995:1–50.
- Gugger M, Reubi JC. GRP receptors in non-neoplastic and neoplastic human breast. *Am J Pathol*. 1999;155:2067–2076.
- Markwalder R, Reubi JC. Gastrin-releasing peptide receptors in the human prostate: relation to neoplastic transformation. *Cancer Res*. 1999;59:1152–1159.
- Reubi JC, Waser B, Friess H, Büchler MW, Laisius JA. Neurotensin receptors: a new marker for human ductal pancreatic adenocarcinoma. *Gut*. 1998;42:546–550.
- Reubi JC, Läderach U, Waser B, Göbbers J-O, Rothermundt P, Laisius JA. Vasoactive intestinal peptide/pituitary adenylate cyclase-activating peptide receptor subtypes in human tumors and their tissues of origin. *Cancer Res*. 2000;60:3105–3112.
- Hessenas C, Bäder M, Meinhold H, et al. Vasoactive intestinal peptide receptor scintigraphy in patients with pancreatic adenocarcinomas or neuroendocrine tumors. *Eur J Nucl Med*. 2000;27:1684–1693.
- Reubi JC, Gugger M, Waser B, Schaer JC. Y1-mediated effect of neuropeptide Y in cancer: breast carcinomas as targets. *Cancer Res*. 2001;61:4636–4641.
- Korner M, Waser B, Reubi JC. Neuropeptide Y receptor expression in human primary ovarian neoplasms. *Lab Invest*. 2004;84:71–80.
- Korner M, Waser B, Reubi JC. High expression of NPY receptors in tumors of the human adrenal gland and extrarenal paraganglia. *Clin Cancer Res*. 2004;in press.
- Reubi JC, Waser B, Vale W, Rivier J. Expression of CRF1 and CRF2 receptors in human cancers. *J Clin Endocrinol Metab*. 2003;88:3312–3320.
- Hennig DM, Laisius JA, Horiuchi Y, Reubi JC. Substance P receptors in human primary neoplasms: tumoural and vascular localisation. *Int J Cancer*. 1995;61:786–792.
- Schumacher T, Eichhorn K, Hofer S, et al. Diffusible brachytherapy (DBT) with radiolabelled substance P in high grade gliomas: first observations [abstract]. *Eur J Nucl Med*. 2001;28:1040.
- Reubi JC, Gugger M, Waser B. Coexpressed peptide receptors in breast cancers as molecular basis for in vivo multireceptor tumor targeting. *Eur J Nucl Med*. 2002;29:855–862.
- Reubi JC, Schaer JC, Waser B, et al. Affinity profiles for human somatostatin receptor subtypes 1–5 of somatostatin radiocytocines selected for scintigraphic and radiotherapeutic use. *Eur J Nucl Med*. 2000;27:273–282.
- Nock B, Nikolopoulou A, Chiotellis E, et al. [<sup>99m</sup>Tc]demobesin 1, a novel potent bombesin analogue for GRP receptor-targeted tumor imaging. *Eur J Nucl Med*. 2003;30:247–258.
- Wild D, Schmitt JS, Ginj M, et al. DOTA-NOC, a high-affinity ligand of somatostatin receptor subtypes 2, 3 and 4 for labelling with various radionuclides. *Eur J Nucl Med Mol Imaging*. 2003;30:1338–1347.
- Ginj M, Chen J, Reubi JC, Maacke HR. Preclinical evaluation of new and highly potent analogs of octreotide for targeted radiotherapy [abstract]. *Eur J Nucl Med Mol Imaging*. 2003;(suppl 2):S198–S199.
- Reubi JC, Eisenwiler KP, Rink H, Waser B, Maacke HR. A new peptide somatostatin agonist with high affinity to all five somatostatin receptors. *Eur J Pharmacol*. 2002;456:45–49.
- Westen HJ, Schottelius M, Scheidhauer K, Reubi JC, Wolf I, Schwager M. Comparison of radiolabelled TOC, TOCA and Mtr-TOCA: the effect of carbonylation on the pharmacokinetics. *Eur J Nucl Med*. 2002;29:28–38.
- Schottelius M, Westen HJ, Reubi JC, Senekowicz-Schmid R, Schwager M. Improvement of pharmacokinetics of radiolabelled tyrosine-octreotide by conjugation with carbonylhydrazide. *Bioconjug Chem*. 2002;13:1021–1030.
- Hoffman TJ, Gali H, Smith CJ, et al. Novel series of <sup>111</sup>In-labeled bombesin analogs as potential radiopharmaceuticals for specific targeting of gastrin-releasing peptide receptors expressed on human prostate cancer cells. *J Nucl Med*. 2003;44:823–831.
- Langer M, La Bella R, Garcia-Garayza E, Beck-Sickinger AG. <sup>99m</sup>Tc-labeled neuropeptide Y analogues as potential tumor imaging agents. *Bioconjug Chem*. 2001;12:1028–1034.
- Behr M, Behr TM, Schmalzer W, Herbst B, Gotschardt M. Indium-111 labelled GLP-1 for in vivo diagnostic of insulinomas [abstract]. *Eur J Nucl Med*. 2002;43(suppl):92P.
- Valkeala R, De Jong M, Bakker WH, et al. Phase I study of peptide receptor radionuclide therapy with [<sup>111</sup>In-DTPA<sup>1</sup>-octreotide]: the Rotterdam experience. *Semin Nucl Med*. 2000;30:110–122.
- Scopinaro F, De Vincentis G, Varvarigou AD, et al. <sup>99m</sup>Tc-bombesin detects prostate cancer and invasion of pelvic lymph nodes. *Eur J Nucl Med Mol Imaging*. 2003;30:1378–1382.
- Krenning EP, Kwekkeboom DJ, Bakker WH, et al. Somatostatin receptor scintigraphy with [<sup>111</sup>In-DTPA<sup>1</sup>-D-Phe<sup>1</sup>] and [<sup>111</sup>In-Tyr<sup>3</sup>-octreotide]: the Rotterdam experience with more than 1000 patients. *Eur J Nucl Med*. 1993;20:716–731.
- Smith-Jones P, Bischof C, Leiner D, et al. "Mauritius" a novel somatostatin analog for tumor diagnosis and therapy [abstract]. *J Nucl Med*. 1998;39(suppl):223P.
- Kwekkeboom DJ, Bakker WH, Kooij PP, et al. Cholecystokinin receptor imaging using an octapeptide DTPA-CCK analogue in patients with medullary thyroid carcinoma. *Eur J Nucl Med*. 2000;27:1312–1317.

# Synthesis and Biodistribution of $^{211}\text{At}$ -Labeled, Biotinylated, and Charge-Modified Poly-L-lysine: Evaluation for Use as an Effector Molecule in Pretargeted Intraperitoneal Tumor Therapy

Sture Lindegren,<sup>\*,1,5</sup> Håkan Andersson,<sup>1</sup> Lars Jacobsson,<sup>1</sup> Tom Bäck,<sup>1</sup> Gunnar Skarnemark,<sup>5</sup> and Börje Karlsson<sup>1</sup>

Department of Radiation Physics, Göteborg University, Sahlgrenska University Hospital, SE-413 45 Göteborg, Sweden, Department of Oncology, Göteborg University, Sahlgrenska University Hospital, SE-413 45 Göteborg, Sweden, and Department of Nuclear Chemistry, Chalmers University of Technology, SE-412 96 Göteborg, Sweden. Received April 25, 2001; Revised Manuscript Received October 23, 2001

Poly-L-lysine (7, 21, and 204 kDa) has been evaluated as an effector carrier for use in pretargeted intraperitoneal tumor therapy. For the synthesis, the  $\epsilon$ -amino groups on the poly-L-lysine were modified in three steps utilizing conjugate biotinylation with biotin amidocaproate *N*-hydroxysuccinimide ester (BANHS), conjugate radiolabeling with  $^{211}\text{At}$  using the intermediate reagent *N*-succinimidyl 3-(trimethylstannyl)benzoate (m-MeATE), and charge modification using succinic anhydride, resulting in an increase in the molecular weight of approximately 80% of the final product. The labeling of the m-MeATE reagent and subsequent conjugation of the polymer were highly efficient with overall radiochemical yields in the range of 60–70%. The in vitro avidin binding ability of the modified polymer was almost complete (90–95%), as determined by binding to avidin beads using a convenient filter tube assay. Following intraperitoneal (ip) injection in athymic mice, the 13 kDa polymer product was cleared mainly via the kidneys with fast kinetics (biological half-life  $T_b \approx 2$  h) and with low whole-body retention. The clearance of the 38 kDa polymer was distributed between kidneys and liver, and the 363 kDa polymer was mainly sequestered by the liver with a  $T_b$  of 8 h. Increased tissue uptake in the thyroid, lungs, stomach, and spleen following the distribution of the large effector molecules (38 and 363 kDa) suggests that degradation of the polymers by the liver may release some of the label as free astatine/astate.

## INTRODUCTION

Intraperitoneal tumors may arise from disseminated carcinomas, especially those originating from the ovaries. Generally, patients with ovarian cancer have advanced disease at the time of diagnosis (FIGO<sup>1</sup> stage IIB–IV) and, as a rule, tumor dissemination is restricted to the peritoneal surface. The standard treatment for ovarian cancer is surgery followed by chemotherapy. However, despite a high initial curative response, most tumors relapse and the 5-year survival is no higher than 30%. The residual and recurrent tumor cells respond weakly to further chemotherapy, and new, more effective forms of treatment are therefore urgently required.

Endoradiotherapy using radiohalogenated monoclonal antibodies has been investigated in recent years in an

effort to improve the therapeutic effect of treatment of ovarian carcinomas (1, 2). The halogen of main interest has been the  $\beta$ -emitter  $^{131}\text{I}$ , which has also been employed in clinical studies (3, 4, 5). Recently,  $^{211}\text{At}$ , the heaviest element in the halogen group, has been the focus of attention for use in radioimmunotherapy (RIT) (6, 7).  $^{211}\text{At}$  is a radionuclide-emitting  $\alpha$ -particles (i.e. high-LET radiation) with a range of 50–80  $\mu\text{m}$  in human tissue. As tumor spread in patients with ovarian cancer is primarily in the form of peritoneal micrometastases,  $^{211}\text{At}$  may be a suitable choice of nuclide for adjuvant intraperitoneal radioimmunotherapy for this form of malignancy.

Despite some promising clinical reports on RIT of ovarian cancer, the clinical application of radiolabeled antibodies has so far been limited, mainly because of the unfavorable in vivo distribution, resulting in low tumor uptake, low target-to-nontarget ratios, and slow clearance rates from normal tissues (8).

Pretargeted radioimmunotherapy (PRIT) in which a tagged antibody is preadministered for tumor targeting, followed by administration of a labeled ligand (effector molecule) as a multistep delivery system, has been proposed to improve the pharmacokinetics of the label in vivo. For this purpose, avidin and biotin are the most commonly used intermediates because of their high-affinity binding characteristics (9, 10). It has been shown, utilizing various protocols based on the biotin–avidin system for PRIT that, due to a more favorable in vivo distribution of the labeled effector molecule, significantly improved tumor uptake and tumor-to-normal-tissue ratios could be achieved (11, 12, 13, 14). In most cases, the

\* To whom correspondence should be addressed. Sture Lindegren, Department of Radiation Physics, Sahlgrenska University Hospital, SE-413 45 Göteborg, Sweden; Fax: +46 31 822 493; E-mail: sture.lindegren@radphys.gu.se.

<sup>1</sup> Department of Radiation Physics, Göteborg University.

<sup>2</sup> Department of Oncology, Göteborg University.

<sup>3</sup> Chalmers University of Technology.

Abbreviations used: BANHS, biotinamidocaproate *N*-hydroxysuccinimide; m-MeATE, *N*-succinimidyl 3-(trimethylstannyl)benzoate; mAb, monoclonal antibody; DMF, dimethylformamide; HPLC, fast protein liquid chromatography; FIGO, International Federation of Gynecology and Obstetrics; HABA, 2-(4'-hydroxyazobenzene)benzoic acid; PBS, phosphate-buffered saline; TNBSA, 2,4,6-trinitrobenzenesulfonic acid; NS[ $^{211}\text{At}$ ]IB, *N*-succinimidyl 3-[ $^{211}\text{At}$ ]iodobenzoate; NS[ $^{211}\text{At}$ ]ATB, *N*-succinimidyl 3-[ $^{211}\text{At}$ ]astatobenzoate.

effector molecule is a conjugate of a biotin and radionuclide, which exhibits rapid *in vivo* clearance and low uptake in normal tissue (15, 16).

In a few investigations, poly-L-lysine has been explored as a multicarrier of biotin and radionuclides for pretargeted radioimmunotherapy (17, 18). The advantages of these polymer conjugates are that increased avidity for avidin and higher specific radioactivity may be achieved. Furthermore, the available molecular weight range of poly-L-lysine may allow increased control of the biodistribution compared with the mono-derivative of biotin.

In this study, the synthesis and distribution of biotinylated, astatinated, and charge-modified poly-L-lysine, as a prospective effector molecule for use in pretargeted intraperitoneal tumor therapy, have been investigated. Three different average sizes of the polymer (7, 21, and 204 kDa) were evaluated with respect to radiolysis after astatine exposure, *in vitro* biotin binding capacity to avidin, and *in vivo* biodistribution and biological half-life in nude mice.

## EXPERIMENTAL PROCEDURES

**Materials.** Poly-L-lysine (7, 21, and 204 kDa), biotinamidocaproate *N*-hydroxysuccinimide ester, *N*-bromosuccinimide (NBS), and *N*-iodosuccinimide (NIS) were purchased from Sigma Chemical Co. Avidin (ImmunoPure Avidin), Avidin beads (ImmunoPure Immobilized Avidin Gel), 2-(4-hydroxyazobenzene)benzoic acid (HABA), and 2,4,6-trinitrobenzenesulfonic acid (TNBSA) were obtained from Pierce Chemical Co. All other nonradioactive commercial chemicals and solvents used were of analytical grade or better.

<sup>211</sup>At was produced by the <sup>209</sup>Bi( $\alpha$ ,2n)<sup>211</sup>At reaction (19) on the Scanditronic MC32-Ni cyclotron at the Cyclotron and PET Unit, Rigshospitalet, Copenhagen, Denmark. Na[<sup>125</sup>I] was obtained from NEN Life Science Products Inc.

**General.** After irradiation, the target was immediately shipped to the Department of Radiation Physics, Göteborg, and the astatine was isolated from the target by dry-distillation, according to the method described previously (19). The radioactivity was measured using an ionization chamber (Capintech CRC-15) utilizing proper settings for <sup>211</sup>At, cross-calibrated for the 70–90 keV <sup>211</sup>Po X-rays in a NaI(Tl) detector (Wizard Wallac  $\gamma$ -well counter, Finland). The biological half-life of the astatinated polymers in athymic mice was determined by measurement of whole-body radioactive content using a NaI(Tl) scintillation detector (Harshaw Chemie B.V.).

High performance liquid chromatography, HPLC, was conducted on a Waters 600/486 system with the Waters Baseline 820 analysis software. Reversed-phase chromatography was performed using a Kromasil C-18 (4.6  $\times$  250 mm) column (EKA-Nobel AB, Sweden), and size-exclusion analysis was carried out on a Superdex-200 FPLC column (Amersham Pharmacia Biotech, Sweden). Preparative gel-permeability chromatography was conducted on disposable Sephadex G-25 PD-10 columns (Amersham Pharmacia Biotech, Sweden). Mass spectral data were obtained by inductively coupled plasma ion source mass spectroscopy (ICP-MS).

**Labeling of *N*-Succinimidyl-3-(trimethylstannyl)-benzoate.** The labeling of *N*-succinimidyl-3-(trimethylstannyl)benzoate, *m*-MeATE, was performed using the procedure previously reported (20). Briefly, to a 1.3-mL reaction vial containing 20–30 MBq <sup>211</sup>At as dry residue

were added 0.5 nmol of *N*-iodosuccinimide and 1.0 nmol of *m*-MeATE in 1% acetic acid/methanol. The *m*-MeATE was reacted with the halogen for 15 min during gentle agitation at room temperature. The reaction was stopped by the addition of 50 nmol of Na<sub>2</sub>S<sub>2</sub>O<sub>5</sub>. Iodination of the precursor was accomplished in essentially the same way as the astatination, except that *N*-bromosuccinimide (NBS) was used as the oxidizing agent.

The labeling efficiency was determined by running an aliquot of the reaction mixture on a reversed-phase C-18 column, isocratically eluted with acetonitrile/2 mM phosphoric acid 60:40 as the mobile phase. The product, *N*-succinimidyl-3-[<sup>211</sup>At]astatoibenzoate (NS[<sup>211</sup>At]AtB) or *N*-succinimidyl-3-[<sup>125</sup>I]iodobenzoate (NS[<sup>125</sup>I]IB), was used immediately, unpurified for conjugation to the biotinylated polymer.

**Modification of Poly-L-lysine, Biotinylation.** Biotinamidocaproate *N*-hydroxysuccinimide ester (BANHS) was dissolved in dimethylformamide (DMF) to a concentration of 5–10 mg/mL. To poly-L-lysine in 0.2 M carbonate buffer pH 8.5 was added a 10–20-fold molar excess of the biotinylation reagent during vigorous agitation, and the reaction was allowed to proceed for 1 h during gentle agitation at room temperature. Further chemistry was conducted on the crude biotinylated product.

**Conjugate Labeling.** Prior to conjugate labeling of the biotinylated polymer, NIS in the labeling mixture was promptly reduced by the addition of 50 nmol of sodium metabisulfite, and the organic fraction of the solvent was evaporated under a gentle stream of nitrogen. To the labeling mixture was added 200  $\mu$ g of the crude biotinylated poly-L-lysine to give a final volume of 50  $\mu$ L, and conjugate labeling was allowed to proceed for 10 min during gentle agitation at room temperature.

**Succinylation.** The biotinylated and labeled polymer was finally reacted with succinic anhydride, in excess over available amines, to convert the remaining unsubstituted amino groups to carboxylic residues. Following conjugate labeling, solid succinic anhydride, in the form of flakes, was added to the reaction mixture. The pH was adjusted with 1 M carbonate buffer, pH 8.5, during the reaction in order to maintain the amino residues unprotonated. After 10 min reaction time, the polymer fraction was isolated by passage over a G-25 PD-10 column (Pharmacia, Sweden).

The final product was analyzed with respect to unbound radioactivity by methanol precipitation according to the method of Reist et al. (21), and the size by gel-filtration chromatography. The biotinylation efficiency was calculated using the HABA dye method (22), and degree of succinylation was determined using the TNBSA spectrophotometric method (23). The average molecular weights of the modified polylysines were estimated to be 13, 38, and 363 kDa.

**Radiolysis of Poly-L-lysine after <sup>211</sup>At Exposure.** To investigate radiolysis effects during labeling, non-modified poly-L-lysine (204 kDa) was exposed to increasing activities, i.e., absorbed doses, of <sup>211</sup>At. Astatine, in chloroform, was added to Eppendorf tubes in a single point series, and the solvent was evaporated. The activities of the dry astatine residues were 0.80, 1.38, 4.85, and 11.7 MBq. A constant amount of poly-L-lysine (50  $\mu$ L, 2 mg/mL) in 0.2 M carbonate buffer, pH 8.5, was then added to each tube.

The astatine was allowed to decay during agitation at 4 °C for 120 h (16.7 half-lives), resulting in absorbed doses to the volume of 0.66, 1.1, 4.0, and 9.5 kGy, as determined using basic dosimetry calculations derived from the following equations:

Number of  $^{211}\text{At}$  decays ( $N$ ):

$$N = \frac{A_0}{\lambda} (1 - e^{-\lambda t}) \text{ for complete decay } N = \frac{A_0}{\lambda}$$

where  $A_0$  is the total radioactivity measured at the start of exposure,  $\lambda$  is the decay constant, and  $t$  is the total exposure time.

Absorbed dose ( $D$ ):

$$D = \frac{E_{\text{abs}}}{m(\text{volume})} \approx \frac{N \bar{E}_\alpha (1.6 \times 10^{-13})}{m(\text{volume})} (\text{Gy})$$

where  $E_{\text{abs}}$  is the absorbed energy in the reaction volume (MeV),  $\bar{E}_\alpha \approx 6.8$  MeV is the mean alpha particle energy (24), and  $m_{\text{volume}}$  is the mass of the solution (kg).

After radiation exposure, the polymer was labeled with  $^{125}\text{I}$  according to the m-MeATE method and charge modified with succinic anhydride as described above. The effect of the radiation, i.e., fragmentation, was analyzed and compared with nonexposed, iodine-labeled, succinylated polymer by size-exclusion chromatography on a Superdex-200 column.

**In Vitro Binding of Modified Polylysine.** The biological function of the biotin moiety on the modified polylysine was examined by binding to avidin beads. Fifty microliters of the avidin bead slurry was transferred to Costar spin-x, 45  $\mu\text{m}$ , filter tubes (Corning Inc., NY). An aliquot of the modified polymer (25 ng) was added, and the volume was adjusted to 150  $\mu\text{L}$  with PBS. The effector molecule was reacted with the beads for 30 min at room temperature during agitation. The beads were then washed three times with PBS, and bound radioactivity was measured in a  $\gamma$ -well counter.

Non-specific binding to avidin was determined by incubating nonbiotinylated, labeled polylysine with the beads, and non-specific binding to the filter tubes was determined by incubation with the modified polymer in tubes not containing avidin beads.

**Animal Experiments.** The tissue distribution and whole-body retention of the 13, 38, and 363 kDa polymers were evaluated in female athymic mice (Balb/C nu/nu), 6–8 weeks of age. Following ip administration of the effector molecule (550–800 kBq in 500  $\mu\text{L}$  of PBS) mice were sacrificed by cervical dislocation at 1, 3, 6, 18, and 24 h postinjection, in groups of four animals per point in time. Whole blood was collected by cardiac puncture immediately after the animals had been killed, and tissues including neck, lungs, stomach, liver, small intestine, large intestine, kidneys, spleen, intraperitoneal fat, and muscle were excised and washed in saline. The tissues were blotted dry and accurately weighed, and the radioactivity was measured in a  $\gamma$ -well counter. All tissue data were corrected for radioactive decay and expressed as the percent of injected radioactivity per gram of organ (%ID/g), except for the neck, where it was expressed as the percent of injected activity (%ID).

The biological half-life of the modified polymers was evaluated by following the whole-body radioactive retention in groups of 5 mice for 24 hours measured with a sodium iodide detector.

## RESULTS

The radioactivity of the irradiated target was in the range of 200 to 300 MBq  $^{211}\text{At}$  upon arrival in Göteborg. Isolation of  $^{211}\text{At}$  was conducted by dry-distillation of the target material, and recovery yields of 70–80% of the

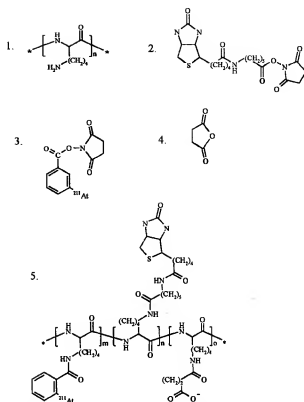


**Figure 1.** Generalized structural formula for (1) poly-L-lysine, (2) *N*-succinimidyl 3-[ $^{211}\text{At}$ ]astatobenzoate (NS[ $^{211}\text{At}$ ]AtB), (3) biotinamidocaproate *N*-hydroxysuccinimide (BANHS), (4) succinic anhydride, (5) modified poly-L-lysine ( $^{211}\text{At}$ -PL<sub>succ</sub>-B).

initial  $^{211}\text{At}$  activity were routinely obtained within a 20-min preparation time. Aliquots of the recovered astatine were immediately used for conjugate labeling via the  $\epsilon$ -amino groups on poly-L-lysine, utilizing the intermediate labeling reagent m-MeATE. Radiohalogenation of the m-MeATE resulted in labeling yields of 85–95% for both the NS[ $^{125}\text{I}$ ]IB and the NS[ $^{211}\text{At}$ ]AtB product. Prior to the conjugate astatine labeling, the poly-L-lysine was biotinylated using biotin amidocaproate *N*-hydroxysuccinimide (BANHS) with an efficiency of 73–85% as determined by the HABA method (22). To avoid workup losses of radioactivity in ensuing conjugations, labeling and charge modification of the biotinylated polylysine were conducted in a single pot without purification of the labeling mixture. After conjugate labeling the poly-L-lysine was subjected to charge modification by complete conversion of the remaining unsubstituted primary amines to carboxylic residues using succinic anhydride. Because of the reaction conditions, the molecular weight of the final product was increased by approximately 80% since the modification by means of the number of substituents per polymer were in the order  $^{211}\text{At} \ll \text{biotin} \ll \text{succinic acid}$ . However, charge modification is essential, as it decreases nonspecific adsorption both in vitro and in vivo. Generalized structural formulas of the reacting species and the final product are shown in Figure 1.

Good conjugation yields of  $70 \pm 5\%$  were achieved in the coupling of NS[ $^{211}\text{At}$ ]AtB to polylysine, corresponding to a mean radiochemical yield of  $63 \pm 4\%$ . Since the labeling procedure involved an excess of the m-MeATE reagent over astatine and the labeling reaction mixture is used in unpurified form for conjugation to the polylysine, the precursor may also be present (i.e. conjugate coupled) in the final product. Organic tin, the Sn(CH<sub>3</sub>)<sub>3</sub>

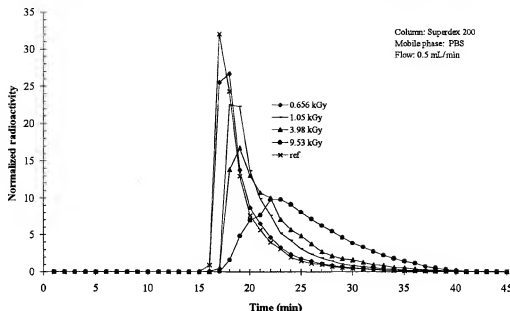


Figure 2. Size-exclusion analysis of poly-L-lysine (204 kDa) exposed to 0.656–9.53 kGy of  $^{211}\text{At}$ . Determination were performed on the  $^{125}\text{I}$ -labeled and succinylated derivative.

Table 1. Tissue Distribution of  $^{211}\text{At}$  Labeled, Biotinylated, and Charge-Modified Poly-L-lysine (386 kDa average molecular weight) in Athymic Mice<sup>a</sup>

tissue	$^{211}\text{At}$ -PL <sub>succ</sub> -B (363 kDa)				
	1 h	3 h	6 h	18 h	24 h
blood	2.02 ± 0.63	2.48 ± 1.03	1.21 ± 0.13	0.49 ± 0.10	0.34 ± 0.17
neck <sup>b</sup>	0.09 ± 0.05	0.59 ± 0.18	1.10 ± 0.32	0.92 ± 0.19	0.85 ± 0.53
lung	2.72 ± 0.50	7.48 ± 1.53	6.46 ± 0.38	2.32 ± 0.47	1.65 ± 0.62
liver	5.45 ± 0.71	3.58 ± 0.73	1.18 ± 0.32	0.36 ± 0.09	0.25 ± 0.10
stomach	3.36 ± 1.19	8.69 ± 1.80	9.90 ± 2.67	4.76 ± 1.30	3.88 ± 1.48
small intestine	0.92 ± 0.19	2.50 ± 0.81	1.98 ± 0.50	0.68 ± 0.23	0.56 ± 0.31
large intestine	1.05 ± 0.48	2.01 ± 0.43	1.81 ± 0.37	0.75 ± 0.20	0.61 ± 0.22
kidney	3.00 ± 0.73	3.75 ± 0.73	2.67 ± 0.30	1.17 ± 0.27	0.86 ± 0.40
spleen	6.23 ± 0.38	9.48 ± 2.57	4.71 ± 0.93	1.02 ± 0.50	0.64 ± 0.37
ip fat	3.07 ± 1.54	2.82 ± 0.89	1.72 ± 0.52	0.51 ± 0.07	0.52 ± 0.22
muscle	1.18 ± 0.52	0.84 ± 0.33	0.53 ± 0.19	0.15 ± 0.03	0.14 ± 0.03

<sup>a</sup> Results are given as mean ± standard deviation of the percent of injected dose per gram tissue (%ID/g); *n* = four animals per time point. <sup>b</sup> Results are expressed as the percent of injected dose (%ID).

group, may be toxic if released in vivo, and the modified polymers were therefore subjected to ICP-MS analysis. Only <10 pg tin, corresponding to <0.0003% of in put amount of the m-MeATE precursor was detected in the spectra. This is probably due to differences in solubility of the precursor and the labeled reagent in the conjugation buffer.

The radiochemical purity of the products was always greater than 95%, as determined by methanol precipitation and by size-exclusion analysis. However, when subjecting the polymer to astatine activities that resulted in a high absorbed dose to the reaction volume, radiolysis effects, i.e., fragmentation, of the polylysine, occurred. As can be seen in Figure 2, the polymer is gradually decomposed when exposed to absorbed doses above 660 Gy, with an initially high degree of large fragments at 1100 Gy and increasingly smaller fragments at higher exposures.

The biotin binding ability of the modified polymer product was examined by means of its reaction with avidin beads using a fast, convenient filter tube assay. Almost complete biotin binding (90–95%) to the beads was achieved with low, nonspecific binding to the tubes. Even when labeling at high absorbed doses, in the range where fragmentation occurred, the degree of biotin bind-

ing was high. Low nonspecific binding to avidin beads was demonstrated by subjecting the beads to nonbiotinylated labeled polylysine.

The tissue distribution and whole-body retention of the 13, 38, and 363 kDa molecular weight effector molecules were evaluated in nude mice following intraperitoneal administration. The tissue distribution data for the polymers from one to 24 h are summarized in Tables 1–3. As can be seen, the distributions of the 38 and 363 kDa effector molecule show uptake in stomach (14.74 and 9.90 %ID/g), lungs (6.74 and 7.48 %ID/g), and spleen (7.64 and 9.48 %ID/g) reaching a maximum at 1–3 h and 3–6 h postinjection. The radioactivity was thereafter slowly cleared from the tissues. The thyroid, known to accumulate astatide (25), shows increasing uptake at 3 to 6 h (0.65 and 1.1 %ID) with a slight decrease over the remaining time of observation. Note that the thyroid was not dissected from the neck, and the results are therefore expressed as the percent of injected dose (%ID). All other organs show low uptake including the blood, which exhibited a maximum uptake of (2.48 %ID/g) at 3 h.

Compared with the larger polymers, the tissue distribution of the 13 kDa effector molecule shows lower uptake in all tissues except for the kidneys, 1 h postin-

**Table 2. Tissue Distribution of  $^{211}\text{At}$ -Labeled, Biotinylated, and Charge-Modified Poly-L-lysine (38 kDa average molecular weight) in Athymic Mice<sup>a</sup>**

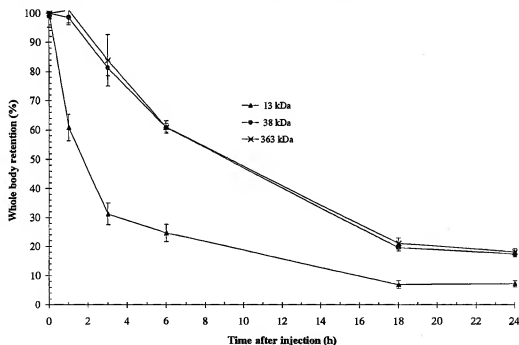
tissue	$^{211}\text{At}$ -PL <sub>enc</sub> -B (38 kDa)				
	1 h	3 h	6 h	18 h	24 h
blood	3.00 ± 0.88	1.37 ± 0.22	0.83 ± 0.12	0.29 ± 0.06	0.31 ± 0.04
neck <sup>b</sup>	0.21 ± 0.04	0.64 ± 0.09	0.62 ± 0.12	0.50 ± 0.20	0.41 ± 0.07
lung	4.48 ± 1.07	6.74 ± 1.39	4.67 ± 0.74	1.65 ± 0.31	1.69 ± 0.23
liver	3.48 ± 0.47	1.47 ± 0.17	0.88 ± 0.15	0.25 ± 0.05	0.27 ± 0.03
stomach	5.93 ± 2.16	14.74 ± 2.45	8.64 ± 3.90	2.48 ± 0.59	3.34 ± 1.22
small intestine	1.93 ± 0.49	1.76 ± 0.14	1.16 ± 0.24	0.53 ± 0.17	0.77 ± 0.14
large intestine	2.00 ± 0.20	1.74 ± 0.20	1.11 ± 0.10	0.40 ± 0.08	0.67 ± 0.12
kidney	14.67 ± 1.58	3.89 ± 0.52	2.32 ± 0.40	0.95 ± 0.31	0.85 ± 0.07
spleen	7.64 ± 1.19	7.37 ± 1.65	4.28 ± 1.28	0.93 ± 0.33	0.64 ± 0.11
ip fat	4.99 ± 0.59	3.20 ± 0.42	1.91 ± 0.30	0.45 ± 0.06	0.61 ± 0.32
muscle	2.22 ± 0.65	0.41 ± 0.08	0.26 ± 0.04	0.11 ± 0.03	0.14 ± 0.01

<sup>a</sup> Results are given as mean ± standard deviation of the percent of injected dose per gram tissue (%ID/g); *n* = four animals per time point. <sup>b</sup> Results are expressed as the percent of injected dose (%ID).

**Table 3. Tissue Distribution of  $^{211}\text{At}$ -Labeled, Biotinylated, and Charge-Modified Poly-L-lysine (13 kDa average molecular weight) in Athymic Mice<sup>a</sup>**

tissue	$^{211}\text{At}$ -PL <sub>enc</sub> -B (13 kDa)				
	1 h <sup>b</sup>	3 h	6 h	18 h	24 h
blood	3.15 ± 0.95	0.81 ± 0.09	0.51 ± 0.10	0.21 ± 0.04	0.15 ± 0.04
neck <sup>c</sup>	0.36 ± 0.37	0.25 ± 0.07	0.28 ± 0.12	0.16 ± 0.06	0.16 ± 0.07
lung	5.36 ± 0.78	4.53 ± 0.38	3.26 ± 0.67	1.23 ± 0.16	0.93 ± 0.19
liver	1.37 ± 0.19	0.76 ± 0.05	0.55 ± 0.11	0.18 ± 0.03	0.16 ± 0.03
stomach	3.71 ± 0.53	5.55 ± 1.55	3.90 ± 1.02	1.68 ± 0.21	1.85 ± 0.39
small intestine	1.37 ± 0.24	1.15 ± 0.31	0.77 ± 0.18	0.35 ± 0.09	0.40 ± 0.32
large intestine	2.05 ± 0.41	1.19 ± 0.09	0.83 ± 0.12	0.32 ± 0.06	0.27 ± 0.03
kidney	18.53 ± 1.26	2.31 ± 0.23	1.36 ± 0.25	0.54 ± 0.11	0.38 ± 0.04
spleen	4.85 ± 1.11	3.58 ± 0.50	2.58 ± 0.59	0.51 ± 0.06	0.62 ± 0.40
ip fat	4.10 ± 2.40	0.88 ± 0.08	0.65 ± 0.15	0.22 ± 0.05	0.19 ± 0.05
muscle	0.72 ± 0.15	0.41 ± 0.04	0.27 ± 0.06	0.17 ± 0.09	0.13 ± 0.06

<sup>a</sup> Results are given as mean ± standard deviation of the percent of injected dose per gram tissue (%ID/g); *n* = four animals per time point. <sup>b</sup> *n* = Three animals. <sup>c</sup> Results are expressed as the percent of injected dose (%ID).

**Figure 3.** The whole-body retention of the 13, 38, and 363 kDa effector molecule in nude mice, following intraperitoneal administration. Results are given as mean ± SEM for four animals per time point.

jection, which may be due to the rapid clearance mainly through the kidneys. The whole-body retention of the astatinated polymers is presented in Figure 3. The results show that whole-body clearance is fast, with

biological half-lives of 2 and 8 h for the low- and high-molecular-weight effector molecules, respectively. This is also reflected in the low tissue content at the later points in time.

## DISCUSSION

Since the development of the hybridoma technology (26) monoclonal antibodies have been used for a variety of applications. Using this method it is possible to produce monoclonal antibodies specific to virtually any molecule of interest. In vivo, one of the challenges has been to develop a novel radioimmunopharmaceutical for tumor imaging and therapy. However, due to the size and passive distribution processes of in vivo administered antibodies, only a small fraction of the injected activity will bind to tumor cells. The remaining non-tumor-bound antibody is evenly distributed and slowly cleared from the body, causing undesirable background and elevated dose to normal tissue. To circumvent the unfavorable distribution of labeled antibodies, pretargeting strategies utilizing the high-affinity binding characteristics between biotin and avidin as intermediates for multistep administration, have been proposed by several investigators (12, 13, 14). Various biotin derivatives have been developed for cross-linking and for labeling with radionuclides to provide effector molecules for pretargeting.

The aim of this study was to produce biotin-polylysine-based effector molecules for use in pretargeted ovarian tumor therapy. Ovarian tumors disseminate primarily to the peritoneal surface as microtumors, and therefore a suitable choice of nuclide may be the  $\alpha$ -emitter  $^{211}\text{At}$ . Following the decay, the  $\alpha$ -particles deposit a considerable amount of energy in a micro-volume, and calculations have shown that only a few astatine decays per cell are required to cause lethal radiation damage (27). Previous experiments by our research group have also demonstrated the high cell-killing effect of astatine in vitro (28) and in vivo (7) when subjecting ovarian cancer cells and microtumors to the astatine-labeled ovarian-tumor-specific monoclonal antibody MOv18. On the basis of the encouraging results of those studies, improvement in the pharmacokinetics to minimize the irradiation of normal tissue was suggested, employing a pretargeting strategy that involves polylysine as an effector carrier. Poly-L-lysine was used since each molecule, depending on the polymerization degree, contains a number of  $\epsilon$ -amino groups that can readily be derivatized with different  $N$ -acylation reagents, thus allowing bifunctional conjugate modification. Apart from this facile chemistry, polylysine can be obtained as mono-amino acid- or copolymers of different molecular weights, which may permit increased control of the biodistribution of the effector molecule.

Applications utilizing polylysine as carriers for nuclides have previously been proposed, such as a polychelating agent for high-specific-activity metal-nuclide binding of antibodies, for use in single-photon emission computed tomography (SPECT) and magnetic resonance tomography, and for therapy (29). The application of polylysine as an effector carrier for use in PRIT has also been reported (17, 18).

In this study, polylysine (7, 21, and 204 kDa) was modified by conjugate coattachment of the biotin reagent (BANHS), the astatine-labeled reagent  $\text{NS}^{211}\text{AtATB}$ , and succinic anhydride in a simple three-step procedure. The product could easily be obtained, with the reaction conditions employed,  $^{211}\text{At}$  activities of 10–20 MBq (100 kBq/ $\mu\text{g}$ ), in a short preparation time, and preliminary experiments suggest that the procedure can be scaled up to higher astatine activities, e.g. for clinical applications. However, it should be noted that the polylysine is sensitive to radiolysis from the astatine decay in the reaction volume. The molecule can be subjected to an

absorbed dose of about 700 Gy without any apparent damage, as determined by size-exclusion chromatography analysis. Increasing the dose above this level resulted in gradual fragmentation with random molecular breakdown at 700–1000 Gy and almost complete decomposition at higher doses (4000–10000 Gy). This is in good agreement with the observations of Larsen and Bruland who studied  $\alpha$ -particle-induced radiolysis effects on antibodies and found that an absorbed dose of 1000 Gy could be tolerated with no or minor effects on the immunoreactivity (30).

The only biologically active part of the effector molecule is the biotin moiety which, surprisingly, was not affected to any high extent by the radiation dose, as determined by binding the effector molecule exposed to a high-absorbed dose to avidin beads. We suggest that the radiation resistance is dependent on the size of the molecule, implying that biotin could withstand much higher absorbed doses than the polymers. In this study, biotin substitution was performed with a 10–20 fold excess of reagent over polymer to ensure uniform attachment on a molar basis, which resulted in approximately 8–16 biotin molecules per polymer. Uniform biotinylation of the low specific radioactive product was confirmed by high binding efficiency to avidin beads. A very high degree of biotin attachment to the polymer is possible, with ultimately complete biotinylation, except for the label, which would give a tremendous increase in avidity for avidin. However, most of the biotin derivatives commercially available have limited aqueous solubility, and this may affect the labeling chemistry and the solubility of the final product (31). Moreover, problems associated with cleavage of the biotin nuclide or carrier bond in vivo due to systemic biotinidase activity when utilizing the commercially available reagents have been reported (32, 33). To circumvent these problems Foulon et al. have developed new biotin compounds for labeling with radiohalogens, e.g.  $^{211}\text{At}$  and iodine isotopes, which are resistant to biotinidase activity (16). Several new biotin derivatives for conjugate labeling have also been explored by Wilbur et al. with regard to solubility and avidin binding characteristics, as well as biotinidase resistance to identify the derivative with the best properties for in vivo applications (31, 34).

The effector molecules studied in the present work were evaluated regarding the tissue distribution following ip injection in nude mice during 24 h postadministration. Significant differences in tissue uptake between the 13 kDa and the larger polymers were seen, which are related to different clearance routes. All molecules enter the circulation from the peritoneal cavity, and their sizes predetermine that the 13 kDa polymer is cleared mainly via the kidneys, the 38 kDa polymer through liver and kidneys and the 363 kDa polymer is sequestered primarily by the liver. Compared with the 13 kDa polymer, a higher uptake of the 38 and 363 kDa polymers was observed in the thyroid gland, stomach, lungs, and spleen, which may reflect the release of astatine/astatide after degradation in the liver. This might be a limiting factor for prospective clinical use, but the astatine/astatide uptake may be decreased by the use of blocking agents, as proposed by Larsen et al., thus limiting the absorbed dose to these tissues (33). The normal tissue at greatest risk is the bone marrow but, because the residence time of the three effector molecules in the circulation following intraperitoneal administration is short, and provided that there are no active uptake mechanisms, the dose to the bone marrow is likely to be limited. Compared with astatinated IgG antibodies, the

radioactive content in the blood is of the order of at least 10 times less for the large polymers and a factor of 20 less for the small polymer (36). Therefore, increased absorbed dose to tumor tissue might be achieved in PRIT utilizing polylysine as the effector carrier as higher activities of the astatinated effector molecule can be administered without increasing the radiotoxic effects on normal tissues, i.e., the bone marrow.

In summary, the preparation, in vitro avidin binding characteristics and biodistribution of biotinylated, astatinated, and charged modified poly-L-lysine of different molecular weights for prospective use as an effector molecule in pretargeted intraperitoneal tumor therapy were investigated. Following ip administration, the three modified polymers studied showed low whole-body retention with clearance routes determined by the size of the molecules. Somewhat higher uptakes of radioactivity in normal tissues were observed for the high-molecular-weight effector molecules, suggesting that for clinical applications a low-molecular-weight poly-L-lysine should be used for derivatization. However, application using a complete pretargeted intraperitoneal tumor model may contribute to lowering normal tissue uptake due to reduced escape of the effector molecule from the peritoneal cavity by binding to its mAb-avidin conjugate at the tumor target. Therefore, further investigations will be focused on more homogeneous preparations of both high- and low-molecular-weight poly-L-lysine for the modification, new biotinidase-resistant water-soluble derivatives and scale-up of the labeling procedure to meet the requirements for patient studies.

#### ACKNOWLEDGMENT

We would like to thank Elisabet Warnhammar (Department Oncology, Göteborg University, Sweden) and Jörgen Elgquist (Department of Radiation Physics, Göteborg University, Sweden) for excellent technical assistance with the animal study. Thanks are due to Dr. Stig Palm (Department of Radiation Physics, Göteborg University, Sweden) for help with the dosimetry evaluation and Arvid Odegaard-Jensen (Department of Nuclear Chemistry, Chalmers University of Technology) for help with mass spectral analysis. This work was supported by grants from the Swedish Cancer Foundation (Grant 3548) and the King Gustaf V Jubilee Clinic Cancer Research Foundation in Göteborg, Sweden.

#### LITERATURE CITED

- (1) Senekowisch, R.; Schmid, P.; Möllenstädt, S.; Kriegel, H.; and Pabst, H. W. (1989) Experimental model for radioimmunotherapy of human ovarian carcinoma with I-131-labeled monoclonal antibody OC125. *Strahlenther onkol*, 165, 564–566.
- (2) Møllthoff, C. F. M., Pinedo, H. M., Schlüper, H. M. M., and Boven, E. (1992) a) Influence of dose and schedule on therapeutic efficacy of <sup>131</sup>I-labeled monoclonal antibody 13H2 in a human ovarian cancer xenograft model. *Int. J. Cancer* 51, 108–115.
- (3) Epenetos, A. A., Munro, A. J., Stewart, S., Rampling, R., Lambert, H. E., McKenzie, C. G., Soutter, P., Rahemtulla, A., Hooker, G., Sivalapenka, G. B., Snook, D., Courtney-Luck, N., Dhokia, B., Krausz, T., Taylor-Papadimitriou, J., Durbin, H., and Bodmer, F. (1987) Antitumor-guided irradiation of advanced ovarian cancer with intraperitoneally administered radiolabeled monoclonal antibodies. *J. Clin. Oncol.* 5, 1890–1899.
- (4) Møllthoff, C. F., Buist, R. M., Kenemans, P., Pinedo, H. M., and Boven, E. (1992) Experimental and Clinical Analysis of

the Characteristics of a Chimeric Monoclonal Antibody, MOv18, Reactive With an Ovarian Cancer-Associated Antigen. *J. Nucl. Med.* 33, 2000–2005.

- (5) Crippa, F., Bolis, G., Seregni, E., Gavoni, N., Scarfone, G., Ferraris, C., Buraggi, G. L., and Bombardieri, E. (1995) Single-dose intraperitoneal radioimmunotherapy with the murine monoclonal antibody I-131 MOv18: Clinical results in patients with minimal residual disease of ovarian cancer. *Eur. J. Cancer* 31A, 686–690.
- (6) Zalutsky, M. R., McLendon, R. E., Garg, P. K., Archer, G. E., Schuster, J. M., and Bigner, D. D. (1994) Radioimmunotherapy of neoplastic meningitis in rats using an  $\alpha$ -particle-emitting immunconjugate. *Cancer Res.* 54, 4719–4725.
- (7) Andersson, H., Lindgren, S., Bäck, T., Jacobsson, L., Leser, C., and Horvath, G. (2000) Radioimmunotherapy of nude mice with intraperitoneally growing ovarian cancer xenograft utilizing <sup>111</sup>Ac-labeled monoclonal antibody MOv18. *Anticancer Res.* 20, 459–462.
- (8) Halpern, E., and Dillman, R. O. (1987) Problems associated with radioimmunodetection and possibilities for future solutions. *J. Biol. Response Mod.* 6, 235–262.
- (9) Stoldt, H. S., Afrab, F., Chinol, M., Paganelli, G., Luca, F., Testori, A., and Geraghty, J. G. (1997) Pretargeting Strategies for Radio-Immunoguided Tumour Localisation And Therapy. *Eur. J. Cancer* 33, 186–192.
- (10) Hnatowich, D. J., Virzi, F., and Ruskowski, M. (1987) Investigation of Avidin and Biotin for Imaging Applications. *J. Nucl. Med.* 28, 1294–1302.
- (11) Chinol, M., Casallini, P., Maggiolo, M., Canevari, S., Omodeo, E. S., Calicetti, P., Veronesi, F. M., Cremonesi, M., Chiolerio, F., Nardone, E., Siccardi, A. G., and Paganelli, G. (1998) Biochemical modifications of avidin improve pharmacokinetics and biodistribution, and reduce immunogenicity. *Br. J. Cancer* 78, 189–197.
- (12) Zhang, M., Yao, Z., Sakahara, H., Saga, T., Nakamoto, Y., Sato, N., Zhao, S., Nakada, H., Yamashina, I., and Kunoshi, J. (1998) Effect of administration route and dose of streptavidin or biotin on the tumor uptake of radioactivity in intraperitoneal tumor with multistep targeting. *Nucl. Med. Biol.* 25, 101–105.
- (13) Bretz, H. B., Weiden, P. L., Beaumier, P. L., Axworthy, D. B., Seiler, S. Su, F.-M., Graves, S., Bryan, K., and Reno, J. M. (1999) Clinical optimization of pretargeted radioimmunotherapy with antibody-streptavidin conjugated and <sup>90</sup>Y-DOTA-biotin. *J. Nucl. Med.* 41, 131–140.
- (14) Paganelli, G., Belloni, C., Magnani, P., Zito, F., Pasini, A., Sassi, I., Meroni, M., Mariani, M., Vignali, M., Siccardi, A. G., and Fazio, F. (1992) Two-Step Tumour Targeting in Ovarian Cancer Patients Using Biotinylated Monoclonal Antibodies and Radioactive Streptavidin. *Eur. J. Nucl. Med.* 19, 332–339.
- (15) Wilbur, D. S., Hamlin, D. K., Pathare, P. M., and Weerawarna, S. A. (1997) Biotin reagents for antibody pretargeting: synthesis radiolodination, and in vitro evaluation of biotinidase resistant biotin derivatives. *Bioconjugate Chem.* 8, 572–584.
- (16) Foulon, C. F., Alston, K. L., and Zalutsky, M. R. (1998) Astatine-211-labeled biotin conjugates resistant to biotinidase for use in pretargeted radioimmunotherapy. *Nucl. Med. Biol.* 25, 81–88.
- (17) Torchlun, V. P. (1999) Biotin-conjugated polychelating agent. *Bioconjugate Chem.* 10, 146–149.
- (18) del Rosario, R. B., and Wahl, R. L. (1992) Biotinylated iodopolylysine for pretargeted radiation delivery. *J. Nucl. Med.* 33, 1147–1151.
- (19) Lindgren, S., Bäck, T., and Jensen, H. J. (2001) Dry-distillation of astatine-211 from irradiated bismuth targets: a time-saving procedure with high recovery yields. *Appl. Radiat. Isot.* 55, 157–160.
- (20) Lindgren, S., Andersson, H., Bäck, T., Jacobsson, L., Karlsson, B., and Skarnemark, G. (2001) High-efficiency astatination of antibodies using N-iodosuccinimide as the oxidising agent in labeling of N-succinimidyl 3-(trimethylstannyl)benzoate. *Nucl. Med. Biol.* 28, 33–39.
- (21) Reist, C. J., Foulon, C. F., Alston, K., Bigner, D. D., and Zalutsky, M. R. (1999) Astatine-211 labelling of internalizing

- anti-EGFRvIII monoclonal antibody using N-succinimidyl 5-[<sup>211</sup>At]astato-3-pyridinecarboxylate. *Nucl. Med. Biol.* **26**, 405–411.
- (22) Green N. M. (1965) A spectrophotometric assay for avidin and biotin based on binding of dyes by avidin. *Biochem. J.* **94**, 23c–24c.
- (23) Cayot P., and Tainturier G. (1996) The quantification of protein amino groups by the trinitrobenzenesulfonic acid method: A reexamination. *Anal. Biochem.* **249**, 184–200.
- (24) Weber D., Eckerman K., Dillman T., and Ryman J. (1989) *MIRD: Radionuclide data and decay schemes*, The Society of Nuclear Medicine, New York.
- (25) Hamilton, J. G., Asling, C. W., Garrison, W. M., and Scott, K. G. (1953) The accumulation, metabolism and biological effects of astatine in rats and monkeys. *Univ. Calif. Publ. Pharmacol.* **2**, 283–343.
- (26) Köhler, G., and Milstein, C. (1975) Continuous cultures of fused cells secreting antibody of predefined specificity. *Nature* **256**, 495–497.
- (27) Ritter, R. H., Cleaver, J. E., and Tobias, C. A. (1977) Radiation induce a large proportion of nonrejoining DNA breaks. *Nature* **266**, 635–655.
- (28) Palm, S., Bäck, T., Claesson, I., Delle, U., Hultborn, R., Jacobsson, L., Köpf, I., and Lindegren, S. (2000) In vitro effects of free <sup>211</sup>At, <sup>211</sup>At–Albumin, and <sup>211</sup>At-monoclonal antibody compared to external photon irradiation for two human cancer cell lines. *Anticancer Res.* **20**, 1005–1012.
- (29) Torchilin, V. P., Kilbanov, A. L., Nossiff, N. D., Stinkin, M. A., Strauss, H. W., Haber, E., Smirnov, V. N., and Khaw, B. A. (1987) Monoclonal Antibody Modification With Chelate-Linked High-Molecular-Weight Polymers: Major Increase in Polyvalent Cation Binding Without Loss of Antigen Binding. *Hybridoma* **6**, 229–240.
- (30) Larsen, R. H., and Bruland, Ø. S. (1995) Radiolysis of radioimmunoconjugates. Reduction in antigen-binding ability by  $\alpha$ -particle radiation. *J. Labeled Compd. Radiopharm.* **34**, 1009–1018.
- (31) Wilbur, D. S., Pathare, P. M., Hamlin, D. K., Stayton, P. S., To, R., Klumb, L. A., Buhler, K. R., and Vesella, R. L. (1999) Development of new biotin/streptavidin reagents for pretargeting. *Biomol. Eng.* **16**, 113–118.
- (32) Hymes, J., and Wolf, B. (1996) Biotinidase and its role in biotin metabolism. *Clin. Acta* **255**, 1–11.
- (33) Foulon, C. F., Shoultz, B. W., and Zalutsky, M. R. (1997) Preparation and Biological Evaluation of Astatine-211 Labeled Biotin Conjugate: Biotinyl-3-[<sup>211</sup>At]astatoanilide. *Nucl. Med. Biol.* **24**, 135–143.
- (34) Wilbur, D. S., Chyan, M.-K., Pathare, p. M., Hamlin, M. B., Brownfelter, M. B., and Kegly, B. B. (2000) Biotin reagents for antibody pretargeting. 4. Selection of biotin conjugates for in vivo application based on their dissociation rate from avidin and streptavidin. *Bioconjugate Chem.* **11**, 569–583.
- (35) Larsen, R. H., Slade, S., and Zalutsky, M. R. (1998) Blocking [<sup>211</sup>At]astatide accumulation in normal tissues: Preliminary evaluation of seven potential compounds. *Nucl. Med. Biol.* **25**, 351–357.
- (36) Garg, P. K., Harrison, C. L., and Zalutsky, M. R. (1990) Comparative tissue distribution of the  $\alpha$ -emitter <sup>211</sup>At and <sup>125</sup>I as labels of a monoclonal antibody and F(ab')<sub>2</sub> fragment. *Cancer Res.* **50**, 3514–3520.

BC010054D

## TERMINAL MODIFICATIONS INHIBIT PROTEOLYTIC DEGRADATION OF AN IMMUNOGENIC MART-1<sub>27–35</sub> PEPTIDE: IMPLICATIONS FOR PEPTIDE VACCINES

Laurence H. BRINCKERHOFF<sup>1</sup>, Vladimir V. KALASINIKOV<sup>2</sup>, Lee W. THOMPSON<sup>1</sup>, Galina V. YAMSHCHIKOVA<sup>1</sup>, Richard A. PIERCE<sup>2,3</sup>, Holly S. GALAVOTTI<sup>1</sup>, Victor H. ENGELHARD<sup>2,3</sup> and Craig L. SLINGLUFF, JR.<sup>1\*</sup>

<sup>1</sup>Department of Surgery, University of Virginia, Health Sciences Center, Charlottesville, VA

<sup>2</sup>Department of Microbiology, University of Virginia, Health Sciences Center, Charlottesville, VA

<sup>3</sup>Beirne B. Carter Center for Immunology Research, University of Virginia, Health Sciences Center, Charlottesville, VA

**Peptide epitopes for tumor-reactive cytotoxic T-lymphocytes (CTL) have been identified on human cancers and are being used in tumor vaccine trials. However, the pharmacokinetics and pharmacodynamics of such peptides have been inadequately studied. It is predicted that immunogenic tumor peptides would have short half-lives *in vivo*. The goal of the present work was to evaluate the stability of the immunogenic peptide MART-1<sub>27–35</sub> in fresh normal human plasma (NHP) and to identify modifications that convey protection against enzymatic destruction without loss of immunogenicity. We evaluated the stability of the MART-1<sub>27–35</sub> peptide (AAGIGILTV) and modified forms of that peptide for stability and immune recognition in an *in vitro* model. The peptides were incubated in plasma for varied time intervals and evaluated for their ability to reconstitute the epitope for MART-1<sub>27–35</sub>-reactive CTL. Loss of CTL reactivity signaled loss of immunoreactive peptide. When 1  $\mu$ M MART-1<sub>27–35</sub> peptide was incubated in plasma prior to pulsing on target cells, CTL reactivity was lost within 3 hr, and the calculated half-life of this peptide was 22 sec. This degradation was mediated by peptidases. The stability of MART-1<sub>27–35</sub> was markedly prolonged by C-terminal amidation and/or N-terminal acetylation (peptide capping), or by polyethylene-glycol modification (PEGylation) of the C-terminus. These modified peptides were recognized by CTL. The MART-1<sub>27–35</sub> peptide is very unstable in plasma. It is probable that it and other immunogenic peptides will be similarly unstable *in vivo*. Immunogenicity of these peptides might be enhanced by creating modifications that enhance stability. *Int. J. Cancer* 83: 326–334, 1999.**

© 1999 Wiley-Liss, Inc.

In the United States in 1997, there were approximately 7,500 deaths due to metastatic melanoma. The impact of conventional systemic therapy for metastatic melanoma is minimal, with best response rates for conventional therapy nearing only 30% and cure rates well below 10%. The identification of MHC-associated peptides that function as epitopes for melanoma-reactive CTL has led to hope that peptide-based vaccines would be effective therapy for melanoma (Cox *et al.*, 1994). Although there have been indications of some protective immune responses against melanoma induced by peptide-based vaccinations, the overall anti-tumor responses have not been optimized (Jaeger *et al.*, 1996). The presentation of immunogenic peptide by professional antigen presenting cells (APC), such as dendritic cells (DCs), is thought to be crucial for the induction of an anti-tumor immune response by peptides *in vivo* (Nair *et al.*, 1997). Thus, for a peptide-based vaccination to be effective, it is reasoned that 4 sequential events must take place after the peptides are injected into the skin or s.c. tissue of a melanoma patient. Firstly, professional APCs must migrate to the vaccination site. Secondly, the peptide must bind to a Class I MHC molecule on the APC; thirdly, this peptide-MHC complex on the APC must induce a CD8<sup>+</sup> T-cell response; and fourthly, this T-cell response must confer a clinically significant anti-tumor effect. Failure in one of these events may compromise effective immunization. However, the intradermal events have not been well studied, and there has been little direct evaluation of the fate of immunizing peptides once injected into the skin and s.c. tissues of melanoma patients.

Therefore, it appears critical for the success of peptide-based melanoma vaccines to understand the effects of the environment into which the immunogenic peptides are being injected. The skin is an enzymatically active organ, and specific endo- and exopeptidases have been isolated from the dermis and epidermis (Boderke *et al.*, 1997). Therefore, in vaccinations that utilize subcutaneous injections, peptides may be degraded by skin peptidases prior to effecting a significant immunologic response. The stability of immunogenic peptides may well be critical to the clinical effectiveness of melanoma peptide vaccines administered intradermally, however, the stability of these peptides has been inadequately studied to date.

When biologically active peptides are used clinically in their natural form, their biologic effects are often rapidly lost *in vivo* due to rapid elimination of the active form of the peptide (Lee, 1988). Naturally occurring peptides such as somatostatin and vasopressin have short half-lives *in vivo*, so their use as therapeutic reagents has required synthesis of modified forms with longer half-lives, such as octreotide and dDAVP (Lee, 1988). Use of immunogenic peptides in their native form is rational in the attempt to stimulate a specific CD8<sup>+</sup> T-cell response against peptides naturally presented on the surface of melanoma cells in association with the Class-I MHC molecules. However, if these peptides are degraded before loading onto APCs, then they are not likely to function well as immunogens. Furthermore, there is increasing concern that the dose of peptide, whether free or pulsed onto DCs, may be critically important for the induction of high-affinity tumor-specific T-cells. If peptides used in tumor vaccines are rapidly degraded in the dermis and s.c. tissue, then the effective peptide dose may not be predictable from the administered dose.

Therefore, the stability of the immunogenic peptides used for vaccination in the intradermal environment may well impact the immunogenic potential of a peptide-based vaccine. *In vitro*, serum-based assays have permitted estimation of the half-lives of some short peptides to be between 5 min and 2 hr (Powell *et al.*, 1992). The time required for DCs to initiate a migratory response toward an inflammatory signal has been estimated to be 1.5–2 hr, and maximal numbers of DCs are reached after about 24 hr to several days (Weiss *et al.*, 1997). Thus, it is critical to define the stability of melanoma peptides being used in melanoma vaccines. If their half-lives *in vivo* are substantially shorter than the time required for dendritic cells to migrate to the immunization site, then

Supported in part by NIH grants CA57653 (to CLS), by the Cancer Center (NIH P30CA44579) at the University of Virginia (Cancer Center Core Grant for Biomolecular Core Facility), by the Cancer Research Institute's Elaine R. Shepard Clinical Investigator Award in Cancer Immunology (to CLS), Argemex (to CLS), and by the USPHS R37 AI20963 (to VHE).

\*Correspondence to: Department of Surgery, University of Virginia, Health Sciences Center, P.O. Box 10005, Charlottesville, VA 22906, USA. Fax: +1-804-243-6844. E-mail: cls8h@virginia.edu

Received 14 October 1998; Revised 26 May 1999

vaccines using them in unmodified form may not stimulate effective immune responses.

If peptides that function as epitopes for melanoma-reactive CTL are rapidly degraded *in vivo*, it may be useful to increase their stability with conservative modifications. A risk with any modification of these peptides is that it may decrease affinity for the MHC or for the T-cell receptor (TCR). Modifications of individual amino acids have been reported to have marked effects on both affinities (Parkhurst *et al.*, 1996). There is evidence that the proteolytic degradation of some short peptides may be markedly inhibited by a number of modifications of the N- and C-terminal residues (Powell *et al.*, 1993). Presumably, this is effective at blocking exopeptidase activity. While this approach has been effective for non-MHC-associated peptides with biologic activity (Marbach *et al.*, 1993) and even with peptides that bind to Class II MHC molecules (Maillet *et al.*, 1995), the effects of such modifications have not been investigated for peptides associated with Class I MHC molecules. The stringency of the Class I MHC-peptide interactions is so high that small modifications may have marked effects on biologic activity. If a modified form of a Class I MHC-associated melanoma peptide is more stable than the naturally occurring peptide and is still able to stimulate a specific T-cell response, then its use in vaccination may lead to increased clinical effectiveness.

It would be desirable to be able to measure the peptide stability and T-cell responses *in vivo* directly after injection into the s.c. tissue of melanoma patients, however, accurate technical methods for such analysis do not exist. It is generally accepted that *in vitro* models utilizing different biologic media, including human serum or plasma, and a method for detecting intact peptide are useful for the identification of stable, biologically active peptide homologues for use in the clinical setting (Maillet *et al.*, 1995; Powell *et al.*, 1992). In other systems, increased peptide stability in serum-based *in vitro* models correlates well with increased peptide stability in the *in vivo* setting (Powell *et al.*, 1993). Although the entire array of enzymes located in human serum and skin have not been fully characterized, the rationale for using fresh human serum to model the biologically active environment of the skin is that both are rich in endo- and exopeptidases (Lee, 1988). Therefore, if a peptide is stable in human plasma, there is a reasonable basis for believing that it may similarly be protected from degradation by skin peptidases.

We have developed an *in vitro* assay method that utilizes fresh, non-heat-inactivated NHP as a biologically active medium and have used melanoma-reactive CTL for detection of intact peptide. Thus, our assay system includes a measure that depends both on peptide binding to the Class I MHC and on T-cell receptor recognition. We have focused on the MART-1<sub>27-35</sub> peptide (AAGIG-LTV) as a melanoma peptide commonly used in vaccinations (Kawakami *et al.*, 1994). We hypothesized that this peptide is unstable in human plasma and that modifications may protect it from degradation without significantly decreasing immune recognition.

## MATERIAL AND METHODS

### Tumors

The melanomas VMM5 and DM6 are cultured cell lines that express the HLA-A\*0201 molecule. T2 is an HLA-A\*0201<sup>+</sup> human T-cell/B-cell fusion with a TAP-dependent, antigen-processing defect provided by Dr. P. Cresswell (Henderson *et al.*, 1992). Each is maintained with RPMI 1640 media (GIBCO, Grand Island, NY) supplemented with 10% fetal calf serum (FCS, Sigma, St. Louis, MO), glutamine and antibiotics (RPMI).

### CTL lines

The VMM5 CTL line is a well-characterized line reactive to multiple shared melanoma peptide epitopes associated with HLA-A\*0201<sup>+</sup>, including the MART-1<sub>27-35</sub> peptide and the gp100<sub>280-288</sub> (YLEPGPVTA) peptide (Cox *et al.*, 1994, and data not shown). These CTL were developed from lymphocytes of the melanoma patient VMM5, using described methods (Cox *et al.*, 1994). Briefly, the CTL lines were developed by *in vitro* stimulations first with autologous irradiated tumor every 10–14 days. After 30 days of *in vitro* culture, irradiated allogeneic DM6 melanoma cells expressing shared antigens were used for subsequent restimulations to select for reactivity against shared HLA-A\*0201-associated peptide epitopes. CTL lines were maintained in RPMI supplemented with 20 Cetus units/ml IL-2.

The VMM18 CTL line is an HLA-A\*0301-restricted CTL line generated from lymphocytes of another patient. This line was generated by stimulation, *in vitro*, with autologous tumor cells, and it recognizes several HLA-A\*0301-restricted peptides, including gp100<sub>17-25</sub> (ALLAVGATK) (Skipper *et al.*, 1996).

### Preparation of synthetic peptides

The MART-1<sub>27-35</sub> peptide, the gp100 peptides YLEPGPVTA (residues 280–288) and ALLAVGATK (residues 17–25), and the influenza M1 peptide were synthesized by standard Fmoc chemistry using a Gilson (Middleton, WI) model AMS422 peptide synthesizer, and purified to more than 98% by reversed-phase HPLC on a Vydac (Hesperia, CA) C-4 column with 0.05% trifluoroacetic acid: water and an acetonitrile gradient. The modified peptides (Table I) were synthesized using the Symphony/Multiplex multivessel automated peptide synthesizer (Rainin, Woburn, MA) operating in the standard Fmoc mode of peptide synthesis. After cleavage from resin, all peptides were purified by reversed-phase HPLC. The molecular masses of these purified peptides were determined using matrix-assisted laser desorption/ionization time-of-flight mass spectrometer using  $\alpha$ -cyano-4-hydroxycinnamic acid as a matrix. All were more than 95% pure and had correct molecular masses.

Synthesis of 2 of these modified peptides required specific additional methods. The asparagine N-linked glycopeptide, Glyco-MART-1, was synthesized using three-dimensional orthogonal solid-phase strategy (Fmoc/Abu/allyl). For post-synthesis modifica-

TABLE I - COMPARISON OF THE MODIFIED MART-1 PEPTIDES TO THE NATIVE MART-1<sub>27-35</sub> PEPTIDE

Peptide name	Peptide sequence	Modifications		M.W.	IC <sub>50</sub> ( $\mu$ M)	Max lysis (% dose)	TSC <sub>50</sub> (relative dose)
		N-Terminus	C-Terminus				
MART-1	Ala-Ala-Gly-Ile-Gly-Ile-Leu-Thr-Val	—	—	813.5	0.5	77%	5 nM (1X)
PEG-MART-1	Ala-Ala-Gly-Ile-Gly-Ile-Leu-Thr-Val-NH-PEG <sub>3000</sub>	—	NH-PEG <sub>3000</sub>	~5800	>35	78%	2,500 nM (500X)
D-MART-1	D-Ala-Ala-Gly-Ile-Gly-Ile-Leu-Thr-D-Val	D-Ala	D-Val	813.5	NT	75%	100 nM (20X)
Glyco-MART-1	Asn(B-D-GlcNHAc)-Ala-Ala-Gly-Ile-Gly-Ile-Leu-Thr-Val	Asn(B-D-GlcNHAc)	—	1130.7	NT	75%	5 nM (1X)
Cap-MART-1	Ac-Ala-Ala-Gly-Ile-Gly-Ile-Leu-Thr-Val-amide	Acetyl	Amide	854.5	65	69%	25 nM (5X)
N-MART-1	Ac-Ala-Ala-Gly-Ile-Gly-Ile-Leu-Thr-Val	—	—	855.5	35	75%	2.5 nM (0.5X)
C-MART-1	Ala-Ala-Gly-Ile-Gly-Ile-Leu-Thr-Val-amide	—	Amide	812.5	7	82%	0.25 nM (0.05X)

<sup>1</sup>IC<sub>50</sub> is the concentration required for 50% inhibition of binding of a standard peptide to HLA-A\*0201 molecules. TSC<sub>50</sub> is the sensitizing concentration of peptide required to induce half maximal lysis in a reconstitution assay. The relative dose, compared with unmodified MART-1 peptide, is shown in parentheses. Data represent a summary of 4 experiments. NT, not tested.

tion, Fmoc-Asp (Oallyl) residue was incorporated. After selective catalytic allyl removal, the resulting  $\beta$ -carboxyl of Asp was coupled with 2-acetamido-1-amino-1,2-dideoxy- $\beta$ -D-glucopyranose to obtain a Fmoc-protected resin-bound glycopeptide (Kates *et al.*, 1994). This peptide contains the Asp-Ala sequence prone to form an aspartimide derivative as a side product. To protect the Asp-Ala amide bond and to suppress undesired reactions during peptide synthesis, modification of the N-(2-acetoxy-4-methoxybenzyl) (AcHmb) group has been proposed (Offer *et al.*, 1996). We tried both approaches, with and without AcHmb-protection, in practical glycopeptide synthesis. The N-AcHmb protection of the Ala residue was on-resin, incorporated using published procedures (Ede *et al.*, 1996). Both approaches gave the desired glycopeptide Glyco-MART-1 with good yield, but with AcHmb-protection, the crude product was better quality and did not contain the aspartimide by-product.

The PEGylated peptide, PEG-MART-1, was synthesized with a 2-step procedure. In the first step, an Fmoc peptide was synthesized by standard solid-phase peptide methodology and then cleaved from resin with Fmoc protection. In the second step, the resulting peptide block with free C-end carboxyl group was reacted in solution with methoxypolyoxyethylene amine (prepared from methoxypolyethylene glycol with a m.w. of 5000, Sigma). The Fmoc protection was cleaved with excess of piperidine, and the resulting product was purified by gel filtration followed by preparative reversed-phase HPLC at elevated temperature (50°C).

#### Plasma

Whole blood was drawn into heparinized tubes from healthy human volunteers and layered onto a Ficoll separation gradient. The plasma was collected from the top layer after centrifugation. The plasma was used fresh within 24 hr of isolation, without heat inactivation or cryopreservation.

For use in one experiment, acid-treated plasma was created by the addition of 12 M HCl to NHP until a pH of 1–1.5 was obtained. The plasma remained at this pH for 1 hr after which 12 M NaOH was added to neutralize the plasma.

#### Assay protocols to evaluate stability of tumor peptides in human plasma

To determine the stability of the MART-1<sub>27–35</sub> peptide in NHP over time, we developed a protocol in which the MART-1<sub>27–35</sub> peptide was incubated for varied time intervals in human plasma or control media, then pulsed onto target cells. To determine if the peptide persisted over time in these media, recognition by MART-1<sub>27–35</sub>-reactive CTL was evaluated by a chromium-release assay.

Concentrated peptide solutions were prepared in water and stored at 4°C, where they are stable. Fresh non-heat inactivated plasma was obtained from a normal donor by Ficoll separation. One ml of this NHP was then aliquoted into a series of 1 ml Eppendorf tubes. Control media, Hank's balanced salt solution (HBSS, Gibco) or RPMI 1640 without additives, was then aliquoted into an equal series of Eppendorf tubes. Each pair of Eppendorf tubes (NHP and control media) was placed at 4°C. At selected time points, the test peptides were added to a pair of tubes, then incubated at 37°C for a specific time interval, *e.g.*, 24 hr, 3 hr, 1 hr, 50 min, 30 min, 10 min and 0 min. The test peptides were added from concentrated stock solutions to create final concentrations of either 1  $\mu$ M or 10  $\mu$ M. To minimize evaporative losses, the Eppendorf tubes remained capped throughout the incubations. The volume of peptide introduced to the 1 ml of test solution was less than 40  $\mu$ l.

Meanwhile, T2 cells were labeled with 200  $\mu$ l of  $^{51}\text{Cr}$  for 1.5–2 hr in a 37°C water bath and were diluted in RPMI. The T2 cells were then aliquoted into a 96-well V-bottom plate with 1,000 cells per well. After incubation in serum or control media as outlined above, the peptide solutions were then removed from 37°C, and triplicate wells of  $^{51}\text{Cr}$ -labeled T2 cells were then incubated 1 hr with 50  $\mu$ l of peptide from each Eppendorf tube. VMM5 CTL

reactive to the MART-1<sub>27–35</sub> peptide were then added at an effector to target ratio of 10:1. After 4 hr of incubation, the chromium released into the supernatants was collected and counted. Percent-specific lysis was calculated. Thus, this assay assessed CTL reactivity as a measure of intact peptide presented on HLA-A\*0201 molecules of the T2 target cells. Similar assays for stability of the 2 gp100 peptides were performed, using VMM18 CTL and EBV-transformed VMM18 B cell line for the A3 restricted peptide ALLAVGATK (gp100<sub>17–25</sub>).

#### Evaluation of the affinity of synthetic peptides for the HLA-A\*0201 molecule

We used a described equilibrium binding assay that measures the ability of test peptides to compete with a radiolabeled standard peptide for binding to a Class I MHC molecule (Chen *et al.*, 1994). Briefly, the standard peptide FLPSDYFSPV, an HLA-A\*0201 restricted analogue of hepatitis B virus core protein (HBc), residues 18–27, was iodinated and incubated with purified Class I MHC molecules (10–50 nM) at room temperature with various doses of the test peptides, together with 5–10 nM of the labeled peptide and 1  $\mu$ M human  $\beta$ 2-microglobulin (Calbiochem, La Jolla, CA) in PBS, pH 7.0, 0.05% NP-40, 1 mM PMSF, 1.3 mM l,10-phenanthroline, 73  $\mu$ M pepstatin A, 8 mM EDTA, and 200  $\mu$ M TLCK. After 48 hr, Class I MHC-peptide complexes were separated from free peptide by gel filtration on either a TSK2000 (7.8 mm  $\times$  15 cm) column eluted with PBS pH 6.5, 0.5% NP-40, 0.1% Na<sub>2</sub>S<sub>2</sub>O<sub>3</sub> or a Sephadex G-50 column (22 ml bed volume) eluted with the same buffer at pH 7.0. Class I MHC-bound and -free radioactivity was measured, and the doses of test peptides yielding 50% inhibition of the binding of the labeled peptide (IC<sub>50</sub>) were calculated.

#### Stimulation of CTL *in vitro* with synthetic peptides

To determine the ability of a modified MART-1<sub>27–35</sub> peptide to stimulate CTL responses *in vitro*, lymphocytes were stimulated with peptide and evaluated by ELISPOT assay. Lymph node cells from the melanoma patient VMM120 were stimulated once *in vitro*, either with the MART-1<sub>27–35</sub> peptide or the Cap-MART-1 peptide by incubating the lymph node cells with 40  $\mu$ M concentrations of peptide for 2 hr at 37°C prior to washing the cells to remove unbound peptide. The cell cultures were then maintained in RPMI + 10% FCS + 20 units/ml IL-2 for 14 days at 37°C, 5% CO<sub>2</sub>. At the end of these 2 weeks, the cultured lymphocytes were evaluated by ELISPOT assay to identify the number of CTL reactive to peptide.

#### ELISPOT assay

Immunol 2 flat-bottom 96-well plates (Dynatech, Chantilly, VA) were coated with anti-IFN $\gamma$  monoclonal antibody (MAb) (M-700A, Endogen, Woburn, MA). Lymphocytes ( $1.5 \times 10^6$ ) were mixed with an equal number of T2 cells alone or T2 cells pulsed with peptide. Serial dilutions of that cell mixture were made in complete medium, such that the numbers of lymphocytes ranged from 150,000–5,000 per well. The plates were incubated at 37°C, 5% CO<sub>2</sub> for 18 hr. After extensive washing with washing buffer (H<sub>2</sub>O, 0.025% Tween 20), plates were incubated with biotin-labeled secondary antibody to IFN $\gamma$  (M-701-B, Endogen), then washed again and incubated with avidin conjugated with alkaline phosphatase. Then the plates were developed with BCIP substrate in 1% low-melting agarose. The next morning, the number of blue spots, corresponding to the number of cells secreting IFN $\gamma$ , were counted in each well by 2 individuals. Each sample was tested in triplicate. The number of spots produced by lymphocytes incubated with T2 alone was compared with that produced by lymphocytes incubated with T2 pulsed with each of the test peptides. The frequency of T-cells reactive to peptide was calculated based on this difference. Statistical significance was tested by a 2-tailed *t*-test.

## RESULTS

*Determination of the stability of the MART-1<sub>27-35</sub> peptide in fresh NHP as detected by reconstitution of CTL epitopes*

Synthetic MART-1<sub>27-35</sub> peptide was pre-incubated in fresh NHP or control media prior to pulsing onto <sup>51</sup>Cr-labeled T2 cells. These peptide-pulsed target cells were then incubated with MART-1<sub>27-35</sub>-reactive CTL. Lysis of peptide-pulsed T2 cells thus represented persistence of intact peptide. When 1  $\mu$ M MART-1<sub>27-35</sub> peptide was pre-incubated in control media (HBSS or RPMI without FCS), there was no decay in CTL reactivity noted past 90 min (Fig. 1a), nor for the length of any assay up to 20 hr (data not shown). However, when the peptide was incubated in NHP (non-heat inactivated), CTL reactivity was noted to be well below 50% of maximal lysis after just 20 min and was undetectable within less than 60 min (Fig. 1a).

To calculate the concentration of intact peptide that correlates with the observed lysis of peptide-pulsed T2 cells at each time point in Fig. 1a, a dose titration of the MART-1<sub>27-35</sub> peptide was simultaneously performed, where that peptide was not pre-incubated in plasma prior to pulsing on T2 cells. A chromium-release assay performed with T2 cells pulsed with peptide ranging in concentration from 0.5 fM to 50  $\mu$ M revealed half-maximal lysis between 5 nM and 50 nM. Similar results were obtained regardless of whether the assay itself was performed in fresh human plasma or control media (RPMI+1% BSA), suggesting that the degradation of peptide observed in Fig. 1a is not substantially affected by the medium used during the chromium-release assay itself (Fig. 1b).

Based on these data in Fig. 1a and b, averaging the data for the 2 curves in Fig. 1b, an estimate of the quantity of intact MART-1<sub>27-35</sub> peptide was calculated for each data point in Fig. 1a. These calculations are presented graphically in Fig. 1c. The initial peptide concentration of 1  $\mu$ M represents approximately 200–200 $\times$  the amount required for half-maximal target-cell lysis and approximately 1000 $\times$  the amount required for detectable lysis by VM5 CTL. This quantity of the MART-1<sub>27-35</sub> peptide induced 75% specific T2 lysis after 100 sec in control medium (Fig. 1a), which was the initial time point of the stability assay. For peptides incubated in NHP, the specific lysis of T2 cells at that early time point was 66%, which corresponds to a peptide concentration of approximately 100 nM. Thus, in 100 sec, the amount of intact peptide decreased from 1  $\mu$ M to 100 nM, approximately 99% of the total amount of peptide (Fig. 1).

The calculated concentration of peptide was plotted against the time of incubation in NHP. The best-fit line correlated the inverse of the peptide concentration with the time of incubation (Fig. 1c). Thus, the degradation of MART-1<sub>27-35</sub> peptide in NHP is consistent with second order rate kinetics, such that the rate of degradation decreases as the concentration of the substrate decreases. Using the best-fit line for these data, an estimate of the second order rate kinetics for this system can be defined by the following equation, where K = slope = 0.0027 ml/ng-min. The correlation coefficient R<sup>2</sup> for this best-fit line is 0.97 (Fig. 1c). From this, the half-life of the peptide (at an initial concentration of 1  $\mu$ M) can be estimated using the following equation:

$$t_{1/2} = \frac{1}{K[\text{peptide}]_0} = \frac{1}{(0.0027 \text{ ml/ng-min}) * (1,000 \text{ ng/ml})} = \frac{1}{2.7 \text{ min}^{-1}} = 22 \text{ sec.}$$

*Loss of the MART-1<sub>27-35</sub> peptide in NHP is due to enzymatic degradation via peptidases*

We hypothesized that the loss of the MART-1<sub>27-35</sub> peptide in NHP was secondary to peptidase activity. If this were the case, then denaturing proteins in NHP or the addition of protease inhibitors should eliminate the loss of MART-1<sub>27-35</sub>. To denature proteins in

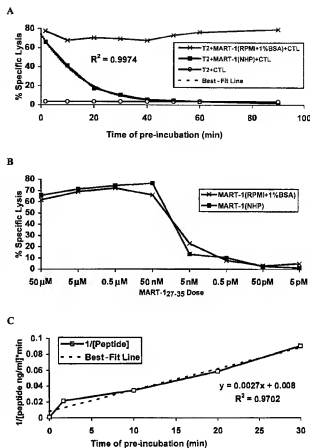


**FIGURE 1**—Degradation kinetics of the MART-1<sub>27-35</sub> peptide in NHP. Loss of CTL reactivity to peptide pulsed target cells is correlated with a dose-titration assay, permitting estimation of the quantity of intact peptide present after pre-incubation times of up to 30 min. In (a), 1  $\mu$ M MART-1<sub>27-35</sub> peptide in 1 ml fresh NHP or HBSS was pre-incubated at 37°C for variable time intervals, then 50  $\mu$ l of these solutions were pulsed onto <sup>51</sup>Cr-labeled T2 cells. Recognition by MART-1<sub>27-35</sub>-reactive VM5 CTL (effector:target ratio 10:1) was evaluated by a chromium-release assay. Specific lysis of T2 cells plus peptide pre-incubated in plasma (solid squares) or control media (RPMI + 1% BSA, x's) is plotted for 8 time points over 90 min of pre-incubation time. A best-fit line for the peptides pre-incubated in plasma is plotted (dashed line) and correlates well with the observed data points (R<sup>2</sup> = 0.9974). Reactivity of CTL against T2 cells alone is less than 5% (circles). For (b), peptides were not pre-incubated in serum but were simply added to <sup>51</sup>Cr-labeled T2 cells in plasma (solid squares) or control media (x's) for the duration of the 4-hr chromium-release assay to determine if the presence of NHP during the chromium-release assay (after peptide pulsing) affects reactivity. Using the mean of values from the 2 superimposable curves from (b) above, the quantity of peptide associated with each of the data points in (a) was estimated and plotted in (c) as 1/[peptide] vs. pre-incubation time (open squares). These observed data approximate a straight line. A best-fit line (dashed) has an R<sup>2</sup> value of 0.9702 and represents second-order kinetics.

NHP, we acidified the NHP with 12N HCl to a final pH of 1–1.5. After 1 hr, this pH was neutralized with 12N NaOH. The assay protocol was then followed as above, utilizing this denatured human plasma (DHP) and comparing its effects to those of fresh NHP. Consistent with prior observations, 1  $\mu$ M of the MART-1<sub>27-35</sub> peptide was unstable in NHP and stable in HBSS at 37°C (Fig. 2a). However, when 1  $\mu$ M of the MART-1<sub>27-35</sub> peptide was pre-incubated in the DHP, no loss of the peptide was detected over 20 hr

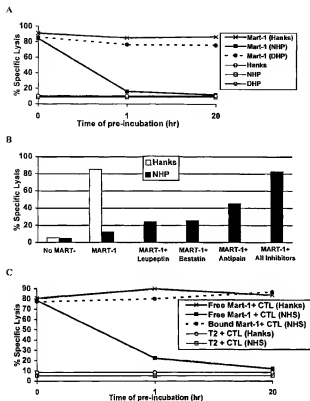


**FIGURE 2.** Loss of MART-1<sub>27-35</sub> peptide in fresh human plasma is due to plasma proteases. To determine if the degradation of that peptide was mediated by plasma protease inhibitors, the peptide MART-1<sub>27-35</sub> was pre-incubated in fresh human plasma or denatured human plasma, with or without protease inhibitors prior to addition of VM5 CTL (effector:target ratio of 10:1). Percent specific lysis was measured. For (a), human plasma was either used fresh or was used after denaturation by acidification as described in Material and Methods. Specific lysis of T2 cells pulsed with 1  $\mu$ M MART-1<sub>27-35</sub> after pre-incubation in control media (x's on solid line), fresh NHP (closed squares on solid line) or acid-denatured human plasma (DNP, closed circles on dashed line) is plotted for 3 time points representing pre-incubation of 0, 1 and 20 hr. Control wells without MART-1<sub>27-35</sub> peptide were associated with 10% lysis or less. In (b), Leupeptin, Antipain and Bestatin at a final concentration of 1 mM were added to MART-1<sub>27-35</sub> peptide (10  $\mu$ M) prior to a 5-hr pre-incubation of peptide in fresh NHP or control media (HBSS). Each protease inhibitor delayed the degradation of the MART-1<sub>27-35</sub> peptide in NHP to some extent, but a combination of the 3 inhibitors had an additive effect. In (c) 1  $\mu$ M MART-1<sub>27-35</sub> peptide was pre-incubated for 0, 1 or 20 hr in HBSS (x's) or NHP (solid squares) prior to pulsing on T2 cells and addition of VM5 CTL. Also, 1  $\mu$ M MART-1<sub>27-35</sub> peptide was pulsed onto T2 cells then incubated NHP for 0, 1 or 20 hr (dashed line with closed circles) prior to addition of VM5 CTL. Specific lysis of target cells was measured. Lysis of T2 cells without peptide was less than 10%.

of pre-incubation. These data are consistent with our hypothesis that the loss of the MART-1<sub>27-35</sub> peptide in NHP was mediated by peptide activity.

To confirm this hypothesis further, we then attempted to inhibit the decay of MART-1<sub>27-35</sub> peptide in NHP with protease inhibitors. When 10  $\mu$ M MART-1<sub>27-35</sub> peptide was incubated in NHP plus 1 mM of either of the endopeptidase inhibitors, leupeptin or antipain, or 1 mM of the exopeptidase inhibitor, bestatin, MART-1<sub>27-35</sub> peptide degradation was partially inhibited (Fig. 2b). Furthermore, the combination of both the endo- and exopeptidase inhibitors was additive in retarding the loss of the MART-1<sub>27-35</sub> peptide in human

plasma, suggesting that multiple enzymes may be involved in the degradation process.

Next, we evaluated whether the MART-1<sub>27-35</sub> peptide would be protected against proteolytic degradation if first bound to an MHC molecule. As seen previously, 1  $\mu$ M free MART-1<sub>27-35</sub> was stable in HBSS and unstable in NHP. However, when the MART-1<sub>27-35</sub> peptide was first pulsed onto T2 cells for 1 hr prior to being incubated with NHP, no loss of CTL reactivity against those peptide-pulsed target cells was noted for up to 20 hr (Fig. 2c).

#### Determination of the stability of the gp100<sub>280-288</sub> and gp100<sub>17-25</sub> peptides in fresh normal human plasma.

To determine whether the stability of nonamer peptides in fresh NHP may be generalizable or whether it was uniquely a property of the MART-1 peptide, 2 other peptides known to be naturally processed and presented on the cell surface were evaluated in a similar manner. The gp100 peptide corresponding to amino acid residues 280-288 (YLEPGPVTA) is naturally processed and presented in association with HLA-A\*0201, and it is recognized by VM5 CTL (Cox *et al.*, 1994). When incubated in fresh NHP, the ability of 10  $\mu$ M YLEPGPVTA to reconstitute an epitope for VM5 CTL persisted at 1 hr but disappeared after 20 hr, whether incubated in 100% FCS (not heat inactivated, data not shown) or in 100% fresh NHP (Fig. 3a). The concentration of this peptide required for half-maximal lysis is 1-10 pM (Cox *et al.*, 1994), so the 10  $\mu$ M concentration is approximately 10<sup>6</sup>-fold in excess.

The gp100 peptide corresponding to amino acid residues 17-25 (ALLAVGATK) is naturally processed and presented in association with HLA-A\*0301, and it is recognized by VM18 CTL (Skipper *et al.*, 1996). When incubated in fresh NHP, the ability of 10  $\mu$ M ALLAVGATK to reconstitute an epitope for VM18 CTL fell to half-maximal at 1 hr and disappeared by 20 hr in 100% fresh NHP (Fig. 3b). The concentration of this peptide required for half-maximal lysis is 1-10 nM (Skipper *et al.*, 1996), so the 10  $\mu$ M concentration is approximately 10<sup>6</sup>-fold in excess. Thus, it can be estimated that approximately 99.9% of this peptide is degraded within the first hour of incubation in plasma.

#### Modification of the MART-1 peptide increases the *t*<sub>1/2</sub> in human plasma without destroying the T-cell epitope

Multiple modifications of peptides have been reported to increase peptide stability *in vivo*. We selected 6 of these modifications to apply to the MART-1<sub>27-35</sub> peptide, and they are outlined in Table I. Each modification was selected because it had been reported to increase the stability of other small peptides *in vivo* with minimal changes in peptide configuration or characteristics. The PEG moiety added to the C-terminus of the MART-1<sub>27-35</sub> peptide had a m.w. of approximately 5,000. It was hypothesized that this moiety, though large when compared to the MART-1<sub>27-35</sub> peptide, might be in a position not to significantly inhibit immune recognition. To achieve glycosylation of the MART-1<sub>27-35</sub> peptide, we added a glycosylated asparagine residue to the N-terminus of the MART-1<sub>27-35</sub> sequence. The C-terminal amino acid capping of the MART-1<sub>27-35</sub> peptide resulted in a peptide of slightly lower molecular weight than the naturally occurring peptide due to substitution of the amide group for a hydroxyl group. We hypothesized that the modified peptides would still be antigenic and that they would confer a significant protection against enzymatic degradation.

We first evaluated whether the modified peptides could reconstitute an epitope for VM5 CTL. When dose was not limited, each of the modified peptides was capable of reconstituting the T-cell epitope sufficiently to induce the same maximal level of target cell lysis by VM5 CTL, however, this was achieved at different peptide concentrations (Table I). Half-maximal lysis was achieved with PEG-MART-1, D-MART-1 and Cap-MART-1 peptides at 500 $\times$ , 20 $\times$  and 5 $\times$  more peptide than the unmodified MART-1 peptide. The Glyco-MART-1 peptide was equivalent to the unmodi-

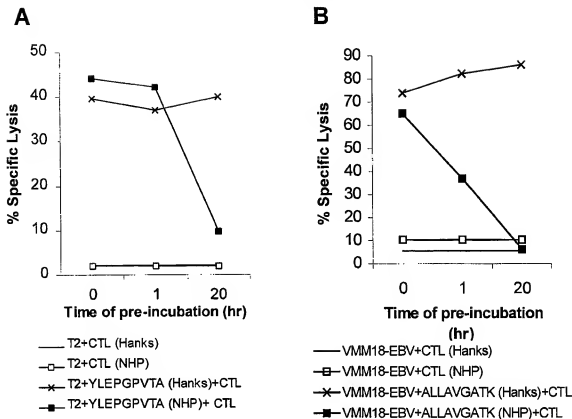


**FIGURE 3**—Stability of HLA-A\*0201-restricted and HLA-A\*0301-restricted gp100 peptides in fresh human plasma. After incubation for 0, 1 or 20 hr in fresh NHP, FCS or Hanks, peptides were added to antigen-presenting cells and tested as targets in 4-hr chromium-release assays to determine the presence or absence of detectable epitopes for these CTL. In (a), HLA-A2-restricted peptide 946 (gp100<sub>939-946</sub>) was pulsed onto T2 cells and evaluated with VMM5 CTL. In (b), HLA-A3-restricted peptide ALLAVGATK (gp100<sub>17-22</sub>) was pulsed onto HLA-A3<sup>+</sup> VMM18-EBV transformed B cells and evaluated with VMM18 CTL.

fied MART-1 peptide in its ability to reconstitute the CTL epitope. In contrast, the N-MART-1 and the C-MART-1 peptides reconstituted the CTL epitope more effectively than the native MART-1<sub>27-35</sub> peptide such that half-maximal lysis was achieved with 1/2 and 1/20<sup>th</sup> as much peptide, respectively (Table I).

Next we evaluated whether these modified peptides conferred any protection against enzymatic degradation in NHP. The assay was initiated with 10  $\mu$ M concentrations of each peptide so that there would be maximal lysis at the beginning of the study with each of the modified peptides (Fig. 4). The results represent the lysis induced by the intact modified MART-1 peptides after 20 hr of incubation at 37°C. This represents the longest incubation time tested. As previously seen, the native MART-1 peptide is unstable in human plasma. Even though glycosylation of the N-terminus and D-amino acid substitution of the N- and C-termini have proven successful in prolonging the half-life of other small peptides (Maille et al., 1995; Powell et al., 1993), here neither conferred any significant protection against degradation. Significantly increased half-lives were noted with the PEGylated MART-1, Cap-MART-1, N-MART-1 and C-MART-1 peptides. All of these modifications extended the stability of the native MART-1<sub>27-35</sub> peptide in NHP such that there was maximal or near maximal lysis even with peptides incubated 20 hr in NHP (Fig. 4).

The binding affinity of these modified peptides was measured in an equilibrium binding assay, and the concentration required for 50% inhibition of binding of a standard peptide are listed (Table I), such that higher values represent weaker binding. The peptides Cap-MART-1, N-MART-1 and C-MART-1 all bind to the HLA-

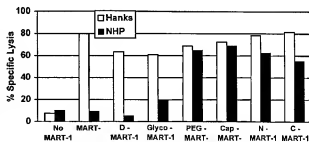


**FIGURE 4**—Stability of modified MART-1 peptides in fresh human plasma. Each of the modified MART-1 peptides were added to HBSS (clear bars) or NHP (black bars) and pre-incubated at 37°C for 20 hr prior to pulsing onto <sup>51</sup>Cr-labeled T2 cells. Specific lysis of T2 cells pulsed with these modified peptides was measured in a chromium-release assay. The D-MART-1 and the Glyco-MART-1 peptides were no more stable in NHP than the native MART-1<sub>27-35</sub> peptide. However, the PEG-MART-1, Cap-MART-1, N-MART-1 and C-MART-1 peptides were significantly more stable in NHP.

A\*0201 molecule, but with lower affinity than the MART-1 peptide.

The Cap-MART-1 peptide was evaluated for its ability to stimulate a MART-1-reactive CTL line *in vitro*. Lymphocytes from a tumor-free lymph node from HLA-A2<sup>+</sup> melanoma patient VMM120 were stimulated *in vitro* with the naturally occurring

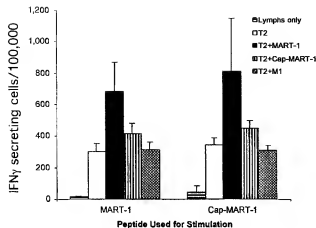


**FIGURE 5**—Immunogenicity of Cap-MART-1 peptide. VMM120 lymph node cells were stimulated *in vitro* either with the natural MART-1 peptide or with the modified Cap-MART-1 peptide for 14 days, then resulting cultured lymphocytes were evaluated by ELISPOT assay for the number of peptide-specific IFN- $\gamma$ -secreting lymphocytes. Reactivity to MART-1 peptide, to Cap-MART-1 peptide and to the influenza M1 peptide are compared with standard deviations of triplicate values marked for each data bar. Comparing responses to T2 + peptide to responses to T2 alone, *p* values for significance are as follows. MART-1 stimulated lymphocytes: T2 + MART-1 vs. T2 (*p* < 0.001); T2 + Cap-MART-1 vs. T2 (*p* < 0.008); T2 + M1 vs. T2 (*p* = 0.73); Cap-MART-1 stimulated lymphocytes: T2 + MART-1 vs. T2 (*p* < 0.008); T2 + Cap-MART-1 vs. T2 (*p* < 0.003); T2 + M1 vs. T2 (*p* = 0.12).

MART-1 peptide (AAGIGILTV) or with Cap-MART-1 peptide. After 14 days, the T-cell response to the naturally occurring MART-1 peptide was measured by ELISPOT assay. There was no significant difference in the reactivity to MART-1 after stimulation with MART-1 itself (382 responding T-cells per  $10^5$ ) or after stimulation with the Cap-MART-1 peptide (465 responding T-cells per  $10^5$ ) (Fig. 5). There was also reactivity to the Cap-MART-1 peptide in both cases (112 and 105 responding T-cells per  $10^5$ , respectively). These reactivities were all significantly above background reactivity to T2 cells alone. Reactivity to the influenza M1 peptide was not significantly above background in either culture. (Fig. 5)

#### DISCUSSION

There has been increased enthusiasm for the use of naturally occurring biologically active peptides in the clinical setting. An important step in the development of many clinically effective peptide-based therapies has been the production of analogues that retain the biologic activity while resisting elimination *in vivo* (Marbach *et al.*, 1993). The identification of peptide epitopes for melanoma-reactive CTLs has led to their use in melanoma vaccines. Modifications of individual amino acid residues in Class I MHC-associated peptides have been reported, which have been designed to increase affinity for the MHC and to increase immunogenicity (Parkhurst *et al.*, 1996; Valmori *et al.*, 1998), but these modifications were not designed to increase stability to peptidase activity and have not been tested for their effect on stability *in vivo*. The stability of Class II MHC-associated peptides in heat-inactivated FCS has been reported (Maille *et al.*, 1995), and the degradation of a murine peptide and of a human MAGE-3 peptide by serum peptidases has been assessed by mass spectrometry (Ayyoub *et al.*, 1998). These results confirm the expectation that synthetic peptides are susceptible to degradation in serum. In addition, Ayyoub *et al.* (1998) demonstrated approaches for stabilizing certain peptide bonds by creating peptide analogues. However, these studies did

not evaluate the effect on antigenicity of modifications that may increase stability. We have undertaken the present study with the premise that it is critical to understand how the stability of immunogenic peptides may affect the potential clinical effectiveness of peptide-based melanoma vaccines. In particular, we have evaluated the antigenicity of a modification that markedly increases peptide stability.

We have found that the MART-1<sub>27-35</sub> peptide is very unstable in NHP, with a calculated half-life of 22 sec at a 1  $\mu$ M concentration and that its degradation was a result of plasma peptidase activity, probably involving multiple peptidases with exo- and endopeptidase activities. Although this calculated half-life is the result of indirect measures, it is clear that the half-life for the MART-1<sub>27-35</sub> peptide in NHP is very short and that in a matter of minutes, less than 1% of the original peptide dose remains intact in human plasma. This conclusion is based purely on an *in vitro* model, however, it is known that the dermis contains multiple peptidases with exo- and endopeptidase activity (Boderke *et al.*, 1997), and in the case of the peptide hormone somatostatin findings related to stability in human plasma were accurately extrapolated to the *in vivo* setting (Marbach *et al.*, 1993). Thus, it is reasonable to expect that the findings in the present report can be similarly extrapolated to the *in vivo* setting. We expect that free, unmodified peptides administered intradermally will experience rapid degradation similar to that observed with the MART-1<sub>27-35</sub> peptide in plasma.

Additional experiments with antigenic gp100 peptides, restricted by HLA-A\*0201 or HLA-A\*0301, reveal that rapid degradation of free peptides in human plasma is a common phenomenon and is not a property unique to the MART-1<sub>27-35</sub> peptide. The HLA-A\*0301-associated peptide ALLAVGATK reconstitutes an epitope for VMM18 CTL at low nanomolar concentrations (Skipper *et al.*, 1996), and the data shown in Fig. 3b suggest that 99.9% of this peptide is degraded within 1 hr. The A\*0201-associated peptide YLEPGVTA reconstitutes an epitope for VMM5 CTL at much lower concentrations in the low picomolar range (Cox *et al.*, 1994), so it is not surprising that maximal reactivity is still observed after 1 hr. However, at 20 hr, reactivity is reduced to near background levels (Fig. 3a).

It is reasonable to expect that peptides must be intact long enough to bind to an APC for there to be an effective immune response induced by the vaccination. Therefore, peptidase-mediated degradation of the MART-1<sub>27-35</sub> peptide may have important implications for vaccinations when considered in combination with data on APC migration. The estimated minimal response time for a DC to begin migrating toward an inflammatory site has been estimated to be between 1.5–2 hr and may only reach completion after 24–48 hr (Weiss *et al.*, 1997). Therefore, it seems likely that, in the setting of vaccines using free, unmodified peptide, the majority of injected peptide would be degraded prior to the arrival of DCs at a vaccination site. Conversely, injected peptide that is not degraded may bind to Class I MHC molecules on non-APC cells that lack the co-stimulatory molecules needed to induce an immunologic response and thus may induce tolerance. Certainly, adjuvants administered with peptide-based vaccines may well alter the susceptibility of peptides to peptidases. This requires additional study, but there is some evidence that local inflammation actually increases peptidase activity (Boderke *et al.*, 1997). Regardless of an incremental effect of adjuvants, however, it seems likely that vaccinations using the Class I MHC-associated melanoma peptides may not be as effective as DC-based therapies because the immunogenic peptide may be degraded prior to the arrival of these antigen-presenting cells at the vaccination site. Therefore, modified Class I-associated melanoma peptides that are protected from endo- and exopeptidase degradation but retain antigenicity may be useful for the next generation of peptide-based vaccines.

Recent vaccine trials using melanoma peptides at this and other institutions have used unmodified peptides with free N-terminal and C-terminal ends (personal communications, Drs. Alexander Knuth, Frankfurt, Germany; Angela Shaver, National Cancer

Institute, Bethesda, MD; Walter Storkus, Pittsburgh, PA; and data not shown). However, we have found that capping of both or either of the N- and C-termini or PEGylation increases the stability of the MART-1<sub>27-35</sub> peptide. Although *in vivo* experiments will be required to evaluate the net immunogenicity of the Cap-MART-1 peptide, preliminary *in vitro* data provide evidence that fresh lymphocytes from a melanoma patient stimulated with the Cap-MART-1 analogue will develop reactivity to the natural MART-1<sub>27-35</sub> peptide at an equivalent level to that obtained after stimulation with the MART-1<sub>27-35</sub> peptide itself (Fig. 5). The lower reactivity to the Cap-MART-1 peptide observed with both cultures is consistent with the data in Table 1, that the binding affinity for HLA-A\*0201 is lower than that of unmodified MART-1 peptide. This may explain why the concentration of Cap-MART-1 required for epitope reconstitution is 5-fold higher than that required for MART-1<sub>27-35</sub>.

In contrast to prior experience with other peptides (Powell *et al.*, 1993), N-terminal glycosylation and d-isomer substitution of the N- and C-terminal amino acids did not significantly stabilize the MART-1<sub>27-35</sub> peptide. In fact, the d-MART-1 peptide had a shorter half-life as compared with the unmodified MART-1 peptide in human plasma (data not shown). These data raise a question of whether the effect of any modification will be uniformly generalizable to all of the immunogenic melanoma peptides.

It appears that some modifications may have effects unrelated to stability alone. In this study, the PEG modification not only increased the stability of the MART-1<sub>27-35</sub> peptide in NHP but also increased the solubility of the hydrophobic MART-1<sub>27-35</sub> peptide (data not shown). The increased solubility of the PEG-MART-1 peptide may increase peptide uptake by APC, or in contrast, the increased solubility may result in increased diffusion away from the immunization site, thus leading to decreased loading onto the APC. We theorize that the mechanism for the increased stability of PEGylated peptides is steric hindrance of the degradative enzymes. However, PEGylation of MHC-binding peptides may likewise produce steric hindrance in the peptide-MHC interaction or in the TCR interaction with antigen. Such steric hindrance may also explain the increased peptide dose required for half maximal lysis, when using this modification. The PEG moiety used for the PEG-MART-1 peptide is large, with a m.w. of 5,000, and it markedly decreased affinity for the MHC (Table 1). Therefore, it may be beneficial to use a smaller PEG moiety for future

modifications. It may also be beneficial to extend the C-terminal side of the MART-1 peptide before adding the PEG moiety, in hopes of decreasing steric hindrance for T-cell receptor engagement.

We assume that increased *in vivo* stability of melanoma Class I MHC-associated peptides used in vaccinations will increase the amount of peptide being loaded onto APCs at the vaccination site. It is this combination of immunogenic peptide plus APCs that is probably critical for the production of an optimal immune response. However, *in vivo* studies are needed to evaluate the overall impact of increased peptide stability on the induced anti-tumor immune response. Modified peptides with increased stability *in vivo* may diffuse into the systemic circulation and become tolerogenic, as seen with IV infusion of immunogenic peptides in mice (Aichele *et al.*, 1995). Or, by effectively increasing the actual dose delivered to the patient, these modified peptides may preferentially induce low-affinity CTL. Likely, there is a balance to be achieved in peptide stability that may permit optimal presentation of immunogenic peptides.

The discovery of specific peptide epitopes for melanoma-reactive CTL has brought optimism for the development of an effective, well-tolerated therapy for melanoma. Although purified MHC Class I-associated peptides can induce CTL-mediated responses in animal models (Jaeger *et al.*, 1996), the results thus far from clinical trials have left some opportunity for improvement. In the present study, we have shown that the MART-1<sub>27-35</sub> peptide is rapidly degraded when exposed to endo- and exopeptidases and that this degradation can be blocked with N- and C-terminal modifications. These data raise the questions of whether peptides that are currently being used in peptide-based vaccine trials for melanoma are unstable and whether these modifications are generalizable for universal protection. These findings certainly support the use of antigen presenting cells, such as DCs, pre-pulsed with peptides, in tumor vaccines. In addition, these findings may well provide a means to improve peptide-based vaccines using free peptide. However, *in vivo* experiments directly addressing the impact of using peptides that have increased stability in vaccinations will be required to address the complex nature of vaccination biology. Increased understanding of how these peptides interact with the melanoma patient is critical for the realization of their potential effectiveness.

## REFERENCES

- AICHELE, P., BROUSCHIA-RIEM, K., ZINKERNAGEL, R.M., HENGARTNER, H. and PIRCHER, H. T-cell priming versus T-cell tolerance induced by synthetic peptide. *J. exp. Med.*, **182**, 261-266 (1995).
- AYYOUB, M., MONSARRAT, B., MAZARGUIL, H. and GAIRIN, J.E., Analysis of the degradation mechanisms of MHC class I-presented tumor antigenic peptides by high performance liquid chromatography/electrospray ionization mass spectrometry: application to the design of peptide-resistant analogues. *Rapid Commun. Mass Spectrom.*, **12**, 557-564 (1998).
- BODERKE, P., MERKLE, H.P., COLLANDER, C., PONEC, M. and BOODE, H., Localization of aminopeptidase activity in freshly excised human skin: direct visualization by confocal laser scanning microscopy. *J. invest. Dermatol.*, **108**, 83-86 (1997).
- CHEN, Y., SIDNEY, J., SOUTHWOOD, S., COX, A.L., SAKAGUCHI, K., HENDERSON, R.A., APPELLA, E., HUNT, D.F., SETTE, A., and ENGELHARD, V.H., Naturally processed peptides longer than nine amino acid residues bind to the class I MHC molecules HLA-A2.1 with high affinity and in different conformations. *J. Immunol.*, **152**, 2874-2881 (1994).
- COX, A.L., SKIFFER, J., CHEN, Y., HENDERSON, R., DARROW, T.L., SHABANOWITZ, J., ENGELHARD, V.H., HUNT, D.F. and SLINGOFF, C.L., Jr., Identification of a peptide recognized by five melanoma-specific human cytotoxic T-cell lines. *Science*, **264**, 716-719 (1994).
- EDD, N.J., ANG, K.H., JAMES, I.W. and BRAY, A.M., Incorporation of 2-hydroxy-4-methoxybenzyl protection during peptide synthesis via reductive alkylation on the solid phase. *Tetrahedron Lett.*, **37**, 9097-9100 (1996).
- HENDERSON, R.A., MICHEL, H., SAKAGUCHI, K., SHABANOWITZ, J., APPELLA, E., HUNT, D.F. and ENGELHARD, V.H., HLA-A2.1-associated peptides from a mutant cell line: a second pathway of antigen presentation. *Science*, **255**, 1264-1266 (1992).
- JAAGER, E., BERNHARD, H., ROMERO, P., RINGHOFFER, M., ARAND, M., KARBACH, J., ILSMANN, C., HAGEDORN, M. and KNUTH, A., Generation of cytotoxic T-cell responses with synthetic melanoma-associated peptides *in vivo*: implication for tumor vaccines with melanoma-associated antigens. *Int. J. Cancer*, **66**, 162-169 (1996).
- KATES, S.A., DE LA TORRE, B.G., ERITJA, R. and ALBERICO, F., Solid-phase N-glycopeptide synthesis using allyl side-chain protected Fmoc-amino acids. *Tetrahedron Lett.*, **35**, 1033-1034 (1994).
- KAWAKAMI, Y., ELIJAH, S., SAKAGUCHI, K., ROBBINS, P.F., RIVOLINI, L., YANNELLI, J.R., APPELLA, E., and ROSENBERG, S.A., Identification of the immunodominant peptides of the MART-1 human melanoma antigen recognized by the majority of HLA-A2-restricted tumor infiltrating lymphocytes. *J. exp. Med.*, **180**, 347-352, (1994).
- LEE, V.H.L., Enzymatic barriers to peptide and protein absorption. *CRC Crit. Rev. Therap. Drug Carrier Systems*, **5**, 69-97 (1988).
- MAILLIERE, B., MOURIER, G., HERVE, M. and MENIZ, A., Fine chemical modification at the N- and C-termini enhance peptide presentation in T cells by increasing the lifespan of both free and MHC-complexed peptides. *Mol. Immunol.*, **32**, 1377-1385 (1995).
- MARKBACH, P., BRINER, U., LEMARIE, M., SCHWEITZER, A. and TERASAKI, T., From somatostatin to somatostatin: pharmacodynamics and pharmacokinetics. *Digestion*, **54** (Suppl. 1), 9-13 (1993).
- NAIR, S.K., BOCKZKOWSKI, D., SNYDER, D. and GILBOA, E., Antigen-

- presenting cells pulsed with unfractionated tumor-derived peptides are potent tumor vaccines. *Europ. J. Immunol.*, **27**, 589–597 (1997).
- OFFER, J., QUIBELL, M., and JOHNSON, T., On-resin solid-phase synthesis of asparagine N-linked glycopeptides: use of N-(2-acetoxy-4-methoxybenzyl) (AcHmb) aspartyl amide-bond protection to prevent unwanted asparagine formation. *J. chem. Soc. [Perkin 1]*, **2**, 175–182 (1996).
- PARKHURST, M.R., SALGALLER, M.L., SOUTHWOOD, S., ROBBINS, P.F., SETTE, A., ROSENBERG, S.A., and KAWAKAMI, Y., Improved induction of melanoma-reactive CTL with peptides from the melanoma antigen gp100 modified at the HLA-A\*0201-binding residues. *J. Immunol.*, **157**, 2539–2548 (1996).
- POWELL, M.F., GREY, H., GAETA, F., SETTE, A., and COLON, S., Peptide stability in drug development: a comparison of peptide reactivity in different biologic media. *J. pharm. Sci.*, **81**, 731–735 (1992).
- POWELL, M.F., STEWART, T., OTVOS, L., URGE, L., GAETA, F.C.A., SETTE, A., ARRIENIUS, T., THOMSON, D., SODA, K., and COLON, S.M., Peptide stability in drug development. II. Effects of single amino acid substitution and glycosylation on peptide reactivity in human serum. *Pharm. Res.*, **10**, 1268–1273 (1993).
- SKIPPER, J.C.A., KITTESEN, D.J., HENDRICKSON, R.C., DEACON, D.D., HARTHUN, N.L., WAGNER, S.N., HUNT, D.F., ENGELHARD, V.H., and SLINGLUFF, C.L., Jr., Shared epitopes for HLA-A3-restricted melanoma-reactive human CTL include a naturally processed epitope from Pmel-17/gp100. *J. Immunol.*, **157**, 5027–5033 (1996).
- VALMORI, D., FONTENEAU, J.F., LIZANA, C.M., GERVOIS, N., LIENARD, D., RIMOLDI, D., JONGENEEL, V., JOTEREAU, F., CEROTTINI, J.C., and ROMERO, P., Enhanced generation of specific tumor-reactive CTL *in vitro* by selected Melan-A/MART-1 immunodominant peptide analogues. *J. Immunol.*, **160**, 1750–1758, (1998).
- WESS, J.M., SLEEMAN, J., RENKL, A.C., DITTMAR, H., TERMEER, C.C., TAXIS, S., HOWELLS, N., HOFMANN, M., KOHLER, G., SCHOFF, E., PONTA, H., HERRLICH, P., and SIMON, J.C., An essential role for CD44 variant isoforms in epidermal Langerhans cell and blood dendritic cell function. *J. Cell Biol.*, **137**, 1137–1147 (1997).

Engineering the Fc region of immunoglobulin G to modulate *in vivo* antibody levelsCarlos Vaccaro<sup>1</sup>, Jinchun Zhou<sup>1</sup>, Raimund J Ober<sup>1,2</sup> & E Sally Ward<sup>1</sup>

We have engineered the Fc region of a human immunoglobulin G (IgG) to generate a mutated antibody that modulates the concentrations of endogenous IgGs *in vivo*. This has been achieved by targeting the activity of the Fc receptor, FcRn, which serves through its IgG salvage function to maintain and regulate IgG concentrations in the body. We show that an IgG whose Fc region was engineered to bind with higher affinity and reduced pH dependence to FcRn potentially inhibits FcRn-IgG interactions and induces a rapid decrease of IgG levels in mice. Such FcRn blockers (or 'Abdegs', for antibodies that enhance IgG degradation) may have uses in reducing IgG levels in antibody-mediated diseases and in inducing the rapid clearance of IgG-toxin or IgG-drug complexes.

The engineering of the variable regions of IgG to generate effective therapeutic antibodies for both targeting and blocking effects is now a widely used approach<sup>1,2</sup>. In contrast, modulation of Fc-receptor function by manipulating the Fc regions of IgGs is relatively unexplored. Here we have investigated such an approach with the aim of developing therapeutics that decrease IgG levels *in vivo*. Such reagents could have potential applications in the treatment of diseases, such as systemic lupus erythematosus, in which autoreactive antibodies play a role<sup>3</sup>. In addition, they may have utility in the clearance of antibodies complexed with toxic molecules such as drugs or toxins.

There is a paucity of methods for modulating IgG levels *in vivo*, primarily owing to the limited understanding of the mechanisms by which antibody concentrations are controlled. However, recent studies have shown that the major histocompatibility complex (MHC) class I-related receptor, FcRn, plays a central role in regulating the transport of IgG within and across cells of diverse origin<sup>4–11</sup>. Thus, in addition to its earlier known activity in the transport of maternal IgG to offspring<sup>12,13</sup>, FcRn regulates IgG concentrations both in the serum and throughout the body<sup>14–16</sup>. The current model for FcRn function is as follows: IgGs are taken up into cells, most likely by fluid-phase pinocytosis, as the near-neutral pH of the extracellular milieu is generally not permissive for FcRn-IgG interactions<sup>17,18</sup>. IgGs that bind to FcRn in early, acidic endosomes following uptake are recycled (or transcytosed) and released at the cell surface by exocytosis<sup>11</sup>. In contrast, IgGs that do not bind enter the lysosomal pathway and are degraded<sup>10</sup>. IgGs can fail to be salvaged by FcRn for several reasons. They may have relatively low affinity for FcRn and as a result not compete favorably with other IgGs for interaction, or the IgG concentration may be saturating for FcRn binding. IgG homeostasis in the body is therefore maintained, at least at the level of IgG breakdown, by the saturable nature of FcRn.

The FcRn interaction site on IgG has been mapped using a combination of site-directed mutagenesis, functional analyses and X-ray crystallography<sup>19–22</sup>. It encompasses residues at the CH2-CH3

domain interface of IgG that include Ile253, His310, His435 and, in most mouse isotypes, His436 (ref. 23). In most human IgG isotypes and mouse IgG2b, residue 436 is tyrosine (ref. 23). The IgG-FcRn interaction is also highly pH dependent, with tight binding at pH 6.0, which becomes progressively weaker as near-neutral pH is approached<sup>17,18</sup>. Information concerning the molecular details of the FcRn interaction site offers opportunities to engineer antibodies with altered pharmacokinetics and distribution<sup>24–26</sup>.

Rather than using knowledge of IgG-FcRn interactions to generate IgGs with longer (or shorter) serum half-lives<sup>20,24–26</sup>, we engineered an antibody that, through its Fc-mediated binding to FcRn, enhances the clearance rates of endogenous IgGs. The rationale for the current study is that modified antibodies with increased affinity for FcRn relative to their wild-type counterparts will inhibit the interaction of endogenous IgGs, thereby increasing degradation of the latter. The inhibitory capacity of the engineered antibody would be further enhanced if the pH dependence of the IgG mutant-FcRn interaction were decreased, because, compared with naturally occurring IgGs, the engineered IgG would bind more stably to FcRn during exocytic events at the cell surface<sup>11</sup>. We have therefore generated a human IgG1 variant that, as a result of mutations in the Fc region, has suitable properties for the blockade of FcRn activity. We show that this engineered antibody inhibits FcRn-mediated recycling of IgG *in vitro* and enhances the clearance rates of endogenous IgGs in mice. Such antibodies, or 'Abdegs' (antibodies that enhance IgG degradation), may have applications in the treatment of antibody-mediated diseases and in other situations where FcRn inhibition is desirable.

## RESULTS

## Generation and FcRn binding properties of an Abdeg

An effective Abdeg should have increased affinity for FcRn at both acidic and near-neutral pH relative to its parent wild-type IgG. In earlier studies a mutated variant of human IgG1 was generated in

<sup>1</sup>Center for Immunology, University of Texas Southwestern Medical Center, 6000 Harry Hines Blvd., Dallas, Texas 75390-9093, USA. <sup>2</sup>Department of Electrical Engineering, University of Texas at Dallas, Richardson, Texas 75080, USA. Correspondence should be addressed to E.S.W. (sally.ward@utsouthwestern.edu).

Received 13 June; accepted 9 August; published online 25 September 2005; doi:10.1038/nbt1143

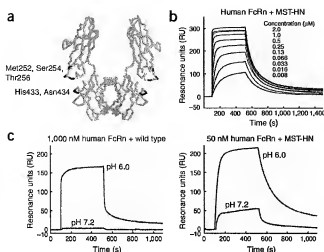


**Figure 1** The MST-HN Abdeg binds to human FcRn with increased affinity and reduced pH dependence. (a)  $\alpha$ -carbon trace of the X-ray crystallographic structure of human IgG1 (Fc region<sup>49</sup>) with location of residues targeted for mutagenesis in the MST-HN mutant (Met252, Ser254, Thr256, His433 and Asn434) indicated in black (drawn using Rasmol, courtesy of Roger Sayle, Bioinformatics Research Institute, University of Edinburgh). (b,c) SPR analyses of the interaction of human FcRn with wild-type human IgG1 (wild type) or MST-HN Abdeg. Coupling densities for the data shown are 671 RU (MST-HN) or 719 RU (wild-type human IgG1). Recombinant human FcRn was injected over the flow cells at the concentrations indicated in PBS plus 0.01% Tween 20 pH 6.0 (b,c) or pH 7.2 (c) at a flow rate of 10  $\mu$ l/minute. Sensorgrams showing equilibrium binding analysis of the interaction of human FcRn with MST-HN Abdeg (b), interaction of human FcRn with wild-type human IgG1 and MST-HN Abdeg at pH 6.0 and pH 7.2 (c). Concentrations of human FcRn used in c correspond to about three times the  $K_{D1}$  value at pH 6.0 for the respective interactions. Representative sensorgrams of at least duplicate injections are shown (b,c). All data were zero adjusted and reference-cell subtracted.

which Met252, Ser254, Thr256, His433, Asn434 and Tyr436 were changed to Tyr252, Thr254, Glu256, Lys433, Phe434 and His436 ('MST-HNY') with the goal of increasing serum half-life<sup>46</sup>. The mutations of these residues, which are located at the CH2-CH3 domain interface (Fig. 1a), result in increased affinity at pH 6.0 and reduced pH dependence (that is, increased binding at near-neutral pH) for binding to both mouse and human FcRn<sup>26</sup>. With the aim of analyzing the role of residue 436 of human IgG1, which differs between mouse and human IgG1 (histidine in most mouse isotypes; tyrosine in human IgG1<sup>23</sup>) in binding to FcRn, we mutated Tyr436 of human IgG1 to histidine. This mutation resulted in an approximate threefold reduction in affinity for binding to human FcRn (J.Z., E. Mateos and E.S.W., unpublished data), suggesting that the Y436H mutation in the MST-HNY variant might be detrimental to binding. This prompted us to make an engineered variant of human IgG1 containing mutations of Met252, Ser254, Thr256, His433 and Asn434 to Tyr252, Thr254, Glu256, Lys433 and Phe434 (MST-HN; Fig. 1). As shown by surface plasmon resonance (SPR) analyses, MST-HN has a substantially increased binding affinity for human FcRn at pH 6.0 ( $K_{D1}$  = 15.5 nM for MST-HN;  $K_{D1}$  = 370 nM for wild-type human IgG1) and retains significant binding activity at pH 7.2 (Fig. 1). We also used SPR to analyze the interaction properties of MST-HN with mouse FcRn. The mutant bound to mouse FcRn with high affinity at pH 6.0 ( $K_{D1}$  = 1.2 nM) and retained good affinity at pH 7.2 ( $K_{D1}$  = 7.4 nM). The MST-HN variant therefore bound more tightly to mouse FcRn than to human FcRn, consistent with earlier studies indicating that, relative to mouse FcRn, human FcRn generally has lower affinities for IgGs<sup>26,27</sup>.

### The MST-HN Abdeg colocalizes with FcRn in endothelial cells

We analyzed the properties of the MST-HN Abdeg using *in vitro* assays with human microvascular endothelial cells (HMEC-1) transfected with mouse FcRn-green fluorescent protein (GFP). HMEC-1 cells

were used extensively in our earlier studies to analyze the intracellular trafficking of FcRn and IgGs<sup>10,11</sup>. The uptake of fluorescently labeled MST-HN Abdeg at a concentration of 20  $\mu$ g/ml (~125 nM) into transfected cells was first compared with that of 20  $\mu$ g/ml fluorescently labeled human or mouse IgG1 (both wild type). Fluorescence imaging showed that the mutated IgG1 accumulated in the cells to substantially higher levels than either wild-type mouse or human IgG1, which were undetectable under our imaging conditions (Fig. 2). Colocalization of the MST-HN Abdeg with mouse FcRn-GFP was extensive, indicating that the Abdeg interacts with FcRn within cells. First, the Abdeg's high affinity and reduced pH dependence for FcRn promotes binding to surface FcRn under the conditions of the assay. This would be expected to facilitate uptake of the Abdeg by receptor-mediated pathways. Second, the Abdeg's binding properties may result in poor release of this IgG during exocytic events involving FcRn at the plasma membrane.

### The MST-HN Abdeg can inhibit recycling of IgGs *in vitro*

We next analyzed the ability of the MST-HN Abdeg to inhibit recycling of IgG in human endothelial cells transfected with mouse

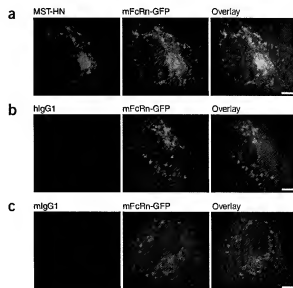


**Figure 2** The MST-HN Abdeg accumulates to higher levels in FcRn-GFP-expressing endothelial cells relative to wild-type human or mouse IgG1. Uptake of Alexa 647-labeled MST-HN Abdeg (a), wild-type human IgG1 (b) or wild-type mouse IgG1 (c) by HMEC-1 cells transfected with mouse FcRn (mFcRn)-GFP. Transfected cells were pulsed with 20  $\mu$ g/ml labeled IgG1 for 60 min, washed, fixed and mounted. The same imaging conditions (exposure times) were used for imaging of Alexa 647-labeled IgGs, and Alexa 647 is pseudocolored in red. Bars, 5  $\mu$ m.

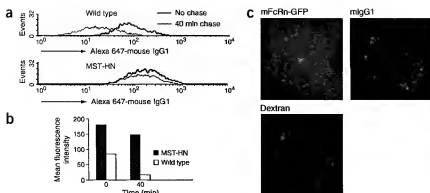


**Figure 3** Inhibition of recycling of mouse IgG1 from HMEC-1 cells transfected with mouse FcRn-GFP. (a) Histogram plots showing the amounts of Alexa 647-labeled mouse IgG1 at different chase times after pretreatment of cells with either MST-HN Abdeg or wild-type human IgG1. (b) Mean fluorescence intensities (background subtracted) of Alexa 647 fluorescence for each time point/treatment for the data shown in a. (c) Images of mouse FcRn (mFcRn)-GFP-transfected cells to show distribution of Alexa 546-labeled mouse IgG1 and Alexa 647-labeled dextran (lysosomal tracer) after pretreatment with the MST-HN Abdeg. Data are representative of at least two independent experiments. Bar, 5  $\mu$ m.

FcRn-GFP. Cells were preincubated with the MST-HN Abdeg or wild-type human IgG1 for 60 min, and then fluorescently labeled mouse IgG1 added for a further 60 min. Uptake and recycling of mouse IgG1 at the end of the pulse and after a 40-min chase period, respectively, were quantified by flow cytometry. Immediately after the pulse period, mouse IgG1 had accumulated to higher levels in cells pretreated with the MST-HN Abdeg relative to those pretreated with wild-type human IgG1 (Fig. 3a,b). In addition, during the chase period substantially more mouse IgG was recycled out of the cells pretreated with wild-type human IgG1 relative to Abdeg-treated cells (Fig. 3a,b).

We also used fluorescently labeled dextran as a lysosomal tracer to assess the intracellular location of the mouse IgG1 in HMEC-1 cells that had been pretreated with the MST-HN Abdeg. Microscopy analyses of these cells indicated colocalization of dextran and mouse IgG1 (Fig. 3c). Taken together, the data show that pretreatment of cells with the MST-HN Abdeg resulted in decreased recycling and accumulation of mouse IgG1 in the lysosomal pathway.

#### The MST-HN Abdeg can enhance IgG clearance *in vivo*

We also investigated the effect of the MST-HN Abdeg on the clearance rates of IgGs in mice. Mice were injected with radiolabeled ( $^{125}$ I) wild-type human IgG1, and 72 h (3 d) later groups of mice were treated with 500 or 200  $\mu$ g MST-HN Abdeg or 500  $\mu$ g wild-type human IgG1. Figure 4 shows the levels of radioactivity remaining in the mice at different times during the experiment. These levels were assessed using whole-body counting and therefore indicate whole-body rather than serum levels of labeled IgG1. After injection of 500  $\mu$ g MST-HN Abdeg, a rapid decrease in radioactivity levels in the mice was observed (Fig. 4). A similar, but less marked effect, was observed for mice treated with 200  $\mu$ g MST-HN Abdeg (Fig. 4). The levels of radioactivity dropped to  $12 \pm 4.6\%$  (500- $\mu$ g treatment group) or

$20 \pm 3.8\%$  (200- $\mu$ g treatment group) of the injected dose 120 h (5 d) after injection of the MST-HN Abdeg. In contrast, treatment of mice with 500  $\mu$ g of wild-type human IgG1 had no observable effect on the clearance rate of the radiolabeled IgG1 (Fig. 4).

#### The MST-HN Abdeg can reduce IgG concentrations *in vivo*

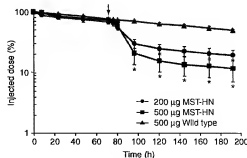
The effect of injection of the MST-HN Abdeg on the levels of endogenous IgGs in the serum of mice was also analyzed. Endogenous (steady-state) serum IgG levels were determined, and mice were subsequently injected with either 500  $\mu$ g MST-HN Abdeg or 500  $\mu$ g wild-type human IgG1. Relative to treatment with wild-type human IgG1, injection of the MST-HN Abdeg resulted in significant decreases in endogenous serum IgG levels, which persisted for about 96 h (4 d) (Fig. 5).

Taken together, the data show that the MST-HN Abdeg reduced levels of both exogenous and endogenous IgGs in mice when used at doses that were substantially lower than the whole-body load of endogenous IgGs. Further, as we have analyzed the *in vivo* effects of the MST-HN Abdeg on IgG levels in both the serum compartment and whole body, our observations indicate that inhibition of FcRn function by Abdeg acted at diverse sites throughout the body.

#### DISCUSSION

Manipulating the Fc region rather than the variable regions of IgGs is a relatively unexplored approach whose potential is now beginning to be realized<sup>2</sup>. We have described a route to lower IgG levels *in vivo* by using IgGs engineered in their Fc region to target the IgG-FcRn interaction site. In contrast to earlier studies in which IgG-FcRn interactions were modulated to alter the *in vivo* persistence of a therapeutic antibody<sup>24-26</sup>, the Abdeg was designed to alter the levels of endogenous, unmanipulated IgGs by enhancing their clearance rates.

**Figure 4** Enhancement of clearance of injected wild-type human IgG1 by MST-HN Abdeg. Swiss Webster mice (six mice/group) were injected with  $^{125}$ I-labeled wild-type human IgG1 and the persistence of the labeled IgG1 monitored by whole-body counting. Mice were injected with 500  $\mu$ g wild-type human IgG1, or 200  $\mu$ g or 500  $\mu$ g MST-HN Abdeg, 72 h later (indicated by arrow). Levels of remaining  $^{125}$ I-labeled human IgG1 were determined at the indicated times. The data shown are means of the remaining radioactivity in the different groups of mice. Error bars indicate s.d. \*, data for these time points for mice treated with 500 or 200  $\mu$ g MST-HN Abdeg are significantly different between the two groups, with  $P < 0.03$  (Student's *t*-test). Data are representative of two independent experiments.



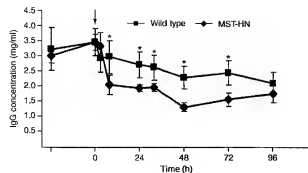


**Figure 5** Enhancement of clearance of endogenous IgGs by MST-HN Abdeg. The serum IgG levels in Swiss Webster mice were quantitated by ELISA. Mice (6 mice/group) were subsequently injected with 500  $\mu$ g wild-type human IgG1 or 500  $\mu$ g MST-HN Abdeg (indicated by arrow) and serum IgG levels monitored at the indicated times post-injection of these antibodies. Data shown are means of the serum IgG levels in the two different groups of mice, with s.d. indicated by error bars. \*, data for these time points are significantly different between the two groups, with a  $P < 0.009$  (Student's *t*-test). Data are representative of two independent experiments.

FcRn is known to be involved in transporting IgGs within and across cells of diverse origin, and in so doing, to regulate IgG concentrations and transport throughout the body<sup>4-11,28</sup>. We show that a mutated, human IgG1-derived antibody (MST-HN) with higher affinity for binding through its Fc region to FcRn at both pH 6.0 and 7.2 relative to its wild-type counterpart competes effectively with wild-type IgGs for FcRn-mediated transport. The binding properties of the Abdeg confer the ability to enhance the clearance of endogenous IgGs in mice.

The intracellular routing of FcRn and its IgG ligand has recently been analyzed using live-cell fluorescence imaging<sup>10,11</sup>. Although the steady-state levels of FcRn on the plasma membrane are generally low relative to cytosolic levels<sup>4-6,10,14,29</sup>, FcRn is directly involved in exocytic events involving transported IgG at the plasma membrane<sup>11</sup>. Surface expression of FcRn, even if only transient, would allow Abdeg such as MST-HN to bind, which in turn would facilitate more efficient uptake relative to fluid-phase processes. The MST-HN Abdeg therefore has several advantages over naturally occurring, pH-dependent IgGs in competing for FcRn binding. First, it can bind with high affinity at the cell surface. Second, it can outcompete IgGs that have lower affinity for FcRn within the sorting endosome<sup>10</sup>. Third, the mutated IgG1 would not be efficiently released during exocytic events involving FcRn<sup>11</sup>. Thus, as shown here, the MST-HN Abdeg accumulates at substantially higher levels in FcRn-expressing endothelial cells relative to wild-type mouse and human IgG1.

We have shown that the MST-HN Abdeg reduces mouse IgG levels both in serum and in the whole body. FcRn is expressed not only in endothelium but also in epithelia of the gut, lung and kidney<sup>4,7,8</sup>. We therefore expect that Abdeg such as MST-HN will have access to FcRn at a diverse array of body sites, including epithelial barriers.

Enhanced IgG degradation in humans may be desirable in multiple therapeutic situations. For example, Abdeg could be tested for the treatment of diseases caused by high levels of autoreactive antibodies, such as systemic lupus erythematosus and immune thrombocytopenic purpura (ITP)<sup>30</sup>. Further, FcRn is directly involved in the maternal-fetal transport of IgGs<sup>31,32</sup>, indicating that Abdeg might also be used to inhibit the passage of deleterious (auto)antibodies to the fetus. Alternatively, it may be possible to couple antibody-mediated

clearance of toxins or drugs from the body with the subsequent delivery of an Abdeg to enhance degradation of IgG-antigen complexes. A possible disadvantage of using Abdeg in therapy is that they systemically induce degradation of all IgGs and are relatively nonspecific compared with therapies that target a particular protein. As a consequence, Abdeg might be more attractive as reagents in situations where short-term effects are desired, rather than as a long-term treatment modality. However, it might be possible to develop ways of targeting Abdeg to specific tissues so that local effects predominate.

Intravenous gamma globulin (IVIg) has been used with some efficacy to treat autoimmune diseases such as ITP, myasthenia gravis and multiple sclerosis<sup>33</sup>. However, the mechanisms of action underlying these effects are a matter of debate. Proposed mechanisms include the blockade of Fc $\gamma$  receptors on phagocytes, anti-idiotypic effects, activation of inhibitory Fc $\gamma$  receptors and prevention of complement activation<sup>34-36</sup>. It has also been proposed that IVIg enhances clearance of endogenous, disease-associated IgGs<sup>34,37</sup>, and recent data in the murine K/BxN arthritis model support this<sup>38</sup>. However, the doses of IVIg that are needed to lower endogenous IgGs are in the range of the whole-body load of IgG. In contrast, owing to its competitive advantage in binding, the effective dose of MST-HN Abdeg (or any other Abdeg with equivalent properties) is much lower. Indeed, in the current study we show that wild-type human IgG1, when used at the same dose as the MST-HN Abdeg, has no effect on the clearance of endogenous IgGs in mice. This lack of effect is observed despite the approximately five- to tenfold higher affinity of (wild-type) human IgG1 relative to mouse IgGs for binding to mouse FcRn<sup>27</sup>.

Mouse and human FcRn have significant differences in binding specificities<sup>39</sup>. The molecular basis for this has recently been determined by site-directed mutagenesis and binding studies<sup>40</sup>. However, despite these differences, relative to wild-type human IgG1 the MST-HN mutant has increased affinity and reduced pH dependence for binding to both mouse and human FcRn. These binding properties for human FcRn suggest that the MST-HN mutant might have uses as an Abdeg in humans. In addition, other engineered IgG variants that share binding properties with the MST-HN mutant<sup>26</sup> may have activities as Abdeg.

In summary, we show that it is possible to generate an IgG with a mutated Fc region that efficiently inhibits FcRn function. As a consequence, this Abdeg reduces the levels of IgGs *in vivo*. The similarities between human and mouse FcRn function suggest that analogous approaches may be effective in humans. The use of engineered antibodies that, through their Fc region, are effective inhibitors of FcRn function therefore offers a potential therapeutic modality for the treatment of antibody-mediated diseases.

## METHODS

**Mice.** Swiss Webster mice (females, 6–8 weeks old) were purchased from Harlan Sprague and housed in the Animal Resources Center at UT Southwestern Medical Center. All procedures with mice were approved by the Institutional Review Board at UT Southwestern.

**Expression vectors.** The expression vector for a humanized anti-lysozyme heavy chain (human IgG1<sup>41</sup>) was generously provided by Jefferson Foote. The human IgG1 constant region was mutated by the PCR with mutagenic oligonucleotides and splicing by overlap extension<sup>42</sup>. The following mutations were made: Met252 to Tyr, Ser254 to Thr, Thr256 to Glu, His343 to Lys and Asn434 to Thr ('MST-HN'). Sequences of mutagenic oligonucleotides are provided in **Supplementary Data** online. After mutagenesis, altered regions were sequenced to ensure insertion of the desired mutation without second site

mutations. The mutated Fc gene was redoned into the final expression construct using standard methods.

A plasmid encoding mouse FcRn linked to enhanced GFP was generated using an analogous strategy to that described for human FcRn and the vector pEGFP-N1<sup>10</sup> (Clontech). The mouse FcRn  $\alpha$ -chain gene was isolated from murine SV40-transformed endothelial cells<sup>43</sup>. A mouse  $\beta$ 2-microglobulin expression plasmid was generated using the PCR to redone the  $\beta$ 2-microglobulin gene from an insert cell vector<sup>48</sup> into pC87 (ref. 44) (generously provided by Michael Roth, UT Southwestern Medical Center).

Generation of transfectants for antibody expression. NSO cells expressing a human anti-lysozyme specific light chain (HuLy5 (ref. 41); generously provided by Jefferson Foote) were transfected by electroporation, and transfectants selected as described<sup>41</sup>. Culture supernatants were screened for expression of antibody by enzyme-linked immunosorbent assay (ELISA) using hen egg lysozyme (Sigma)-coated plates and horseradish peroxidase (HRP)-conjugated anti-human Fc (Sigma). Positive clones were expanded further for protein production.

Expression, purification and labeling of recombinant proteins. Recombinant human IgG1 proteins (wild type and MST-HN variant; both lysozyme specific) were purified from culture supernatants using lysozyme-sepharose as described<sup>41</sup>. Human IgG1 was radiolabeled with <sup>125</sup>I using iodogen according to methods previously described<sup>45</sup>.

The mouse (IgG1) anti-lysozyme antibody, D1.3, was purified from culture supernatants of the D1.3 hybridomas<sup>46</sup> (generously provided by Roy Mariuzza, Center for Advanced Research in Biotechnology, Rockville, MD, USA) using lysozyme-sepharose. Mouse or human IgG1 (wild type or mutants) were labeled using Alexa 546 or Alexa 647 carboxylic acid, succinidyl ester and methods recommended by the manufacturer (Molecular Probes).

Recombinant, soluble human and mouse FcRn were expressed in High-Five cells (Invitrogen) infected with recombinant baculoviruses and protein purified as described<sup>47</sup>.

Surface plasmon resonance analyses. Binding analyses of human or mouse FcRn with immobilized IgGs were carried out as described previously<sup>27,40</sup>. However, the loss of pH dependence of the MST-HN mutant-mouse FcRn interactions necessitated the use of 100 mM glycine, 100 mM NaCl, pH 2.8 buffer to 'strip' the flow cells after each injection at pH 6.0 (rather than the pH 7.2 buffer used in earlier analyses for FcRn-IgG interactions<sup>27</sup>).

FcRn binds to two sites on IgG that are not equivalent<sup>47,48</sup>. Data were therefore fitted to a two-site binding model involving negative cooperativity<sup>49</sup>. This generated estimates for two dissociation constants ( $K_{D1}$  and  $K_{D2}$ ) that are taken to represent occupancy of the higher affinity site ( $K_{D1}$ ) followed by occupancy of the lower affinity site ( $K_{D2}$ )<sup>49</sup>.

Analyses of *in vivo* properties of IgGs. HMEC-1 cells (from the Centers for Disease Control; generously provided by F. Candali) were cotransfected with mouse FcRn-GFP and mouse  $\beta$ 2-microglobulin expression plasmids using Amaxa nucleofector technology (Amaxa) and incubated in phenol red-free Hams 12K medium depleted of bovine IgGs as described<sup>10</sup>. To assess IgG uptake, about 20 h after transfection cells were incubated with 20  $\mu$ M of Alexa 647-labeled, wild-type human or mouse IgG1, or mutated human IgG1 (MST-HN) at 37 °C in a 5% CO<sub>2</sub> incubator for 60 min. Cells were then washed, fixed and mounted for fluorescence microscopy as described<sup>10</sup>.

To assess the recycling of mouse IgG1, transfected cells were incubated with 20  $\mu$ M wild-type or mutated (MST-HN) human IgG1 for 60 min as above, and Alexa 647-labeled mouse IgG1 was added at a concentration of 250  $\mu$ M for a further 60 min. Cells were then washed and processed immediately (no chase) or incubated in phenol red-free Hams 12K medium for a further 40 min. After each treatment, cells were trypsinized, washed and stored on ice. Amounts of cell-associated Alexa 647-labeled mouse IgG1 at each time point were quantified by flow cytometry using a FACScaliber. Data were processed using WinMDI2.8 (J. Trotter, Scripps Research Institute, La Jolla, CA, USA). To assess the intracellular location of mouse IgG1 in MST-HN pretreated transfectants, cells were pretreated as above and then incubated with 250  $\mu$ M Alexa 546-labeled mouse IgG1 and Alexa 647-labeled dextran (Molecular

Probes) for 60 min. Cells were washed, chased in medium for 40 min, and then washed, fixed and mounted for fluorescence microscopy analyses.

**Fluorescence microscopy.** Images were acquired using a Zeiss Axiocvert 200M inverted fluorescence microscope with a 100 $\times$  PlanApo objective as described previously<sup>10</sup>. Data were processed using custom written software in the programming language Matlab (MATLAB/LABSoft p1.0.0; <http://www4.utsouthwestern.edu/wardlab/matlab/>).

**ELISA.** ELISA was used to determine total serum IgG levels in mice. We coated 96-well plates with rabbit anti-mouse IgG (heavy-chain specific; Zymed) and then non-specific sites were blocked with 1% bovine serum albumin in PBS. Dilutions (1:40,000–1:120,000) of serum samples were made in PBS and then added to the wells. Bound mouse IgGs were detected using HRP-conjugated rabbit anti-mouse IgG (heavy- and light-chain specific; Zymed). A standard curve was generated using purified mouse IgGs (The Binding Site).

**Analyses of the *in vivo* effects of mutated human IgG1 molecules.** To assess the effect of the mutated (MST-HN) human IgG1 on the clearance of <sup>125</sup>I-labeled wild-type human IgG1, mice were injected intraperitoneally with <sup>125</sup>I-labeled human IgG1 (wild type) and levels of radioactivity assessed by whole-body counting (using an AtomLab 100 Dose Calibrator). 72 h later, mice were injected intravenously with 500  $\mu$ g of either wild-type human IgG1, or 500 or 200  $\mu$ g mutated (MST-HN) human IgG1. Six mice per treatment group were used. Levels of radiolabeled human IgG1 were determined at the indicated times after injection of wild-type or mutated IgG1 by whole-body counting.

To analyze the effects of the mutated (MST-HN) human IgG1 on the levels of serum IgGs in mice, IgG levels in serum samples taken at two different time points (24 h apart) were determined by ELISA (above). Mice were then injected intravenously with 500  $\mu$ g wild-type human IgG1 or 500  $\mu$ g mutated (MST-HN) human IgG1. Six mice per treatment group were used. Serum levels of endogenous (mouse) IgGs were determined by ELISA at the indicated times after injection.

*Note: Supplementary information is available on the Nature Biotechnology website.*

## ACKNOWLEDGMENTS

We are grateful to Fernando Mateos, Jerry Chao and Rafael Guevara for excellent technical assistance. We also thank Steven Gibbons and Strid Ram for assistance with preparation of the figures. This study was supported by grants from the National Institutes of Health R01 AI 39167, R01 AI 55556 (E.S.W.) and R01 AI 50747 (R.J.O.).

## COMPETING INTERESTS STATEMENT

The authors declare competing financial interests (see the *Nature Biotechnology* website for details).

Published online at <http://www.nature.com/naturebiotechnology/>

Reprints and permissions information is available online at <http://npg.nature.com/reprintsandpermissions/>

- Souriau, C. & Hudson, P.J. Recombinant antibodies for cancer diagnosis and therapy. *Expert Opin. Biol. Ther.* **3**, 305–318 (2003).
- Weiner, L.M. & Carter, P. Tunable antibodies. *Nat. Biotechnol.* **23**, 556–557 (2005).
- Lewis, E.J. & Schwartz, M.M. Pathology of lupus nephritis. *Lupus* **14**, 31–38 (2005).
- Dickinson, B.L. et al. Bidirectional FcRn-dependent IgG transport in a polarized human intestinal epithelial cell line. *J. Clin. Invest.* **110**, 903–911 (1999).
- McCarthy, K.M., Young, Y. & Simister, N.E. Bidirectional transcytosis of IgG by the neonatal Fc receptor expressed in a rat kidney cell line: a system to study protein transport across epithelia. *J. Cell Sci.* **113**, 1277–1285 (2000).
- Anfoh, F., Rodriguez, L., Gafencu, A., Ghelisi, V. & Simionescu, M. Expression of functionally active FcRn and the differentiated bidirectional transport of IgG in human placental endothelial cells. *Hum. Immunol.* **62**, 93–105 (2001).
- Kobayashi, N. et al. FcRn-mediated transcytosis of immunoglobulin G in human renal proximal tubular epithelial cells. *Am. J. Physiol. Renal Physiol.* **282**, F358–F365 (2002).
- Spiekermann, G.M. et al. Receptor-mediated immunoglobulin G transport across mucosal barriers in adult life: functional expression of FcRn in the mammalian lung. *J. Exp. Med.* **196**, 303–310 (2002).
- Claypool, S.M. et al. Bidirectional transepithelial IgG transport by a strongly polarized basolateral membrane Fc $\gamma$  receptor. *Mol. Biol. Cell* **15**, 1746–1759 (2004).
- Ober, R.J., Martinez, C., Vaccaro, C., Zhou, J. & Ward, E.S. Visualizing the site and dynamics of IgG salvage by the MHC class I-related receptor, FcRn. *J. Immunol.* **172**, 2021–2029 (2004).

11. Ober, R.J., Martinez, C., Lai, X., Zhou, J. & Ward, E.S. Exocytosis of IgG as mediated by the receptor, FcRn: an analysis at the single-molecule level. *Proc. Natl. Acad. Sci. USA* **101**, 11076–11081 (2004).
12. Rodewald, R. & Kraehenbuehl, J.P. Receptor-mediated transport of IgG. *J. Cell Biol.* **99**, 159–164 (1984).
13. Simister, N.E. & Rees, A.R. Isolation and characterization of an Fc receptor from neonatal rat small intestine. *Eur. J. Immunol.* **15**, 733–738 (1985).
14. Ghetie, V. et al. Abnormally short serum half-lives of IgG in beta 2-microglobulin-deficient mice. *Eur. J. Immunol.* **26**, 690–696 (1996).
15. Jungbluth, R.P. & Anderson, C.L. The protection receptor for IgG catabolism is the beta 2-microglobulin-containing neonatal intestinal transport receptor. *Proc. Natl. Acad. Sci. USA* **93**, 5512–5516 (1996).
16. Israel, E.J., Wisker, D.F., Hayes, K.C., Schoenfeld, D. & Simister, N.E. Increased clearance of IgG in mice that lack beta 2-microglobulin: possible protective role of FcRn. *Immunology* **89**, 573–578 (1996).
17. Raghavan, M., Bonaguidi, V.R., Morrison, S.L. & Bjorkman, P.J. Analysis of the pH dependence of the neonatal Fc receptor/immunoglobulin G interaction using antibody and receptor variants. *Biochemistry* **34**, 14649–14657 (1995).
18. Popov, S. et al. The stoichiometry and affinity of the interaction of murine Fc fragments with the MHC class I-related receptor, FcRn. *Mol. Immunol.* **33**, 521–530 (1996).
19. Medesan, C., Matsuo, D., Radu, C., Ghetie, V. & Ward, E.S. Deletion of the amino acid residues involved in transcytosis and catabolism of mouse IgG1. *J. Immunol.* **158**, 2211–2217 (1997).
20. Kim, J.K. et al. Mapping the site on human IgG for binding of the MHC class I-related receptor, FcRn. *Eur. J. Immunol.* **29**, 2819–2825 (1999).
21. Martin, W.L., West, A.P.J., Gan, L. & Bjorkman, P.J. Crystal structure at 2.8 Å of an FcRn/heterodimeric Fc complex: mechanism of pH dependent binding. *Mol. Cell* **7**, 867–877 (2001).
22. Shields, R.L. et al. High resolution mapping of the binding site on human IgG1 for Fc gamma RI, Fc gamma RII, Fc gamma RIII, and FcRn and design of IgG1 variants with improved binding to the Fc gamma RI. *J. Biol. Chem.* **276**, 6591–6604 (2001).
23. Kabat, E.A., Wu, T.T., Perry, H.M., Gottesman, K.S. & Foeller, C. (eds.) *Sequences of Proteins of Immunological Interest* (US Dept. of Health and Human Services, Bethesda, MD, 1991).
24. Ghetie, V. et al. Increasing the serum persistence of an IgG fragment by random mutagenesis. *Nat. Biotechnol.* **15**, 637–640 (1997).
25. Hinton, P.R. et al. Engineered human IgG antibodies with longer serum half-lives in primates. *J. Biol. Chem.* **279**, 6213–6216 (2004).
26. Dall'Aquila, W. et al. Increasing the affinity of a human IgG1 to the neonatal Fc receptor: biological consequences. *J. Immunol.* **169**, 5171–5180 (2002).
27. Zhou, J., Johnson, J.E., Ghetie, V., Ober, R.J. & Ward, E.S. Generation of mutated variants of the human form of the MHC class I-related receptor, FcRn, with increased affinity for mouse immunoglobulin G. *J. Mol. Biol.* **332**, 901–913 (2003).
28. Yoshida, M. et al. Human neonatal Fc receptor mediates transport of IgG into luminal secretions for delivery of antigens to mucosal dendritic cells. *Immunology* **20**, 769–783 (2004).
29. Barryman, M. & Rodewald, R. Beta 2-microglobulin co-distributes with the heavy chain of the intestinal IgG-Fc receptor throughout the transepithelial transport pathway of the neonatal rat. *J. Cell Sci.* **108**, 2347–2360 (1995).
30. Semple, J.W. Immune pathophysiology of autoimmune thrombocytopenic purpura. *Blood Rev.* **16**, 9–12 (2002).
31. Israel, E.J., Patel, V.K., Taylor, S.F., Marshak-Rothstein, A. & Simister, N.E. Requirement for a beta 2-microglobulin-associated Fc receptor for acquisition of maternal IgG by fetal and neonatal mice. *J. Immunol.* **154**, 6246–6251 (1995).
32. Firan, M. et al. The MHC class I related receptor, FcRn, plays an essential role in the maternal-fetal transfer of gamma globulin in humans. *Int. Immunol.* **13**, 993–1002 (2001).
33. Takai, T. Fc receptors and their role in immune regulation and autoimmunity. *J. Clin. Immunol.* **25**, 1–18 (2005).
34. Bleeker, W.K., Teeling, J.L. & Hack, C.E. Accelerated autoantibody clearance by intravenous immunoglobulin therapy: studies in experimental models to determine the magnitude and time course of the effect. *Blood* **98**, 3136–3142 (2001).
35. Samuelsson, A., Towers, T.L. & Ravetch, J.V. Anti-inflammatory activity of IVIG mediated through the inhibitory Fc receptor. *Science* **291**, 484–486 (2001).
36. Mouthon, L. et al. Mechanisms of action of intravenous immune globulin in immune-mediated diseases. *Clin. Exp. Immunol.* (suppl.) **1**, 104, 3–9 (1996).
37. Yu, Z. & Lennon, V.A. Mechanism of intravenous immune globulin therapy in antibody-mediated autoimmune diseases. *N. Engl. J. Med.* **340**, 227–228 (1999).
38. Akle, S. et al. The MHC class II-like Fc receptor promotes humoral mediated autoimmune disease. *J. Clin. Invest.* **113**, 1328–1333 (2004).
39. Ober, R.J., Radu, C.G., Ghetie, V. & Ward, E.S. Differences in promiscuity for antibody-FcRn interactions across species: implications for therapeutic antibodies. *Int. Immunol.* **13**, 1551–1559 (2001).
40. Zhou, J., Mateos, F., Ober, R.J. & Ward, E.S. Confirming the binding properties of the mouse MHC class I-related receptor, FcRn, onto the human ortholog by sequential rounds of site-directed mutagenesis. *J. Mol. Biol.* **345**, 1071–1081 (2005).
41. Foote, J. & Winter, G. Antibody framework residues affecting the conformation of the hypervariable loops. *J. Mol. Biol.* **224**, 487–499 (1992).
42. Horton, R.M., Hunt, H.D., Ho, S.N., Pullen, J.K. & Pease, L.R. Engineering hybrid genes without the use of restriction enzymes: gene splicing by overlap extension. *Gene* **77**, 61–68 (1989).
43. O'Connell, K.A. & Eddin, M. A mouse lymphoid endothelial cell line immortalized by simian virus 40 binds lymphocytes and retains functional characteristics of normal endothelial cells. *J. Immunol.* **144**, 521–525 (1990).
44. Brewer, C.B. Cytochrome P-450 plasmid vectors for permanent lines of polarized epithelial cells. *Methods Cell Biol.* **43**, Pt A, 233–245 (1994).
45. Kim, J.K., Tsou, M.F., Ghetie, V. & Ward, E.S. Identifying amino acid residues that influence plasma clearance of murine IgG1 fragments by site-directed mutagenesis. *Eur. J. Immunol.* **24**, 542–548 (1994).
46. Amlt, A.G., Mariluzzi, R.A., Phillips, S.E. & Poljak, R.J. Three-dimensional structure of an antigen-antibody complex at 2.8 Å resolution. *Science* **233**, 747–753 (1986).
47. Schuck, P., Radu, C.G. & Ward, E.S. Sedimentation equilibrium analysis of recombinant mouse FcRn with murine IgG1. *Mol. Immunol.* **36**, 1117–1125 (1999).
48. Martin, W.L. & Bjorkman, P.J. Characterization of the 2:1 complex between the class I MHC-related Fc receptor and its Fc ligand in solution. *Biochemistry* **38**, 12639–12647 (1999).
49. Deisenhofer, J. Crystallographic refinement and atomic models of a human Fc fragment and its complex with fragment B of protein A from *Staphylococcus aureus* at 2.9- and 2.8-Å resolution. *Biochemistry* **20**, 2361–2370 (1981).

## Research Paper

# PEGylation of Octreotide: II. Effect of N-terminal Mono-PEGylation on Biological Activity and Pharmacokinetics

Dong Hee Na,<sup>1</sup> Kang Choon Lee,<sup>2</sup> and Patrick P. DeLuca<sup>1,3,4</sup>

Received October 6, 2004; accepted February 4, 2005

**Purpose.** To determine the optimal polyethylene glycol (PEG)-conjugate of octreotide by evaluating the effects of PEGylation chemistry on the biological activity and pharmacokinetic properties.

**Methods.** Octreotide was chemically modified by reaction with succinimidyl propionate monomethoxy PEG (SPA-mPEG, molecular weight 2000) or succinimidyl butyraldehyde-mPEG (ALD-mPEG, molecular weight 2000 and 5000). The structural conformation of PEG-octreotides was evaluated by circular dichroism (CD), the biological activity was assessed by measuring the decrease of serum insulin-like growth factor-I levels in rats, and a pharmacokinetic study was performed after subcutaneous administration in rats. The stability against acylation was investigated with poly(D,L-lactide-co-glycolide) (PLGA).

**Results.** ALD-mPEG was site-specific in PEGylating octreotide at the N-terminus. The mono-PEG-octreotides prepared with ALD-mPEG (mono-ALDPEG-octreotide), which alkyl bond preserves the amine's positive charge, showed complete preservation of biological activity, whereas the PEG-octreotides prepared with SPA-mPEG showed lower activity. In the CD analysis, the spectra of the mono-ALDPEG-octreotides were nearly superimposable with that of native octreotide. The mono-ALDPEG-5K-octreotide showed significantly improved pharmacokinetic properties compared with mono-ALDPEG-2K-octreotide as well as native octreotide. Both mono-ALDPEG-2K- and mono-ALDPEG-5K-octreotides were stable against acylation by degrading PLGA.

**Conclusions.** The mono-PEGylation of octreotide at N-terminus with ALD-mPEG produced a conjugate that is biologically and structurally active and stable against acylation by PLGA, and therefore it may serve as a candidate for somatostatin microsphere formulations.

**KEY WORDS:** biological activity; octreotide; site-specific PEGylation; pharmacokinetics; stability.

## INTRODUCTION

Octreotide, a synthetic octapeptide analogue of somatostatin, is clinically used for the treatment of acromegaly and certain endocrine tumors (1,2). It has been commercially formulated in poly(D,L-lactide-co-glycolide) (PLGA) microspheres (Sandostatin LAR depot, Novartis Pharma, Basel, Switzerland) for intramuscular administration on a monthly basis. In addition to the convenience of a monthly injection, the depot preparations showed the same or even increased effectiveness compared with three-daily subcutaneous injections in lowering growth hormone and insulin-like growth factor (IGF)-I (3).

Although biodegradable poly(D,L-lactide) (PLA) and PLGA have been widely used for the long-term controlled release of peptides and proteins, the acidic microenvironment inside the matrix due to degradation of PLA and PLGA has

been reported to cause instability (4–6). Recently, it was shown that peptide impurities formed within the degrading PLA or PLGA matrix by acylation with lactic and glycolic acid units (7–9) and that lactoyl and glycolyl adducts of octreotide formed after *in vitro* incubation of microspheres in phosphate buffer saline (10).

The covalent attachment of polyethylene glycol (PEG) to the peptide, PEGylation, appears to be a promising approach for stabilizing octreotide because it has been widely used to improve the chemical and biological stability of salmon calcitonin, a 32-amino-acid peptide (11,12). PEGylated octreotide (PEG-octreotide) showed much better stability than native octreotide against acylation in lactic acid solutions (13). In addition, an interaction study with hydrophilic and hydrophobic PLGA showed that N-terminal PEGylation could effectively prevent acylation of octreotide by degrading PLGA (14). The stability of N-terminally PEGylated octreotide may be attributed to the lowered nucleophilic reactivity of the Lys residue in octreotide and the steric hindrance of the PEG strand.

The objective of this study was to assess the best PEG-octreotide that is biologically active and stable against acylation with PLGA for microsphere delivery. Besides the advantageous effects of PEGylation such as stabilization and longer circulation half-life, the problem of preserving the biological activity of biomolecules after PEGylation is particularly im-

<sup>1</sup> College of Pharmacy, Kyungsu University, Busan, South Korea.

<sup>2</sup> Drug Targeting Laboratory, College of Pharmacy, SungKyunKwan University, Suwon City, South Korea.

<sup>3</sup> University of Kentucky College of Pharmacy, Lexington, Kentucky, USA.

<sup>4</sup> To whom correspondence should be addressed. (e-mail: ppdeluca@uky.edu)

portant with a small peptide. A number of factors, for example, PEGylation site, PEG size, and linkage between peptide and PEG, can affect the biological activity (15). Morpurgo *et al.* reported the effects of the type and location of PEGylation on the structural and biological activity of different mono-PEGylated somatostatin analogue RC160 (16). In the current study, PEG-octreotides with different PEGylation sites and linkages were prepared with two PEG reagents having different functional groups. PEGylation with the *N*-hydroxysuccinimidyl ester-activated PEG nonspecifically resulted in two mono- and one di-PEG-octreotide, whereas that with aldehyde-activated PEG produced *N*-terminally mono-PEGylated octreotide in a site-specific manner (17). Their structural conformations were evaluated by circular dichroism, and biological activity was assessed by measuring the decrease of serum IGF-I levels in rats. The pharmacokinetic parameters were assessed after subcutaneous administration to rats, and the stability against acylation by PLGA was evaluated.

## MATERIALS AND METHODS

### Materials

Octreotide acetate (MW 1019.26) was obtained from Bachem (Torrance, CA, USA). Succinimidyl propionate-monomethoxy PEG (SPA-mPEG, MW 2000) and butyraldehyde-mPEG (ALD-mPEG, MW 2000 and 5000) were purchased from Nektar Therapeutics (Huntsville, AL, USA). Hydrophilic 50:50 PLGA polymers (Resomer RG502H) was supplied by Boehringer Ingelheim (Ingelheim, Germany).  $\alpha$ -Cyano-4-hydroxycinnamic acid ( $\alpha$ -CHCA), Endoproteinase Lys-C (from *Lysobacter* enzymes, sequencing grade), and dithiothreitol (DTT) were purchased from Sigma (St. Louis, MO, USA). Acetonitrile (HPLC grade) was supplied from Fisher Scientific (Fair Lawn, NJ, USA). Trifluoroacetic acid (TFA) was obtained from Pierce (Rockford, IL, USA). All other chemicals were of analytical grade and used as obtained commercially.

### PEGylation of Octreotide

Site-specific PEGylation of *N*-terminus in octreotide with ALD-mPEG was carried out in the presence of 20 mM sodium cyanoborohydride ( $\text{NaCNBH}_3$ ) in 0.1 M acetate buffer at pH 5. The reaction was performed with different molar ratios of 1:1, 1:2, and 1:3 (octreotide:ALD-mPEG) at 4°C overnight. PEGylation with SPA-mPEG at a molar ratio of 1:1, 1:2, and 1:3 (octreotide:SPA-mPEG) was performed in 0.1 M sodium phosphate buffer (pH 6) for 1 h at room temperature. Each reaction was repeated in triplicate. The PEGylation reaction mixtures were loaded onto reversed-phase high-performance liquid chromatography (RP-HPLC) and the PEG-octreotides were isolated. The purified PEG-octreotides were freeze-dried after evaporation of organic solvent with a Speed-Vac (Eppendorf, Hamburg, Germany). The molecular weights of the PEG-octreotides were determined by matrix-assisted laser desorption/ionization time-of-flight mass spectrometry (MALDI-TOF MS).

### Identification of PEGylation Sites

PEGylation sites were identified as described previously (18,19). PEG-octreotides were treated with DTT at a final

concentration of 5 mM for 4 h to reduce the disulfide bond. Thereafter, enzymatic digestion with endoproteinase Lys-C was performed in 0.1 M Tris-HCl buffer (pH 8.0) at 37°C with an enzyme to substrate ratio of 1:100 (w/w) for 4 h. The concentrations of PEG-octreotides were 200  $\mu\text{g/ml}$ . The Lys-C digests were directly analyzed by MALDI-TOF MS. The PEGylation sites were determined by measuring molecular weights of PEG-octreotide fragments digested with Lys-C.

### RP-HPLC

The PEGylation reaction mixtures were loaded onto a HPLC system (2 LC-6A pumps, SIL-6B autoinjector, SPD-6AV detector and SCL-6B system controller from Shimadzu Scientific Instruments, Inc., Columbia, MD, USA). A Prosphere C-18 column ( $4.6 \times 250$  mm, Alltech, Deerfield, IL, USA) with guard column ( $4.6 \times 7.5$  mm) was used with a mobile phase A (0.1% [v/v] TFA in water) and B (0.1% [v/v] TFA in acetonitrile). The gradient elution conditions for octreotides modified with SPA-mPEG and ALD-mPEG were 65:35 to 50:50 and 70:30 to 40:60 (A:B), respectively, for 20 min at a flow rate of 1.0 ml/min, and the chromatograms were recorded by UV detection at 215 nm.

### MALDI-TOF MS

The molecular weights of the PEG-octreotides were obtained on a Kratos Kompact SEQ time-of-flight mass spectrometer (Manchester, UK) (20). The  $\alpha$ -CHCA in 50% acetonitrile in water with 0.1% TFA was used as matrix. Data for 2-ns pulses of the 337-nm nitrogen laser were averaged for each spectrum in a linear mode, and a positive ion TOF detection was performed using an accelerating voltage of 20 kV.

### Circular Dichroism

Circular dichroism (CD) spectra were recorded in the range of 190–250 nm with a Jasco J-710 spectropolarimeter (Easton, MD, USA) using a CD cell of 0.1-cm pathlength and a bandwidth of 1 nm. A scan speed of 20 nm/min was used with an average of five scans per sample. The spectra were expressed as the mean residue molar ellipticity in  $\text{deg}\cdot\text{cm}^2/\text{dmol}$ . Peptide concentrations were precisely determined by RP-HPLC and set to 200  $\mu\text{g/ml}$  in 0.1 M phosphate buffer (pH 7.4).

### Biological Activity

Male Sprague-Dawley rats ( $n = 6$  per sample), weighing 220–250 g, were used to evaluate biological activity of octreotide and PEG-octreotides. The animals were housed in groups of two in a well-ventilated environment under controlled temperature ( $22 \pm 1^\circ\text{C}$ ) and humidity ( $60 \pm 5\%$ ), with food and water available *ad libitum*. The octreotide and PEG-octreotides dissolved in water for injection (WFI) were injected subcutaneously at the back of the neck at a dose of 200  $\mu\text{g}$  peptide/kg. The injections were repeated at 2, 24, and 26 h. A control group received WFI. Blood samples were removed from the tail vein at 0, 2, 4, 24, 26, 28, and 30 h, centrifuged in Microtainer tubes (Becton Dickinson, Franklin Lakes, NJ, USA), and the collected serum was frozen and stored at  $-20^\circ\text{C}$  until analysis. The IGF-I levels were determined by radioimmunoassay (RIA) with a Rat IGF-I RIA kit having a sensitivity of 21 ng/ml (Diagnostic Systems Laboratories,

Webster, TX, USA). Serum IGF-I levels of the animal prior to administration of octreotide were set to 100% (initial value), and the averaged IGF-I levels after administration (at 26, 28, and 30 h) were expressed as percent of initial value.

### Pharmacokinetic Study

Octreotide and PEG-octreotides in WFI (100 µg/ml) were subcutaneously injected into male Sprague-Dawley rats weighing 220–250 g ( $n = 6$  per sample) at a dose of 100 µg/kg octreotide. Samples were taken at 0, 0.5, 1, 2, 3, 4, and 6 h, and the serum octreotide levels were determined by RIA (Peninsula Laboratories Inc., San Carlos, CA, USA). A standard calibration curve was constructed using native or mono-ALDPEG-octreotides. Pharmacokinetic parameters were determined using a noncompartmental pharmacokinetic model using WinNonLin 4.1 software (Pharsight, Mountain View, CA, USA).

### Interaction with Polymers

One hundred milligrams of RG502H was added to 10 ml of octreotide or mono-ALDPEG-octreotide (peptide concentration of 200 µg/ml) in 0.1 M phosphate buffer (pH 7.4) at 37°C. Samples were collected at 1, 3, 7, 14, 21, 28, 35, 42, and 49 days, centrifuged, and the supernatant analyzed by RP-HPLC. The gradient elution conditions for octreotide and mono-ALDPEG-octreotide were 80:20 to 65:35 and 70:30 to 40:60 (A:B), respectively, for 20 min at a flow rate of 1.0 ml/min, and the chromatograms were recorded by UV detection at 215 nm.

### Statistical Analysis

The biological activity and pharmacokinetic parameters were subjected to an unpaired Student's *t* test using Microsoft Excel Software. A *p* value <0.05 was considered as significant.

## RESULTS AND DISCUSSION

### Preparation and Characterization of PEG-Octreotides

General amine PEGylation using SPA-mPEG with *N*-hydroxysuccinimide (NHS) ester structure will modify the N-terminus and Lys residue of octreotide, whereas that with ALD-mPEG, having an aldehyde group, can be site-specific for the N-terminus in the presence of sodium cyanoborohydride at acidic pH (Fig. 1). Specific PEGylation at the

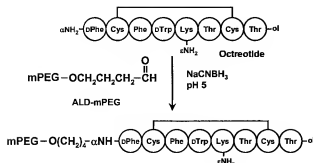


Fig. 1. Schematic diagram for the specific N-terminal PEGylation of octreotide.

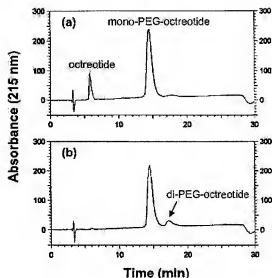


Fig. 2. RP-HPLC chromatograms of octreotides reacted with ALD-mPEG-2K. The reaction molar ratios (octreotide:ALD-mPEG-2K) were 1:2 (a) and 1:3 (b).

N-terminus is based on the difference in reactivity of the  $\alpha$ -amino group in the N-terminus ( $\text{pK}_a = 7.8$ ) and  $\epsilon$ -amino group in the Lys residue ( $\text{pK}_a = 10.1$ ) at acidic pH (21). The N-terminally site-specific PEGylation with ALD-mPEG forms a secondary amine linkage and thus preserves the positive charge on the N-terminal amino group, whereas the PEGylation with SPA-mPEG leads to an amide bond, which removes the charge on the amino groups of the N-terminus or Lys residue.

Figure 2 shows the RP-HPLC chromatograms of octreotide and ALD-mPEG-2K mixtures at different molar ratios. The mono-ALDPEG-octreotide was preferentially produced at a molar ratio of 1:3 (octreotide:ALD-mPEG-2K). Table I shows the characterization of the PEG-octreotides by MALDI-TOF MS after isolation by RP-HPLC and Lys C digestion. Three PEG-octreotides were produced with SPA-mPEG, that is, mono-SPAPEG-Phe<sup>1</sup>-, mono-SPAPEG-Lys<sup>2</sup>-, and di-SPAPEG-octreotide, while a single mono ALDPEG-Phe<sup>1</sup>-octreotide was produced with ALD-mPEG-2K and -5K reagents. The PEGylation sites were determined by measurement of the mass change based on the PEG resistance to the proteolytic cleavage during Lys C digestion (18,19). As the octreotide has only one lysine residue, PEGylation at this site would show no mass change when treated with Lys-C after

Table I. Characterization of PEG-Octreotides by MALDI-TOF MS

Sample	Mass <sup>a</sup> of insect molecule	Mass after Lys C digestion
Mono-ALDPEG-2K-Phe <sup>1</sup> -octreotide	3287	2934
Mono-ALDPEG-5K-Phe <sup>1</sup> -octreotide	6505	6149
Mono-SPAPEG-2K-Phe <sup>1</sup> -octreotide	3243	2930
Mono-SPAPEG-2K-Lys <sup>2</sup> -octreotide	3242	3242
Di-SPAPEG-2K-octreotide	5534	5534

The molecular mass of octreotide is 1019 Da.

<sup>a</sup> The number is centroided mass value of the polydisperse peaks.

Table II. PEGylation of Octreotides at Various Molar Ratios

PEG	Molar ratio (octreotide:PEG)	% Composition in reaction mixture <sup>a</sup>			
		Octreotide	Mono-PEG-Phe <sup>1</sup> -octreotide	Mono-PEG-Lys <sup>5</sup> -octreotide	Di-PEG-octreotide
ALD-PEG-2K	1:1	52 ± 3.9	48 ± 3.9	—	—
	1:2	13 ± 2.2	83 ± 3.5	—	4 ± 1.0
	1:3	1 ± 0.2	89 ± 2.9	—	10 ± 1.2
ALD-PEG-5K	1:1	27 ± 4.1	73 ± 4.1	—	—
	1:2	8 ± 1.5	90 ± 3.0	—	2 ± 0.8
	1:3	—	76 ± 2.8	—	24 ± 2.8
SPA-PEG-2K	1:1	58 ± 2.6	28 ± 3.1	10 ± 2.2	4 ± 1.8
	1:2	23 ± 2.3	44 ± 3.8	13 ± 2.9	20 ± 1.4
	1:3	10 ± 1.1	44 ± 3.2	11 ± 1.9	35 ± 2.6

<sup>a</sup> Mean value ± SD, n = 3.

reduction of the disulfide bond with DTT. However, such treatment of the mono-PEG-octreotide modified at the N-terminus would result in the reduced mass fragment. The mass changes of approximately 350 Da in the mono-ALDPEG forms demonstrate site-specific PEGylation at the N-terminus. The identities of mono- and di-SPAPEG-2K-octreotides were also confirmed by measuring their intact and Lys-C treated masses.

To optimize site-specific PEGylation condition and investigate the site-specificity, the PEGylation reactions of octreotide with ALD-mPEG-2K, -5K, and SPA-mPEG-2K were monitored at different molar ratios (Table II). The PEGylation with ALD-mPEG-2K and -5K resulted in production of each mono-ALDPEG-octreotide with a yield of approximately 90%. When the reaction was performed at the molar ratio of 1:3 (octreotide:ALD-mPEG), the area percents of di-ALDPEG-2K- and di-ALDPEG-5K-octreotides in reaction mixtures were 10% and 24%, respectively. As the presence of di-ALDPEG-octreotide causes difficulty in separating the mono-ALDPEG-octreotide, the molar ratio of 1:2 was selected for isolating each mono-ALDPEG-octreotide. The PEGylation using SPA-mPEG-2K was performed at pH 6 because the  $\alpha$ -amino group of the N-terminus is more susceptible to the PEGylation reaction at low pH (12). However, the yield of mono-SPAPEG-Phe<sup>1</sup>-octreotide did not exceed 44%.

#### Structural Study by Circular Dichroism

Figure 3 shows the CD spectra of octreotide and the mono-PEG-octreotides prepared with ALD-mPEG-2K, -5K, and SPA-mPEG-2K. The spectra of intact octreotide and mono-PEG-octreotides prepared with ALD-mPEG-2K and -5K were nearly superimposable in the range of 190 to 250 nm, suggesting that PEGylation using ALD-mPEG had no significant effect on the secondary structure of the octreotide. However, mono-PEG-octreotides prepared with SPA-mPEG-2K showed spectral changes in the range of 190 to 210 nm, which might indicate some conformational modification. This result strongly supports the importance of the positive charge for preserving the structural conformation after PEGylation, as previously reported by Moriguchi *et al.* with PEGylated RC160 (16). Concerning the possibility of the involvement of thiol group from the reduction of disulfide bond with N-terminal PEGylation using ALD-mPEG and NaCNBH<sub>3</sub>, no spectral change of mono-ALDPEG-octreotides suggests that the disulfide bond is stable and not involved in

the PEGylation process because the reduction of disulfide bond substantially changes the spectra (22).

#### Biological Activity

Octreotide substantially reduces growth hormone and IGF-I levels in patients with acromegaly (2). It binds with a high affinity to somatostatin receptor subtype 2 and 5 and Phe<sup>2</sup>-Trp<sup>4</sup>-Lys<sup>5</sup>-Thr<sup>6</sup> in the structure is known to be essential for biological activity (23). Serum IGF-I is an important

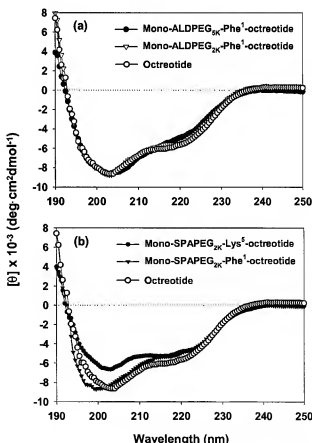


Fig. 3. Circular dichroism of octreotides modified with ALD-mPEGs (a) and SPA-mPEGs (b). The concentrations of PEG-octreotides were set equivalent to 200  $\mu$ g/ml of octreotide.

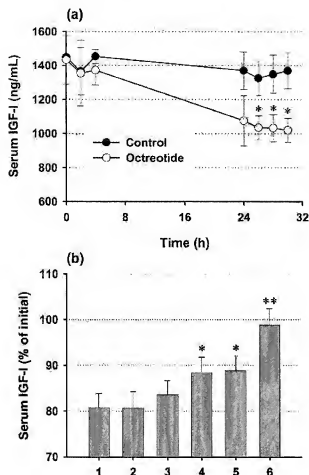


Fig. 4. Biological activities of octreotide and PEG-octreotides. (a) Effect of octreotide on rat IGF-I serum levels after subcutaneous administration at 0, 2, 24, and 26 h. \*Significantly different from control. (b) The changes of rat IGF-I serum levels after 24 h after subcutaneous administration of octreotide and PEG-octreotides (1, octreotide; 2, mono-ALDPEG-2K-octreotide; 3, mono-ALDPEG-5K-octreotide; 4, mono-SPAPEG-2K-Lys<sup>3</sup>-octreotide; 5, mono-SPAPEG-2K-Phe<sup>3</sup>-octreotide; 6, di-SPAPEG-2K-octreotide). Significant differences from native octreotide: \* $p < 0.05$ ; \*\* $p < 0.01$ . Mean  $\pm$  SD,  $n = 6$ .

marker for diagnosis of acromegaly and monitoring the efficacy of treatment (24). The biological activity of PEG-octreotides was evaluated by measuring the capability to decrease serum IGF-I levels in rats. As the IGF-I levels drop slowly in response to somatostatin analogues, multiple samples were administered (25). Figure 4a shows the effect of octreotide serum IGF-I levels after subcutaneous administration to rats. After 24 h, native octreotide showed a reduction of approximately 20% in serum IGF-I levels compared with the initial level. Figure 4b represents the changes of IGF-I levels after 24 h in rats subcutaneously administered with native octreotide and PEG-octreotides. The mono-ALDPEG-octreotides prepared with ALD-mPEG-2K and -5K showed higher reductions of IGF-I levels than the PEG-octreotides prepared with SPA-mPEG. The reduction with mono-ALDPEG-2K-octreotide was comparable to native octreotide. Compared to mono-ALDPEG-2K-octreotide, the lower bioactivity of mono-ALDPEG-5K-octreotide may be

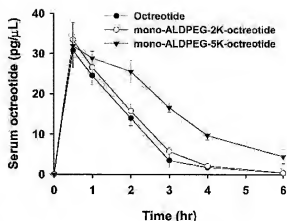


Fig. 5. Average serum concentration-time curves after subcutaneous administration of octreotide, mono-ALDPEG-2K-, and mono-ALDPEG-5K-octreotide. Mean  $\pm$  SD,  $n = 6$ .

attributed to the effect of steric hindrance of PEG on receptor binding. The biological activities of the two mono-SPAPEG-2K-octreotides with different PEGylation sites were not statistically different suggesting the PEGylation site might not have an effect on the biological activity. Di-SPAPEG-2K-octreotide appeared to be inactive. These results further support the importance of the positive charge for preserving the biological activity. The biological activity of somatostatin analogues depends on both their affinity for the cellular receptor and *in vivo* stability. The presence of the positive charge in the primary amino groups of octreotide may be related to the binding affinity to the receptor.

#### Pharmacokinetic Study

PEGylation has been successful in improving the pharmacokinetic properties of peptides and proteins by virtue of increasing the molecular mass and providing protection against proteolytic enzymes (26). Figure 5 shows the average serum concentration-time profiles of octreotide, mono-ALDPEG-2K-, and mono-ALDPEG-5K-octreotide after subcutaneous administration. Although the profile of mono-

Table III. Pharmacokinetic Parameters in Rats After Subcutaneous Administration of Octreotide and PEG-Octreotides ( $n = 6$  per Sample)

	Octreotide	mono-ALDPEG-2K-octreotide	mono-ALDPEG-5K-octreotide
$C_{max}$ (ng/ml)	$30.8 \pm 2.2$	$33.4 \pm 3.2$	$31.9 \pm 2.9$
$t_{1/2}$ (h)	$0.87 \pm 0.3$	$0.83 \pm 0.3$	$1.61 \pm 0.6^a$
$AUC_{0-24h}$ (ng $\cdot$ h/ml)	$54.2 \pm 4.9$	$62.7 \pm 4.6$	$98.0 \pm 6.7^a$
$AUC_{0-\infty}$ (ng $\cdot$ h/ml)	$54.6 \pm 4.8$	$63.2 \pm 4.3$	$108.3 \pm 6.5^a$
Cl (ml/h)	$18.3 \pm 1.9$	$15.8 \pm 1.2$	$9.2 \pm 1.4^a$
$V_{ss}$ (ml)	$22.9 \pm 2.4$	$18.3 \pm 1.4$	$21.5 \pm 2.4$
MRT (h)	$1.46 \pm 1.1$	$1.52 \pm 0.8$	$2.78 \pm 1.5^a$

Mean value  $\pm$  standard deviation.  $C_{max}$ , maximum concentration;  $t_{1/2}$ , biological half-life; AUC, area under the curve; Cl, systemic clearance;  $V_{ss}$ , volume of distribution at steady state; MRT, mean residence time.

<sup>a</sup>Significantly different from native octreotide ( $p < 0.05$ ).

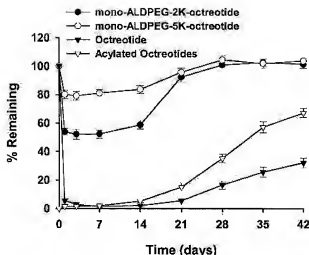


Fig. 6. Interaction of octreotide and mono-ALDPEG-octreotides with PLGA in 0.1 M phosphate buffer (pH 7.4) at 37°C. Mean  $\pm$  SD,  $n = 3$ .

ALDPEG-2K-octreotide was not significantly different from that of native octreotide, mono-ALDPEG-5K-octreotide showed higher serum levels after 1 h compared with octreotide and mono-ALDPEG-2K-octreotide. The pharmacokinetic parameters are shown in Table III. The mono-ALDPEG-5K-octreotide had a longer circulation half-life ( $t_{1/2}$ : 1.61 h) than native octreotide ( $t_{1/2}$ : 0.87 h) and mono-ALDPEG-2K-octreotide ( $t_{1/2}$ : 0.83 h). The AUC was significantly higher for mono-ALDPEG-5K-octreotide than for native octreotide (108.3 vs. 54.6 ng·h/ml). The systemic clearance was significantly lower for mono-ALDPEG-5K-octreotide than for native octreotide (9.2 vs. 18.3 ml/h). The molecular size of PEG plays a crucial role in increasing the circulation time by decreasing the glomerular filtration rate and increasing resistance to proteolytic digestion (26). Knauf *et al.* examined the effects of PEG size on pharmacokinetic

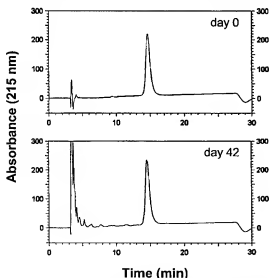


Fig. 7. RP-HPLC chromatograms of mono-ALDPEG-2K-octreotides incubated in 0.1 M sodium phosphate buffer (pH 7.4) at 37°C for 42 days.

behavior using interleukin-2 modified with PEGs of different molecular mass ranging from 0.35 to 20 kDa (27). The circulation half-life remained unaltered with a molecular mass increase of 4 kDa, but increased at a molecular mass >8 kDa. In this study, the attachment of PEG-5K significantly increased the half-life and AUC of octreotide, whereas PEG-2K did not significantly alter the pharmacokinetic behavior.

#### Stability Against Acylation by PLGA

Figure 6 shows the interaction of mono-ALDPEG-octreotides with hydrophilic PLGA (RG502H) in 0.1 M phosphate buffer (pH 7.4) at 37°C. PEGylation of octreotide decreased the initial adsorption to PLGA. Although approximately 95% of the native octreotide was adsorbed within 1 day, the initial adsorption of mono-ALDPEG-2K and mono-ALDPEG-5K-octreotide was 46.2% and 19.9%, respectively. The increase of PEG size is shown to inhibit the interaction with PLGA due to the steric hindrance. As the adsorption is related to the ionic interaction between the carboxylic end groups of the polymer and the primary amino groups of peptide (14), PEG strands might interfere with attraction of the Lys residue to the polymer. At day 28, both mono-ALDPEG-2K- and mono-ALDPEG-5K-octreotides were entirely recovered in an intact form unlike native octreotide with 67% of acylated impurities at day 42. Figure 7 shows RP-HPLC chromatograms of mono-ALDPEG-2K-octreotides before and after incubation with RG502H at pH 7.4 for 42 days. Besides the peaks from the degraded PLGA before 10 min of retention time, only the intact mono-ALDPEG-2K-octreotide was observed with the same peak shape.

#### CONCLUSIONS

N-terminally PEGylated octreotides prepared with the alkyl bond in a site-specific manner showed better structural and biological activity than nonspecifically PEGylated octreotide with amide bond. Both mono-PEG-octreotides prepared with ALDPEG-2K and -5K were also stable against acylation by degrading PLGA. The attachment of ALDPEG-5K to octreotide significantly improved the pharmacokinetic properties compared with that of ALDPEG-2K.

#### ACKNOWLEDGMENTS

This study was supported by Oakwood Laboratories, LLC (Oakwood, OH, USA). The authors appreciate the assistance of Wei Qiu for animal studies. Mass spectral data were obtained at the University of Kentucky Mass Spectrometry Facility. The authors thank Dr. Jack Goodman for MALDI-TOF MS measurements.

#### REFERENCES

1. Marbach, M. Neufeld, and J. Pless. Clinical applications of somatostatin analogues. *Adv. Exp. Med.* 188:339-353 (1985).
2. S. W. Lamberts, A. J. van der Lely, W. W. de Herder, and L. J. Hofland. Octreotide. *N. Engl. J. Med.* 334:246-254 (1996).
3. S. J. Hunter, J. A. Shaw, K. O. Lee, P. J. Wood, A. B. Atkinson, and J. S. Bevan. Comparison of monthly intramuscular injections of Sandostatin LAR with multiple subcutaneous injections of octreotide in the treatment of acromegaly: effects on growth hormone and other markers of growth hormone secretion. *Clin. Endocrinol. (Oxf.)* 50:245-251 (1999).
4. M. van de Weert, W. E. Hennink, and W. Jiskoot. Protein insta-

- bility in poly(lactic-co-glycolic acid) microparticles. *Pharm. Res.* 17:1159-1167 (2000).
5. A. Brunner, K. Mäder, and A. Göpferich. pH and osmotic pressure inside biodegradable microspheres during erosion. *Pharm. Res.* 16:847-853 (1999).
6. K. Fu, D. W. Pack, A. M. Klibanov, and R. Langer. Visual evidence of acidic environment within degrading poly(lactic-co-glycolic acid) (PLGA) microspheres. *Pharm. Res.* 17:100-106 (2000).
7. A. Lucke, J. Kiermaier, and A. Göpferich. Peptide acylation by poly( $\alpha$ -hydroxy esters). *Pharm. Res.* 19:175-181 (2002).
8. A. Lucke, E. Fustella, J. Telfar, A. Gazzaniga, and A. Göpferich. The effect of poly(ethylene glycol)-poly(D,L-lactic acid) diblock copolymers on peptide acylation. *J. Control. Rel.* 80:157-168 (2002).
9. D. H. Na, Y. S. Yoon, S. D. Lee, M. W. Son, W. B. Kim, P. P. DeLuca, and K. C. Lee. Monitoring of peptide acylation inside degrading PLGA microspheres by capillary electrophoresis and MALDI-TOF mass spectrometry. *J. Control. Rel.* 92:291-299 (2003).
10. S. B. Murty, J. Goodman, B. C. Thanoo, and P. P. DeLuca. Identification of chemically modified peptide from poly(D,L-lactide-co-glycolide) microspheres under in vitro release conditions. *AAPS PharmSciTech.* 4:article 50 (2003).
11. K. C. Lee, S. C. Moon, M. O. Park, J. T. Lee, D. H. Na, S. D. Yoo, H. S. Lee, and P. P. DeLuca. Isolation, characterization and stability of positional isomers of mono-PEGylated salmon calcitonins. *Pharm. Res.* 16:818-823 (1999).
12. D. H. Na, Y. S. Yoon, E. J. Park, J. M. Lee, O. R. Cho, K. R. Lee, S. D. Lee, S. D. Yoo, P. P. DeLuca, and K. C. Lee. Stability of PEGylated salmon calcitonin in nasal mucosa. *J. Pharm. Sci.* 93: 256-261 (2004).
13. D. H. Na, S. B. Murty, K. C. Lee, B. C. Thanoo, and P. P. DeLuca. Preparation and stability of PEGylated octreotide for application to microsphere delivery. *AAPS PharmSciTech.* 4:article 72 (2003).
14. D. H. Na and P. P. DeLuca. PEGylation of octreotide: I. Separation of positional isomers and stability against acylation by poly(D,L-lactide-co-glycolide). *Pharm. Res.* 22:736-742 (2005).
15. M. J. Roberts, M. D. Bentley, and J. M. Harris. Chemistry for peptide and protein PEGylation. *Adv. Drug Deliv. Rev.* 54:459-476 (2002).
16. M. Morpurgo, C. Monfardini, L. J. Hoffland, M. Sergi, P. Orsolini, J. M. Dumont, and F. M. Veronese. Selective alkylation and acylation of alpha and epsilon amino groups with PEG in a somatostatin analogue: tailored chemistry for optimized bioconjugates. *Bioconjug. Chem.* 13:1238-1243 (2002).
17. O. B. Kinstler, D. N. Brems, S. L. Lauren, A. G. Paige, J. B. Hamburger, and M. J. Treuheit. Characterization and stability of N-terminally PEGylated rhG-CSF. *Pharm. Res.* 13:996-1002 (1996).
18. D. H. Na, M. O. Park, S. Y. Choi, Y. S. Kim, S. S. Lee, S. D. Yoo, H. S. Lee, and K. C. Lee. Identification of the modifying sites of mono-PEGylated salmon calcitonins by capillary electrophoresis and MALDI-TOF mass spectrometry. *J. Chromatogr. B* 754:259-263 (2001).
19. D. H. Na and K. C. Lee. Capillary electrophoretic characterization of PEGylated human parathyroid hormone with matrix-assisted laser desorption/ionization time-of-flight mass spectrometry. *Anal. Biochem.* 331:322-328 (2004).
20. D. H. Na, Y. S. Yoon, and K. C. Lee. Optimization of the PEGylation process of a peptide by monitoring with matrix-assisted laser desorption/ionization time-of-flight mass spectrometry. *Rapid Commun. Mass Spectrom.* 17:2241-2244 (2003).
21. S. S. Wong. *Chemistry of Protein Conjugation and Cross-linking*, CRC Press, Boca Raton, FL, 1991.
22. S. G. Chang, K. D. Choi, S. H. Jang, and H. C. Shin. Role of disulfide bonds in the structure and activity of human insulin. *Mol. Cells* 16:323-330 (2003).
23. E. Pohl, A. Heine, and G. M. Sheldrick. Structure of octreotide, a somatostatin analogue. *Acta Crystallogr.* D51:48-59 (1995).
24. G. Brabant. Insulin-like growth factor-I: marker for diagnosis of acromegaly and monitoring the efficacy of treatment. *Eur. J. Endocrinol.* 148:S15-S20 (2003).
25. G. Weckbecker, U. Briner, I. Lewis, and C. Bruns. SOM230: A new somatostatin peptidomimetic with potent inhibitory effects on the growth hormone/insulin-like growth factor-I axis in rats, primates, and dogs. *Endocrinology* 143:4123-4130 (2002).
26. P. Caliceti and F. M. Veronese. Pharmacokinetic and biodistribution properties of poly(ethylene glycol)-protein conjugates. *Adv. Drug Deliv. Rev.* 55:1261-1277 (2003).
27. M. J. Knauf, D. P. Bell, P. Hirtzer, Z. P. Luo, J. D. Young, and N. V. Katre. Relationship of effective molecular size to systemic clearance in rats of recombinant interleukin-2 chemically modified with water-soluble polymers. *J. Biol. Chem.* 263:15064-15070 (1988).

## Strategies to improve plasma half life time of peptide and protein drugs

### Review Article

M. Werle<sup>1</sup> and A. Bernkop-Schnürch<sup>2</sup>

<sup>1</sup> ThioMatrix GmbH, Research Center Innsbruck, Innsbruck, Austria

<sup>2</sup> Department of Pharmaceutical Technology, Leopold-Franzens-University, Innsbruck, Austria

Received November 30, 2005

Accepted December 16, 2005

Published online April 20, 2006; © Springer-Verlag 2006

**Summary.** Due to the obvious advantages of long-acting peptide and protein drugs, strategies to prolong plasma half life time of such compounds are highly on demand. Short plasma half life times are commonly due to fast renal clearance as well as to enzymatic degradation occurring during systemic circulation. Modifications of the peptide/protein can lead to prolonged plasma half life times. By shortening the overall amino acid amount of somatostatin and replacing L-analogue amino acids with D-amino acids, plasma half life time of the derivate octreotide was 1.5 hours in comparison to only few minutes of somatostatin. A PEG<sub>240K</sub> conjugate of INF- $\alpha$ -2b exhibited a 330-fold prolonged plasma half life time compared to the native protein. It was the aim of this review to provide an overview of possible strategies to prolong plasma half life time such as modification of N- and C-terminus or PEGylation as well as methods to evaluate the effectiveness of drug modifications. Furthermore, fundamental data about most important proteolytic enzymes of human blood, liver and kidney as well as their cleavage specificity and inhibitors for them are provided in order to predict enzymatic cleavage of peptide and protein drugs during systemic circulation.

**Keywords:** Peptides – Proteins – Plasma half life time – N-C-terminus – PEGylation

### Introduction

Due to the great progress in the field of recombinant technology and biotechnology, it is possible to produce a large number of peptides and proteins in commercial quantities. The majority of these drugs are administered via parenteral routes. Although it is possible to produce a multitude of peptide and protein based drug candidates, many drugs which exhibit promising pharmacological activities fail to show convincing effects *in vivo*. This is due to various reasons, including low stability or unexpected immunogenicity and toxicity. One main problem is that several therapeutic peptides and proteins exhibit a short plasma

half life time. Peptides and proteins often display half life times in the range of few minutes to few hours. Half life times of only few minutes are in most cases not effective in order to deliver sufficient drug amounts to the target tissue. Short plasma half life times are commonly due to fast renal clearance which is connected to the hydrophilic properties of most of these agents as well as their often small size or to enzymatic degradation caused by enzymes occurring in blood, liver and kidney. Strategies to prolong plasma half life time may lead to improved pharmacokinetic profiles of established drugs and may even offer new indications for drug use. Moreover, prolongation of plasma half life time is often a prerequisite for numerous drug candidates for their clinical use at all.

A well known example for a targeted modification is octreotide, a drug which is used in the treatment of gastrointestinal tumors. It is a synthetic peptide based on the amino acid sequence of the endogen hormone somatostatin, which is a 14-peptide tetradecapeptide that inhibits pancreatic exocrine and endocrine secretion. Its clinical application has been limited by its short half life time of only few minutes. To overcome this drawback, octreotide was developed. By shortening the overall amino acid sequence of somatostatin from 14 to 8 and the replacement of L-amino acids by D-amino acids, the enzymatic stability was enhanced which consequently led to an improvement of plasma half life time from few minutes up to 1.5 hours (Harris, 1994).

Due to the fact that a broad variety of proteolytic enzymes occur in the human body, it is important to

Table I. Tissue source of human peptidases/proteases

EC number	Recommended name and synonyms	Blood	Liver	Kidney
2.3.2.2	<i>Gamma-glutamyltransferase</i> gamma-glutamyl transpeptidase, gamma-GPT, gamma-GTase, GGT	X	X	X
3.1.2.12	<i>S-formylglutathione hydrolase</i> FGH, Ubiquitin thioesterase 12		X	
3.3.2.6	<i>Leukotriene-A4 hydrolase</i> LTA-4 hydrolase		X	X
3.4.11.1	<i>Leucyl aminopeptidase</i> aminopeptidase I, cathepsin III, cytosol aminopeptidase, FTBL protein, peptidase S		X	X
3.4.11.2	<i>Membrane alanyl aminopeptidase</i> amino-oligopeptidase, aminopeptidase M, aminopeptidase N, aminopeptidase, microsomal, APN, CD13	X		
3.4.11.3	<i>Cystinyl aminopeptidase</i> alpha-Aminoacyl-peptide hydrolase, insulin-regulated aminopeptidase, IRAP, oxytocinase, P-LAP		X	X
3.4.11.4	<i>Tripeptide aminopeptidase</i> peptidase T			X
3.4.11.5	<i>Prolyl aminopeptidase</i> cytosol aminopeptidase V		X	
3.4.11.6	<i>Aminopeptidase B</i> L-RAP, leukocyte-derived arginine aminopeptidase		X	
3.4.11.7	<i>Glutamyl aminopeptidase</i> aminopeptidase A, angiotensinase A, glutamyl aminopeptidase	X		X
3.4.11.9	<i>X-Pro aminopeptidase</i> aminopeptidase P, AP-P	X		X
3.4.11.14	<i>Cytosol alanyl aminopeptidase</i> Aminopolypeptidase, tripeptidase		X	X
3.4.13.3	<i>X-His dipeptidase</i> aminoacyl-L-histidine hydrolase, carnosinase	X	X	X
3.4.13.9	<i>X-Pro dipeptidase</i> post-proline-cleaving aminopeptidase, prolidase, quiescent cell proline dipeptidase		X	X
3.4.13.18	<i>Cytosol nonspecific dipeptidase</i> DPP8, human cytosolic non-specific dipeptidase, prolyl dipeptidase	X	X	X
3.4.13.19	<i>Membrane dipeptidase</i> MBD, nonspecific dipeptidase			X
3.4.13.20	<i>Beta-Ala-His dipeptidase</i> serum carnosinase	X		
3.4.14.1	<i>Dipeptidyl-peptidase I</i> cathepsin C, cathepsin J, dipeptidyl aminopeptidase I			X
3.4.14.2	<i>Dipeptidyl-peptidase II</i> dipeptidyl peptidase, DP II, DPP-II	X		X
3.4.14.5	<i>Dipeptidyl-peptidase IV</i> (GLP1)-degrading enzyme, ADA binding protein, ADABP, adenosine deaminase binding protein, attractin, CD26, DP IV, glucagon-like peptide 1-degrading enzyme	X		X
3.4.15.1	<i>Peptidyl-dipeptidase A</i> ACE, angiotensin converting enzyme, peptidase P, peptidyl dipeptidase A	X	X	X
3.4.16.2	<i>Lysosomal Pro-X carboxypeptidase</i> endothelial cell prekallikrein activator, HUVEC PK activator, matrix PK activator, PKA, PRCP, prolylcarboxypeptidase, serine protease prolylcarboxypeptidase	X		X
3.4.17.2	<i>Carboxypeptidase B</i> HBPCB, PCB	X		
3.4.17.3	<i>Lysine carboxypeptidase</i> carboxypeptidase N, CPN, Plasma carboxypeptidase B	X	X	X
3.4.17.20	<i>Carboxypeptidase U</i> CPR, TAFI, thrombin-activatable fibrinolysis inhibitor	X	X	

(continued)

Table 1 (continued)

EC number	Recommended name and synonyms	Blood	Liver	Kidney
3.4.17.21	<i>Glutamate carboxypeptidase II</i> Acetylaspartylglutamate dipeptidase, N-Acetylated alpha-linked acidic dipeptidase, Prostate-specific membrane antigen	X		
3.4.18.1	<i>Cathepsin X</i> cathepsin Z, cysteine-type carboxypeptidase		X	
3.4.19.3	<i>Pyroglutamyl-peptidase I</i> aminopeptidase, pyroglutamate, PGPEP1	X		X
3.4.19.9	<i>Gamma-glutamyl hydrolase</i> carboxypeptidase G, folic acid conjugase, polyglutamate hydrolase	X	X	
3.4.21.41	<i>Complement subcomponent C1r</i>	X	X	
3.4.21.42	<i>complement subcomponent C1s</i> protease C1s	X		
3.4.21.B1	<i>hyaluronan-binding serine protease</i> factor seven activating protease, FSAP, PHBP	X	X	X
3.4.21.B7	<i>mannan-binding lectin-associated serine protease 1</i> MASP-1, P100, RaRF	X	X	
3.4.21.B13	<i>protease do</i> HtrA			X
3.4.21.B39	<i>stratum corneum tryptic enzyme</i> K5, kallikrein protein 5, SCTE, stratum-corneum trypsin-like serine protease	X		X
3.4.22.16	<i>cathepsin H</i>		X	X
3.4.22.B13	<i>caspase-9</i>		X	
3.4.22.B40	APAF, ICE-like apoptotic protease 6 <i>caspase-4</i>		X	X
3.4.22.B41	ICH-3 protease, TX protease <i>caspase-5</i>		X	
3.4.23.45	TY protease <i>memapsin 1</i>			X
3.4.24.11	aspartic protease BACE2, protease ASP1 <i>Nephrilysin</i>	X		X
3.4.24.18	acute lymphoblastic leukemia antigen, common acute lymphoblastic leukemia antigen, CALLA, Endopeptidase-2, neutral metallendopeptidase <i>meprin A</i>			X
3.4.24.80	PPH alpha <i>membrane-type matrix metalloproteinase-1</i>		X	
3.4.24.81	<i>ADAM10 endopeptidase</i> metalloproteinase MADM			X
3.4.24.86	<i>ADAM 17 endopeptidase</i> H-TACE, metalloprotease TACE, TNF-alpha processing protease	X		X
3.4.24.B9	<i>ADAM9 endopeptidase</i> cellular disintegrin-related protein, M12.209, MDC-9, meltrin gamma		X	
3.4.24.B13	<i>ADAMTS13 endopeptidase</i> M12.241, van Willebrand factor processing activity, vWF protease	X	X	X

identify the potential enzymes that degrade a certain peptide or protein during systemic circulation. Beside the knowledge regarding tissue localisation of various peptidases and proteases, their cleavage specificity is of particular interest. In the context of enzymatic degradation during systemic circulation, blood, liver and kidney are most important. In order to modify peptides and proteins in an appropriate way to enhance their stability and prolong their plasma half life time it is therefore necessary to know which enzymes cleave the drug and what cleavage specificity is exhibited by the particular proteolytic

enzyme. Beside of proteolytic enzymes, several other types of drug-metabolizing enzymes (DME) occur within the human body such as Cytochrome P450 enzymes. Various reviews dealing with the topic of predicting drug metabolism and human pharmacokinetic parameters from *in vitro* as well as preclinical data are already published (Pelkonen et al., 2005; Obach et al., 1997; Chaturvedi et al., 2001).

It was therefore the aim of this review to provide an overview of the various peptidases and proteases occurring in human blood, liver and kidney and about their

cleavage specificity. Furthermore, methods to evaluate the protective effect of modifications to improve metabolic stability as well as strategies to prolong plasma half life time of peptides and proteins shall be discussed.

## 1. Systemic peptidases and proteases affecting plasma half life time

Referring to plasma half life time, most important compartments concerning enzymatic degradation of peptides

and proteins are in first instance blood, liver and kidney. Orally administered peptides or proteins, which are absorbed from the stomach or the intestine, are transported in the venous blood via the vena portae through the liver to enter systemic circulation.

Parenteral administered drugs have to pass liver and kidney, which are with more than 1 liter blood/min organs which are very well supplied with blood. The liver as well as the kidney contains several proteolytic enzymes. In the kidneys, glomerular ultrafiltrate is pressed

Table 2. Aminopeptidases of human blood, liver and kidney

EC number	Specificity	Localization
3.3.2.6	bifunctional enzyme acting as an epoxid hydrolase and also as an aminopeptidase	Cytosol (erythrocyte, leukocyte, liver) (Samuelson et al., 1989)
3.4.11.1	release of an N-terminal amino acid, Xaa-/Yaa-, in which Xaa is preferably Leu, but may be other amino acids including Pro although not Arg or Lys, and Yaa may be Pro. Amino acid amides and methyl esters are also readily hydrolysed, but rates on arylamides are exceedingly low	Cytoplasm (liver) (Kohno et al., 1986)
3.4.11.2	release of an N-terminal amino acid, Xaa-/Xbb- from a peptide, amide or arylamide, Xaa is preferably Ala, but may be most amino acids including Pro (slow action). When a terminal hydrophobic residue is followed by a prolyl residue, the two may be released as an intact Xaa-Pro dipeptide	Membrane (mucosal membrane) (McClellan et al., 1980)
3.4.11.3	release of an N-terminal amino acid, Cys-/Xaa-, in which the half-cystine residue is involved in a disulphide loop, notably in oxytocin or vasopressin. Hydrolysis rates on a range of aminoacyl arylamides exceed that for the cystinyl derivative, however	Lysosome, mitochondrion, nucleus soluble (Lampelo et al., 1979), membrane (placenta, serum) (Matsumoto et al., 2000)
3.4.11.4	release of N-terminal residue from tripeptide	–
3.4.11.5	release of N-terminal proline from peptide	–
3.4.11.6	release of N-terminal Arg and Lys from oligopeptides when PI' is not Pro, also acts on arylamides of Arg and Lys	Cytosol (leukocyte) (Mendz et al., 1989)
3.4.11.7	release of N-terminal glutamate (and to a lesser extent aspartate) from a peptide	Particle bound (intestine) (Sterchi et al., 1981)
3.4.11.9	release of any N-terminal amino acid, including proline, that is linked to proline, even from a dipeptide or tripeptide	Cytosol (leukocyte, platelet) (Cottrell et al., 2000), extracellular (plasma) (Adam et al., 2002)
3.4.11.14	release of N-terminal amino acid, preferentially alanine, from a wide range of peptides, amides and arylamides	–
3.4.14.1	release of an N-terminal dipeptide, Xaa-Xbb-/Xcc, except when Xaa is Arg or Lys, or Xcc is Pro	Lysosome (kidney) (Cigic et al., 1999)
3.4.14.2	release of an N-terminal dipeptide, Xaa-Xbb-/Xcc, preferentially when Xbb is Ala or Pro. Substrates are oligopeptides preferentially tripeptides	Lysosome (placenta) (Stoeckel-Maschek et al., 2000)
3.4.14.5	release of an N-terminal dipeptide, Xaa-Xbb-/Xcc-, from a polypeptide, preferentially when Xbb is Pro, provided Xcc is neither Pro nor hydroxyproline	Extracellular (seminal plasma, serum), membrane (kidney) (Oefner, 2003)
3.4.19.3	release of an N-terminal pyroglutamyl group from a polypeptide, the second amino acid generally not being Pro	–
3.4.22.16	hydrolysis of proteins, acting as an aminopeptidase as well as an endopeptidase	–
3.4.24.86	narrow endopeptidase specificity. Cleaves Pro-Leu-Ala-Gln-Ala-Val-Arg-Ser-Ser-Ser in the membrane-bound, 26-kDa form of tumor necrosis factor $\alpha$ (TNF $\alpha$ ). Similarly cleaves other membrane-anchored, cell-surface proteins to "shed" the extracellular domains	Cytoplasm (fibroblast, leukocyte) (Reddy et al., 2000), membrane (kidney) (Schloendorff, 2000)

Table 3. Carboxypeptidases of human blood, liver and kidney

EC number	Specificity	Localization
3.4.15.1	release of a C-terminal dipeptide, oligopeptide-/Xaa-Xbb, when Xaa is not Pro, and Xbb is neither Asp nor Glu. Thus, conversion of angiotensin I to angiotensin II, with increase in vasoconstrictor activity, but no action on angiotensin II	Membrane (kidney) (Takada et al., 1981)
3.4.16.2	cleavage of a Pro-/Xaa bond to release a C-terminal amino acid	Lysosome (kidney), membrane (umbilical vein endothelial cell line) (Shariat-Madar et al., 2004)
3.4.17.2	preferential release of a C-terminal lysine or arginine amino acid	—
3.4.17.3	release of C-terminal basic amino acid, preferentially lysine	—
3.4.17.20	release of C-terminal Arg and Lys from a polypeptide	—
3.4.17.21	release of an unsubstituted, C-terminal glutamyl residue, typically from Ac-Asp-Glu or folylpoly- $\gamma$ -glutamates	Membrane (prostate gland) (Gregorkis et al., 1998)
3.4.18.1	release of C-terminal amino acid residues with broad specificity, but lacks action on C-terminal proline. Shows weak endopeptidase activity	—

out of the plasma. Molecules with a molecular mass below 5 kDa and which are not bound to plasma proteins can pass the filter completely, whereas for example only 1% of albumin with a molecular mass of 69 kDa can be found in the glomerular ultrafiltrate. Also secretive and absorptive mechanisms play an important role.

Regarding enzymatic stability, it has to be distinguished between the localisation of the proteolytic enzymes in the particular tissue. Hydrophilic drugs such as peptides and proteins are rather degraded by soluble enzymes occurring in the blood and membrane bound enzymes than by enzymes that occur mainly or exclusively in the cytosol-plasma. Although a broad variety of peptidases and proteases occur in the above mentioned tissues, it must be taken into consideration that most of them exhibit narrow cleavage specificity. In Table 1, an overview about peptidases and proteases occurring in human blood, liver and kidney is provided.

Exopeptidases can be divided into two groups, amino- and carboxypeptidases. Aminopeptidases cleave peptides at the N-terminal whereas carboxypeptidases cleave peptides at the C-terminal site. Several exopeptidases occurring in human blood, liver and plasma as well as there preferred cleavage sites are listed in Tables 2 and 3. Information concerning cleavage specificity of proteolytic enzymes was summarized from the enzyme database at <http://www.brenda.uni-koeln.de>. As mentioned above, the localization of peptidases and proteases in the particular tissue is important. Therefore information about tissue localization is also provided in Tables 2 and 3.

In Table 4, dipeptidases and endopeptidases of human blood, liver and kidney as well as their localization in the particular tissue are shown. Endopeptidases often exhibit

narrow cleavage specificity. However, modification in order to stabilise peptide or protein drugs towards endopeptidases is commonly more challenging than protecting N- or C-terminal sites towards endopeptidase cleavage.

## 2. Methods to evaluate parameters important for peptide/protein drug plasma half life time

### 2.1. *In vitro* test models

A common method to evaluate peptide or protein stability towards systemic metabolism is to incubate the drug at 37 °C and pH 7.4 in serum, plasma or diluted plasma (Fredholt et al., 2000). Samples can be withdrawn at pre-determined time points in order to gain a concentration-time profile. Although this method gives a good overview about the stability enhancement efficacy of modifications in comparison to the unmodified drug, it has to be considered that some proteolytic enzymes occur exclusively in liver or kidney. To verify the influence of these organs regarding enzymatic degradation, homogenates of liver or kidney can be used for enzymatic stability studies (Powell et al., 1992; Boulanger et al., 1992). However, therapeutic peptides and proteins – which are commonly hydrophilic molecules – will be digested to a much higher extent by such homogenates, containing large amounts of cytosolic enzymes, than can be expected under *in vivo* conditions.

Another approach which leads to more detailed results is the incubation of the drug in a medium containing one or more isolated enzymes. In Fig. 1 for example, the time dependent degradation caused by purified porcine kidney dipeptidyl peptidase IV (DP IV) of glucose-dependent

Table 4. Peptidases/proteases of human blood, liver and kidney acting as dipeptidase or endopeptidase

EC number	Specificity	Localization
2.3.2.2.	5-L-glutamyl-peptide + an amino acid = peptide + 5-L-glutamyl amino acid	Extracellular (blood, duodenum) (Shaw, 1983), membrane (pancreas) [Sugimoto et al. (Characterization of gamma-GTP in a human pancreatic cancer cell line)]
3.1.2.12	S-formylglutathione + H <sub>2</sub> O = glutathione + formate	Cytosol (liver) (Uotila et al., 1974)
3.4.13.3	hydrolysis of Xaa-/His dipeptides	Cytosol
3.4.13.9	hydrolysis of Xaa-/Pro dipeptides, also acts on aminoacyl-hydroxyproline analogs, no action on Pro-Pro	Extracellular, cytosol (JURKAT cell) (Chiravuri, 2000)
3.4.13.18	hydrolysis of dipeptides, preferentially hydrophobic dipeptides including prolyl amino acids	—
3.4.13.19	hydrolysis of dipeptides	Membrane (kidney) (Hooper et al., 1990)
3.4.13.20	preferential hydrolysis of the beta-Ala-/His dipeptide (carnosine), and also anserine, Xaa-/His dipeptides and other dipeptides including homocarnosine	—
3.4.19.9	hydrolysis of a gamma-glutamyl bond	Cytoplasm, lysosome, membrane (jejunum) (Gregory et al., 1987), soluble (intracellular, jejunum) (Reisenauer, 1977)
3.4.21.41	selective cleavage of Lys(or Arg)-/-Ile bond in complement subcomponent C1s to form the active form of C1s	—
3.4.21.42	cleavage of Arg-/Ala bond in complement component C4 to form C4a and C4b, and Lys(or Arg)-/Lys bond in complement component C2 to form C2a and C2b: the "classical" pathway C3 convertase	—
3.4.21.B1	endopeptidase activity. Cleaves C-terminal site of Lys and Arg	—
3.4.21.B7	endopeptidase activity. It triggers the activation of complement cascade by activating the C4 and C2 components. It activates the C4 component by cleaving the alpha-chain of C4	—
3.4.21.B13	endoprotease activity. Enzyme can degrade ica, ada, casein and globin	—
3.4.21.B39	proteolytic cleavage of polypeptides	—
3.4.22.16	hydrolysis of proteins, acting as an aminopeptidase as well as an endopeptidase	—
3.4.22.B13	the preferred cleavage sequence is LEHD-/-. Binding of caspase-9 to Apaf-1 leads to activation of the protease which then cleaves and activates caspase-3. Proteolytically cleaves poly(ADP-ribose) polymerase (PARP)	Cytosol (JURKAT cell) (Reisenauer, 1977)
3.4.22.B40	the preferred cleavage sequence is WEHD-/-. Efficient cleavage of p35 and pro-caspase-3	—
3.4.22.B41	the preferred cleavage sequence is WEHD-/-. Caspase-5 has protease activity on its own precursor and cleaves p35 and pro-caspase-3	—
3.4.23.45	broad endopeptidase specificity. Cleaves Glu-Val-Asn-Leu-Asp-Ala-Glu-Phe in the Swedish variant of Alzheimer's amyloid precursor protein	Membrane (Fluhrer et al., 2002)
3.4.24.11	preferential cleavage of polypeptides between hydrophobic residues, particularly with Phe or Tyr at P1'	Membrane (cerebrospinal fluid, plasma) (Spillantini et al., 1990)
3.4.24.18	hydrolysis preferentially on carboxyl side of hydrophobic residues	Membrane (Yamaguchi et al., 1994)
3.4.24.80	endopeptidase activity. Activates progelatinase A by cleavage of the propeptide at Asn37-/Leu. Other bonds hydrolysed include Gly35-/Ile in the propeptide of collagenase 3, and Asn341-/Phe, Asp441-/Leu and Gln354-/Thr in the aggrecan interglobular domain	Cytoplasm, membrane (liver) (Seiki, 2003)
3.4.24.81	endopeptidase of broad specificity	Membrane (kidney) (Anders et al., 2001)
3.4.24.86	narrow endopeptidase specificity. Cleaves Pro-Leu-Ala-Gln-Ala-Val-Arg-Ser-Ser in the membrane-bound, 26-kDa form of tumor necrosis factor $\alpha$ (TNF $\alpha$ ). Similarly cleaves other membrane-anchored, cell-surface proteins to "shed" the extracellular domains	Cytoplasm, membrane (kidney) (Schloendorff et al., 2000)
3.4.24.B9	proteolytic cleavage of proteins	Extracellular (liver) (Hotoda et al., 2002), membrane
3.4.24.B13	proteolytic cleavage of von Willebrand factor	Extracellular (plasma, serum) (Furlan et al., 1996)

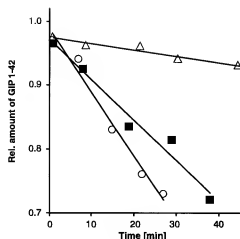


Fig. 1. Quantification of the DP IV-catalyzed GIP1-42 hydrolysis in the presence of specific DP IV-inhibitors using MALDI-TOF MS; ○ represents substrate turnover in the absence of inhibitor; ■ represents turnover in the presence of alanine-thiazolidide and △ represents turnover in the presence of isoleucine-thiazolidide; slightly modified from Pauly et al. (1996)

insulinotropic polypeptide (1-42) (GIP1-42) with and without inhibitors is shown (Pauly et al., 1996). Knowing the theoretical cleavage sites may allow a more specific

alteration of the drug, especially when it is degraded by endopeptidases.

Needless to say that only a small amount of isolated proteolytic enzymes is commercially available and the isolation of certain enzymes can be intricate. Therefore another approach is the utilization of specific enzyme inhibitors. A reasonable proceeding is to first identify the theoretical eligible peptidases and proteases and then to systematically add specific inhibitors to the plasma in order to see if a stabilisation of the drug can be achieved. Thereafter, the drug can be modified in a well-directed manner. Various inhibitors of human peptidases and proteases as well as the molecular mass of the proteolytic enzymes are shown in Tables 5-7.

Renal excretion of most peptides and proteins is determined by glomerular filtration and reabsorption in the proximal tubule. Physico-chemical properties of the compound as well as its plasma protein binding ability can be used to predict renal clearance. Of course these parameters are less predictable where active secretion or reabsorption and saturation kinetics are involved.

If peptides and proteins are degraded by proteolytic enzymes, it is generally important to identify the frag-

Table 5. Inhibitors of human aminopeptidases

EC number	Molecular mass [kDa]	Inhibitors
3.3.2.6	49 (Ohishi et al., 1987)	14,15-Leukotriene A <sub>4</sub> , HgCl <sub>2</sub> , Leukotriene A <sub>4</sub> , Leukotriene A <sub>4</sub> methyl ester, N-Ethylmaleimide, PCMB (Ohishi et al., 1987)
3.4.11.1	326 (Kohno et al., 1986)	1,10-Phenanthroline, Amastatin, Bestatin, EDTA, Iodoacetic acid, N-Ethylmaleimide, p-Chloromercuribenzoate (Kohno et al., 1986)
3.4.11.2	240 (Tokioka-Terao et al., 1984)	1,10-Phenanthroline (McClellan et al., 1980), 8-Hydroxyquinoline (McClellan et al., 1980), Bacitracin (Yamamoto et al., 1994; Langguth et al., 1994), Bestatin (Okagawa et al., 1994), EDTA (Yamamoto et al., 1994), Puromycin (Langguth et al., 1994)
3.4.11.3	340 (Lampelo et al., 1979)	1,10-Phenanthroline, Co <sup>2+</sup> , EDTA, EGTA, L-Methionine, Ni <sup>2+</sup> , Zn <sup>2+</sup> (Lampelo et al., 1979)
3.4.11.4	100 (Lees et al., 1990)	Cd <sup>2+</sup> , Cu <sup>2+</sup> , Hg <sup>2+</sup> , N-Ethylmaleimide, p-Hydroxymercuriphenyl sulfonate, Zn <sup>2+</sup> (Lees et al., 1990)
3.4.11.5	300 (Matsushima et al., 1991)	—
3.4.11.6	220 (Nagata et al., 1991)	Arphamenine A, Arphamenine B, Bestatin, Cd <sup>2+</sup> , Cu <sup>2+</sup> , Hg <sup>2+</sup> , p-Chloromercuribenzoate (Nagata et al., 1991)
3.4.11.7	190 (Nagatsu et al., 1970)	1,10-Phenanthroline, EDTA, Puromycin (Auricchio et al., 1978)
3.4.11.9	140 (Cottrell et al., 2000)	1,10-Phenanthroline, apstatin, Ca <sup>2+</sup> , Co <sup>2+</sup> , Cu <sup>2+</sup> , Dithiothreitol, EDTA, Glutathione, Mg <sup>2+</sup> , Ni <sup>2+</sup> , Zn <sup>2+</sup> (Cottrell et al., 2000)
3.4.11.14	223, 242	Benzylpenicillenic acid, Penicillin, Puromycin (Little et al., 1976)
3.4.14.1	210 (Mantle, 1991)	Leupeptin, NEM, p-Hydroxymercuriphenyl sulfonate (Mantle, 1991)
3.4.14.2	—	Bestatin, Diisopropyl fluorophosphate, phenylmethylsulfonyl fluoride, Tris (Sakai et al., 1987)
3.4.14.5	230-250 (Shibuya-Saruta et al., 1996)	Cd <sup>2+</sup> , Diprotin A, Hg <sup>2+</sup> , Leu, Lys, Met, PCMB, SrCl <sub>2</sub> , Zn <sup>2+</sup> (Shibuya-Saruta et al., 1996), Ala-thiazolidide, Ile-thiazolidide (Pauly et al., 1999, 1996), NVP DPP728 (Ahren et al., 2002), valine-pyrrolidide (Deacon et al., 1998)
3.4.19.3	22 (Mantle et al., 1991)	Amastatin, Chymostatin, Elastatin, Leupeptin (Mantle et al., 1991)
3.4.22.16	28 (Schwartz et al., 1980)	chymostatin B, Iodoacetamide, Leupeptin, Puromycin, Soybean trypsin inhibitor (Schwartz et al., 1980)
3.4.24.86	120 (Schloendorff et al., 2000)	1,10-Phenanthroline, BB 94, Endo-H, Hydroxamate, TACE-pro domain

Table 6. Inhibitors of human carboxypeptidases

EC number	Molecular mass [kDa]	Inhibitors
3.4.15.1	155 (Stewart et al., 1981)	Captopril, EDTA, snake venom peptide (Stewart et al., 1981)
3.4.16.2	115 (Ody et al., 1981)	Diisopropyl fluorophosphate, Pepstatin, phenylmethylsulfonyl fluoride (Ody et al., 1981)
3.4.17.2	32–33 (Marinkovic et al., 1977)	6-Amino-n-hexanoic acid, $\text{Co}^{2+}$ , EDTA, SDS, Urea
3.4.17.3	280 (Schweissfurth, 1984)	2,3-dimercaptopropan-1-ol, 2-Mercaptoethanol, 6-Aminohexanoic acid, $\text{Cd}^{2+}$ , $\text{CoCl}_2$ , EDTA, $\text{Hg}^{2+}$ , $\text{MnCl}_2$ , $\text{NiSO}_4$ , $\text{Zn}^{2+}$ (Schweissfurth, 1984)
3.4.17.20	435 (Wang et al., 1994)	1,10-Phenanthroline, 2-Guandinomethylmercaptosuccinic acid (Wang et al., 1994), 2-Mercaptoethanol, 2-mercaptomethyl-3-guainido-ethylbiopropionic acid, Dithiothreitol, EDTA, Epsilon-aminocaproic acid, guanidinomethylmercaptosuccinic acid, p-Chloromercuribenzoate, peptide inhibitor from Hirudo medicinalis, Folate carboxypeptidase inhibitor (Booma et al., 2001)
3.4.17.21	84 (Carter et al., 1996)	N-Acetyl-beta-L-Asp-L-Glu, Quisqualic acid (Carter et al., 1996),
3.4.18.1	–	CA-074, Chicken cystatin, cystatin C, GFG-semicarbazone, Stef A (Klemencic et al., 2000)

ments because they can exhibit pharmacological activity. It is for example well known that the terminal located helices of teriparatide are essential for bioactivity which is mediated by an activation of cAMP/protein kinase-A (PKA) as well as protein kinase-C (PKC). C-truncated derivatives such as PTH 1–31 are able to stimulate intracellular cAMP accumulation. However, it has been demonstrated that PTH 1–31 is less potent to increase serum calcium levels in mice in comparison to PTH 1–34 (Mohan et al., 2000). Fujimori et al. demonstrated that activation of cAMP/PKA system requires the N-terminal amino acids 1 and 2 whereas the phospholipase-C/PKC system is coupled to a longer domain of the hormone's N-terminus (Fujimori et al., 1992). Also Tsomaia et al. showed that the N-terminal residues (1–4) of the signalling domain plays a significant role in PTH action (Tsomaia et al., 2004). Furthermore it has been demonstrated, that the truncated fragment PTH 2–34 was only 67% as potent as PTH 1–34 and deletion of the first two amino acids at the N terminus abolished the hormone's ability to stimulate cAMP production in UMR-106-01 cells (Civitelli et al., 1994). Moreover, it was shown that also the PTH analogues 3–34, 7–34 and 13–34 did not stimulate cAMP production (Yu et al., 1997).

Fragments of enzymatic peptide/protein drug hydrolysis can be isolated by HPLC and identified by mass spectroscopy (Hernandez-Ledesma et al., 2005). Knowing the cleavage sites of a peptide/protein drug allows a well-directed modification leading to improved enzymatic stability. Also simple methods such as thin layer chromatography can be helpful, especially for the identification of single amino acids cleaved by amino- or carboxypeptidases (Werle et al., 2006).

## 2.2. *In vivo* test models

Results of *in vitro* studies lead to specific modification of the drug in order to enhance its enzymatic stability. The ultimate proof of prolonged plasma half life time however, has to be provided by *in vivo* studies. Above all, *in vivo* studies are necessary for systems which prolong plasma half life time only partly by improving enzymatic stability such as PEGylation or oligomerization. After injection, blood samples are withdrawn at pre-determined time points and the degradation process is stopped for example by adding inhibitors such as EDTA or trifluoroacetic acid to gain a concentration-time curve. In Fig. 2 the time dependent plasma concentration of intravenously administered IFN- $\alpha$ 2b (I) in comparison to a PEGylated derivative (II) is shown. Peptide drugs and proteins can usually be evaluated by HPLC, RIA or ELISA (Song et al., 2002; Ziegler et al., 1984; Kekow et al., 1985).

Beside direct detection of the compound itself it is sometimes possible to monitor the biological response caused by the drug such as a decrease in blood glucose after insulin administration (Krauland et al., 2004).

To predict renal clearance for humans, the use of inter-species allometric scaling approaches has been quite successful (Dedrick, 1973; Boxenbaum, 1982; Sawada et al., 1984). Nevertheless, the practical value of this approach is strongly limited due to the fact that it requires experimentation in four to five species (Lin, 1998). Another and more simple approach for predicting human renal clearance is to use the ratio of glomerular filtration rate (GFR) between rats and humans (Lin, 1995). Ratios of renal clearance for various drugs in rats and humans are roughly similar to the ratio of GFR between these two species.

Table 7. Inhibitors of human di- and endopeptidases

EC number	Molecular mass [kDa]	Inhibitors
2.3.2.2.	300 (Echeteu et al., 1982)	Glutathione (Miller et al., 1976), glycine (Wahlefeld et al., 1983), maleate (Miller, et al., 1976), $\text{NH}_4$ (Miller et al., 1976), urea (Ikeda et al., 1995)
3.1.2.12	52, 58 (Uotila et al., 1974)	Ascorbate, $\text{CaCl}_2$ , $\text{Co}^{2+}$ , $\text{CuSO}_4$ , Folate, Glutathione, $\text{HgCl}_2$ , Iodoacetate, p-Hydroxymercuribenzoate, $\text{Zn}^{2+}$ (Uotila et al., 1974)
3.4.13.3	160 (Lenney et al., 1982)	1,10-Phenanthroline, $\text{Co}^{3+}$ , Dithiothreitol, Homocarnosine (Lenney et al., 1982)
3.4.13.9	108, 185 (Ohhashi et al., 1990)	EDTA (Lenney et al., 1985)
3.4.13.18	63, 85 (Masuda et al., 1994)	Daurorubicin, Doxorubicin (Muszynska et al., 2001), p-Chloromercuribenzoate (Endo et al., 1989)
3.4.13.19	135, 200 (Sugiura et al., 1978)	$\text{Cd}^{2+}$ , $\text{Cu}^{2+}$ , EDTA, $\text{Mn}^{2+}$ , $\text{Ni}^{2+}$ , p-Chloromercuribenzoate, $\text{Pb}^{2+}$ , $\text{Zn}^{2+}$ , 1,10-Phenanthroline, $\text{Co}^{3+}$ , Cysteine, EDTA, N-Bromosuccinimide (Sugiura et al., 1978)
3.4.13.20	160 (Lenney et al., 1982)	—
3.4.19.9	110 (Lavoie et al., 1975)	Gamma-Diglutamate, p-Aminobenzoyleglutamate, Pterine, pteroyldiglutamate, $\text{Zn}^{2+}$ (Wang et al., 1986)
3.4.21.41	17 (Sim et al., 1977)	4-Nitrophenyl-4-guanidinobenzoate, C1-bar-inhibitor, Diisopropyl fluorophosphate, Leupeptin, NaCl (Sim, 1981)
3.4.21.42	113 (Sumi et al., 1974)	3,4-Dichloroisocoumarin, 4-chloro-3-(3-isothiuroidopropoxy)isocoumarin, 4-chloro-3-ethoxy-7-guanidinisocoumarin, 4-chloro-7-guanidino-3-(2-phenylethoxy)isocoumarin, 4-chloro-7-guanidino-3-methoxyisocoumarin, 7-amino-4-chloro-3-(3-isothiuroidopropoxy)isocoumarin (Kam et al., 1992)
3.4.21.B1	70 (Hunfeld et al., 1999)	alpha1-proteinase, alpha2-antiplasmin, Aprotinin, C1-esterase inhibitor, $\text{Co}^{2+}$ , $\text{Cu}^{2+}$ (Hunfeld et al., 1999)
3.4.21.B7	85 (Wong et al., 1999)	alpha-2-Macroglobulin, C1-inhibitor, PefablocSC (Wong et al., 1999)
3.4.21.B13	40 (Yousef et al., 2003)	—
3.4.22.16	28 (Schwartz et al., 1980)	Alpha1-antitrypsin, alpha2-Macroglobulin (Yousef et al., 2003)
3.4.22.B13	—	chymostatin B, Iodoacetamide, Leupeptin, Puromycin, Soybean trypsin inhibitor (Schwartz et al., 1980)
3.4.22.B40	—	acetyl-AEVD-CHO, acetyl-DEVD-CHO, acetyl-IETD-CHO, acetyl-WEHD-CHO, acetyl-YVAD-CHO, benzoyloxycarbonyl-VAD-fluoromethylketone, cowpox serpin CrmA (Garcia-Calvo et al., 1998)
3.4.22.B41	—	acetyl-AEVD-aldehyde, acetyl-DEVD-aldehyde, acetyl-IETD-aldehyde, acetyl-WEHD-aldehyde, acetyl-YVAD-aldehyde, benzoyloxycarbonyl-VAD-fluoromethylketone (Garcia-Calvo et al., 1998)
3.4.23.45	62, 65 (Fluhrer et al., 2002)	acetyl-AEVD-aldehyde, acetyl-DEVD-aldehyde, acetyl-IETD-aldehyde, acetyl-WEHD-aldehyde, acetyl-YVAD-aldehyde, benzoyloxycarbonyl-VAD-fluoromethylketone, cowpox serpin CrmA (Garcia-Calvo et al., 1998)
3.4.24.11	—	$\text{Cu}^{2+}$ , $\text{Zn}^{2+}$ (Kim et al., 2002)
3.4.24.18	200 (Sterchi et al., 1988)	Leu5-enkephalin, Met5-enkephalin, Phosphoramidon, Thiorphan, thiorphan- $\text{NH}_2$ (Spillanti et al., 1990)
3.4.24.80	—	1,10-Phenanthroline, $\text{Ca}^{2+}$ , Captopril, DTT, EDTA, $\text{Zn}^{2+}$ (Sterchi et al., 1988)
3.4.24.81	68 (Colciaghi et al., 2002)	Marimastat, TIMP-2, TIMP-4 (Toth et al., 2002)
3.4.24.86	120 (Schloendorff et al., 2000)	BB3103, o-Phenanthroline, TAPI (Vincent et al., 2001)
3.4.24.89	—	1,10-Phenanthroline, BB 94, EndoH, Hydroxamate, TACE-pro domain
3.4.24.B13	300 (Furlan et al., 1996)	Aprotinin, Benzamidine, Hydroxamates, o-Phenanthroline, phosphoramidon, TIMP-1, TIMP-3 (Amour et al., 2002)
		Citrate, EDTA, EGTA, N-Ethylmaleimide, Z-Phe-Phe- $\text{CHN}_2$ (Furlan et al., 1996)

Therefore, knowledge of renal clearance in rats allows the approximate estimation of human renal clearance using GFR ratios.

### 3. Strategies to improve peptide/protein drug plasma half life time

Although several strategies to improve peptide/protein drug plasma half life are already established, drug mod-

ifications shall be based on an exact knowledge of the enzymatic susceptibility of the particular drug.

It was for example demonstrated, that dermorphin analogues with additional D-amino acid substitutions were cleaved more rapidly than the parent peptides. This may be due to remote secondary structural features which may be important for differential enzyme susceptibility (Darlak et al., 1988). In addition, studies of Rafferty et al. demonstrated that D-amino acid-substituted ana-

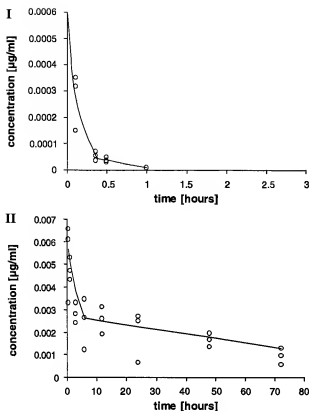


Fig. 2. IFN- $\alpha$ 2b time course following a single 125 µg/kg intravenous bolus dose in male Sprague-Dawley rats. The symbols (open circles) represent the observed concentration data (three points per sampling time) from each treatment group (i.e., graph I for the unconjugated IFN; graph II for the PEG<sub>240K</sub>-IFN- $\alpha$ 2b). The continued lines represent the predicted values according to the best fitted-curve using compartment modelling; slightly modified from Ramon et al. (2005)

logues of growth hormone-releasing factor 1–29-amide did not exhibit significant different plasma half life times after intravenous injection in rats in comparison to the unmodified compound (Rafferty et al., 1988). These two examples emphasize the importance of well directed drug modification.

### 3.1. Modification of N- and C-terminus

As shown in Tables 1–3, several proteolytic enzymes occurring in plasma, liver and kidney which affect therapeutic peptides and proteins are exopeptidases. Therefore, a modification of either or both of the peptide/protein drug termini can in many cases significantly increase enzymatic stability. However, modifications always can lead to a loss of drug activity. One common way of terminal modification is N-acetylation and C-amidation. Brinckerhoff et al. for example significantly pro-

longed plasma stability of the immunogenic peptide MART-I<sub>27–35</sub> by C-terminal amidation and/or N-terminal acetylation (Brinckerhoff et al., 1999). Also N-pyroglytamylation led to an improved enzymatic stability of glucagon-like-peptide-1<sub>7–36</sub> (Green et al., 2004).

Various fatty acids of chain lengths ranging from 4 to 18 were conjugated to RC-160, a somatostatin analogue with anti-proliferative activity. The novel compounds exhibited greater resistance towards trypsin and serum degradation in comparison to unmodified RC-160 (Dasgupta et al., 2002).

Another approach is the specific covalent attachment of PEG to either or both termini of a peptide or a protein drug. The N-terminal modification of glucose-dependent insulinotropic polypeptide (GIP1–30) with 40 kDa PEG abrogated functional activity, whereas C-terminal PEGylation of GIP1–30 maintained full agonism at the GIP receptor and conferred a high level of dipeptidyl peptidase IV (DP IV) resistance. Moreover, the dual modification of N-terminal palmitoyl and C-terminal PEGylation resulted in a full agonist of comparable potency to native GIP that was stable to DP IV cleavage (Salhanick et al., 2005). Also Irwin et al. developed palmitate-derivitized analogues of N-terminal pyroglutamyl GIP which were completely resistant to DP IV degradation (Irwin et al., 2005).

In general, also a head-to-tail cyclization of peptides and proteins by the formation of an amide bond between C- and N-terminus in order to prevent exopeptidase caused degradation is possible. Of course, an alteration of the shape may lead to a loss in activity. Marastoni et al. prepared linear and head to tail cyclic hexapeptide analogues of peptide T. All compounds showed significant bioactivity and the cyclic peptides also proved to be highly resistant to degradation by plasma and brain enzymes (Marastoni et al., 1994).

### 3.2. Replacement of labile amino acids

A replacement of amino acids which are known to be susceptible for enzymatic cleavage is another strategy to delay degradation and therefore to improve plasma half life time. The substitution of L-amino acids with D-amino acids at both termini led to a stabilisation of several peptides (Powell et al., 1993). Various luteinizing hormone releasing hormone (LHRH) analogues which are substituted in positions 6, 10 or both and which furthermore are much more active and possess prolonged activity in comparison to LHRH are on the market including [D-Trp<sup>6</sup>]LHRH (triptorelin), [D-Leu<sup>6</sup>, Pro<sup>9</sup>-NHEt]LHRH (leuprolide), [D-Ser(But)<sup>6</sup>, Pro<sup>9</sup>-NHEt]LHRH (buserelin),

[D-Ser(But)<sup>6</sup>, Aza-Gly<sup>10</sup>]LHRH (goserelin) and [D-Nal(2<sup>6</sup>)<sup>10</sup>]LHRH (nafarelin) (Holland et al., 1996).

Cetorelix, a decapeptide, has a highly modified LHRH sequence, comprising 10 amino acids, five out of which are in a non-natural D-configuration. It is an antagonist of the luteinizing hormone releasing hormone (LHRH) and is highly resistant to degrading enzymes, e.g. chymotrypsin, pronase and nargase, for up to 50 h at 37 °C (Reissmann et al., 1994) which is in sharp contrast to several LHRH agonists which face almost complete degradation within few hours. The proteolytic stability of Cetorelix is underlined in comparison with a diastereomeric analogue comprising L-configured citrulline in position 6 instead of D-citrulline as in Cetorelix. This analogue is highly sensitive to degradation (Pinski et al., 1995).

Also analogues of glucagon-like peptide 1 (GLP-1), which were N-terminally substituted with threonine, glycine, serine or alpha-aminoisobutyric acid were more resistant to dipeptidyl peptidase IV than the unmodified compound (Deacon et al., 1998). By substituting the theoretical chymotrypsin cleavage site of a cystine-knot microprotein, stabilisation towards this peptidase was achieved (Werle et al., 2006). Marx et al. expressed, purified and characterised two chimeras of activated thrombin-activable fibrinolysis inhibitor (TAFIa), in which the non conserved residues were replaced by residues of pancreatic carboxypeptidase B. TAFIa is a labile carboxypeptidase B which is inactivated by conformational instability and proteolysis, whereas pancreatic carboxypeptidase B is a stable protease. One of the mutants displayed a markedly prolonged half life time (Marx et al., 2004). Also the GLP-1 analog [Ser]GLP-1 (7–36) amide, in which the second N-terminal amino acid alanine was replaced by serine was not significantly degraded by human and rat plasma in comparison to unmodified GLP-1 (Ritzel et al., 1998).

Strausberg et al. improved activity and stability of subtilisin by sequentially randomizing 12 amino acid positions in calcium-free subtilisin. The optimal amino acid for each randomized site was chosen based on stability and catalytic properties and became the parent clone for the next round of mutagenesis. Taken together, the 12 selected mutations increased subtilisin half-life at elevated temperature 15,000-fold (Strausberg et al., 2005).

### 3.3. Cyclization

Cyclization of a peptide or protein is a method to decrease proteolytic degradation and to prolong half life time. Growth regulating factor (GRF) and analogues were incu-

bated in porcine plasma at 37 °C. GRF(1–29)-NH<sub>2</sub> displayed a half life time of only 13 minutes. Substitution of Gly15 by Ala15 only slightly prolonged plasma half life time (17 min), whereas side-chain to side-chain cyclization between Asp8 and Lys12 amino acid residues significantly improved the stability of GRF in plasma with 1/2 greater than 2 h. In addition, cyclization between Lys21 and Asp25 also improved GRF stability in plasma. Enzymatic stability and half life time were even more improved by substitution of D-Ala2 for Ala2 in the cyclic analogue (Su et al., 1991). Osapay et al. synthesised a series of cyclic somatostatin analogues containing a lanthionine bridge. The enzymatic stability of lanthionine-somatostatin and sandostatin was studied in rat brain homogenates. Although both compounds exhibited high enzymatic stability, the cyclic lanthionine-somatostatin had a 2.4-fold prolonged half life time in comparison to sandostatin (Osapay et al., 1997). Also a cyclic disulfide bonded analogue of indolicin displayed greatly increased protease stability and the half life time in the presence of trypsin was increased 4.5-fold from 4 to 18 minutes (Rozek et al., 2003). Beside of cyclization in the molecule also a head to tail cyclization as mentioned in Section 3.1 can improve enzymatic stability.

### 3.4. Enzyme inhibition

An interesting approach for prolonging half life time of peptides and proteins might be the co-administration of specific enzyme inhibitors. It already has been demonstrated *in vitro* and *in vivo* that co-administration of enzyme inhibitors to oral dosage forms increases oral bioavailability (Fujii et al., 1985; Langguth et al., 1994; Morishita et al., 1992; Yamamoto et al., 1994). Recently, Pauly et al. (1990) showed the effectiveness of Ile-thiazolidide, a specific dipeptidyl dipeptidase IV inhibitor to increase circulating half life time of GLP-17–36. HPLC analysis of plasma following *in vivo* administration of 125I-labeled peptides showed that inhibition of DP IV by about 70% prevented the degradation of 90.0% of injected 125I-GLP-17–36 within 5 min, whereas only 13.4% remained unhydrolyzed in rats not treated with the DP IV-inhibitor after only 2 min (Pauly et al., 1999). Also the co-administration of the inhibitors NVP DDP728 and valine-pyrrolidide resulted in prolonged plasma half life time of the intact peptide (Ahren et al., 2002; Deacon et al., 1998). Wiedeman and Trevillyan summarized recent advances in the design of potent and selective small molecule inhibitors of DP IV and the potential challenges to the development of DP IV inhibitors for the

treatment of impaired glucose tolerance and type-2 diabetes (Wiedeman et al., 2003).

### 3.5. Increasing molecular mass: PEGylation and oligomerization

As a general rule, substances with a molecular mass below 5 kDa which are not bound to plasma proteins are completely excreted via the renal route, whereas molecules with a molecular mass over 50 kDa cannot or only in very small amounts be found in the glomerular ultrafiltrate. Accordingly, a main reason for short peptide and protein half life time beside enzymatic degradation is their fast renal excretion. Therefore, half life time can be prolonged by increasing drug size. Furthermore, a synergistic effect may be given by additional enzyme inhibition. Beside chemical modification of N- and C-termini which is usually an effective way to inhibit exopeptidases and replacement of labile amino acids, PEGylation offers the possibility to specifically protect endangered termini and furthermore increases molecular mass. Moreover, it is believed that PEGylation within the drug molecule leads to improved enzymatic stability mediated by a steric hindrance of proteolytic enzymes. Examples, where improved stability towards proteolytic digestion after PEGylation of the native protein was achieved are tumor necrosis factor, epidermal growth factor and interferon- $\alpha$ -2b (INF- $\alpha$ -2b) (Li et al., 2002; Lee et al., 2003; Ramon et al., 2005). The stability of INF- $\alpha$ -2b towards trypsin caused degradation was strongly improved by the conjugation of PEG<sub>2,40 K</sub> to the native protein (Ramon et al., 2005). Furthermore, it has already been demonstrated that the effect of protecting PEGylated proteins from proteolysis is especially strong when high-molecular-weight, branched PEGs are used (Monfardini et al., 1995).

Poly(ethyleneglycol) (PEG) exhibits several properties that are of relevance for pharmaceutical applications: high water solubility, high mobility in solution, lack of toxicity and immunogenicity and ready clearance from the body (Delgado et al., 1992; Harris et al., 1997). Interestingly, many of these properties are transferred to PEG-protein or PEG-peptide conjugates. The extent of these features are dependent on the molecular weight of the attached PEG. As demonstrated for example by He et al., only minor changes in immunogenicity of trichosanthin after modification with PEG<sub>5k</sub> was observed, whereas modification with PEG<sub>20k</sub> led to significantly reduced immunogenicity (He et al., 1999). Up to now, there are lots of data about the chemistry of PEGylation published (Kozłowski et al.,

2001). Also a multitude of scientific articles have already been published where the effectiveness of PEG to improve half life time was clearly demonstrated (Sun et al., 2003). Lee et al. for example showed that site specific mono-PEGylation of GLP-1 led to a 16-fold increase in plasma half life time in rats (Lee et al., 2005). Moreover, some PEGylated proteins for human use are already on the market including PEGylated adenosine deaminase and asparaginase as well as  $\alpha$ -Interferon. PEG-Intron, a PEGylated  $\alpha$ -interferon marketed by Schering-Plough and approved by the FDA in 2001 for the treatment of hepatitis C, has an elimination half life time of 50 hours in comparison to 5 hours of the native  $\alpha$ -interferon. Pegasys, a PEGylated  $\alpha$ -interferon developed by Roche even exhibits an elimination half life time of 77 hours. Furthermore it has been shown recently by Ramon et al. that a PEG<sub>2,40 K</sub> conjugate of INF- $\alpha$ -2b exhibited a 330-fold prolonged plasma half life time in rats compared to the native protein (Fig. 2) (Ramon et al., 2005).

Polymers of N-acetylneuraminic acid (polysialic acids) are naturally occurring, biodegradable, highly hydrophilic compounds which have no known receptors in the human body. After intravenous injection, polysialic acids exhibit long half-lives in the blood circulation and can therefore be used as carriers of short-lived drugs and small peptides. Furthermore, polysialic acids can be used in order to increase the circulatory half-life of proteins and thus serve as an alternative to the nonbiodegradable monomethoxypoly(ethylene glycol) (Gregoriadis et al., 2000). Sialylation has been shown to effectively improve enzymatic stability of proteins as well as plasma half life time. Sialylated catalase for example was shown to be much more stable in the presence of specific endoproteases compared to the native enzyme (Fernandes et al., 1996). *In vivo* studies with polysialylated asparaginase in mice also revealed that beside of improved plasma stability also the half life time could be increased. Such an increase was greatest for the construct with the highest polysialylation (Fernandes et al., 1997).

PEGylation and sialylation prolong half life time by a combination of two mechanisms – improvement of enzymatic stability and decrease of renal excretion by increasing molecular mass – whereas oligomerization leads to prolonged half life time in first instance by increasing molecular mass. It was demonstrated for example, that a dimeric human erythropoietin, which was synthesized by chemical crosslinking of the monomeric form exhibited an increased plasma half life time in rabbits of more than 24 h compared to 4 h of the monomeric form. This effect is believed to be due to a decrease in glomerular filtration.

Furthermore, the dimer exhibited a more than 26-fold higher activity *in vivo* (Sytkowski et al., 1998).

### 3.6. Sustained delivery systems

Prolonged plasma half life time can also be achieved without chemical modification of the drug by the utilization of sustained delivery systems. Liposomes, for example, are widely used as drug carriers. As demonstrated by Kim et al., half life time of streptokinase incorporated in liposomes increased 16.3- and 6.1-fold, respectively in comparison to those of streptokinase alone after femoral administration in rats (Kim et al., 1998). Also intraperitoneal administered liposomes containing insulin exhibited a prolonged plasma half life time of 4–5 hours in contrast to free insulin solution in diabetic rats (Khakha et al., 2000). In a pharmacokinetic *in vivo* study, after subcutaneous injections in rats, insulin like growth factor-1 (IGF-I) levels were sustained for 5–7 days with a multivesicular liposome drug delivery system, whereas IGF-I in the free form was cleared in one day (Katre et al., 1998).

Sustained delivery systems based on the biodegradable polymers poly(lactic acid) (PLA) and poly(lactic/glycolic acid) (PLGA) have also been demonstrated to be effective in several *in vivo* studies. Heya et al. demonstrated the potential of PLGA microspheres as a sustained delivery system for thyrotropin releasing hormone (TRH) (Heya et al., 1994) and Okada et al. developed and evaluated a PLGA microsphere sustained delivery system for leuprolerin (Okada, 1997; Okada et al., 1994). In addition, long-acting delivery systems for triptorelin and other LHRH agonists in microcapsules of poly(DL-lactide-co-glycolide) (PLG) or different polymers designed to release a controlled dose of the peptide over a 30-day period were developed (Parmar et al., 1985; Sharifi et al., 1990).

Another approach to achieve sustained delivery of peptide and protein drugs is the utilization of emulsions. A water/oil emulsion containing the hydrophilic markers aprotinin as well as perthechnate displayed enhanced *in vivo* retention (Bjerregaard et al., 2001).

Also cyclodextrins and derivatives are known for several years to provide a sustained release of peptide drugs. Uekama et al. for example demonstrated a significantly retarded release of buserelin *in vitro* in presence of heptakis (2,6-di-O-ethyl)-beta-cyclodextrin (DE-β-CyD) as well as an effective continuous plasma level of buserelin *in vivo* after single subcutaneous injection of a suspension containing a buserelin-DE-β-CyD complex. Figure 3 shows the plasma concentrations of buserelin in rats following

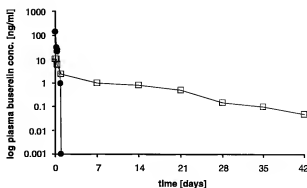


Fig. 3. Plasma levels of buserelin following the subcutaneous administration of the oily suspension containing buserelin acetate or its DE-β-CyD complex (equivalent to 1 mg/kg as buserelin acetate) to rats. ○: Buserelin acetate; ●: DE-β-CyD complex; each point represents the mean  $\pm$  s.e. of 5 rats; modified from Uekama et al. (1989)

the subcutaneous administration of the oily suspension (Uekama et al., 1989).

## 4. Conclusion

To design long-acting analogues of peptide and protein drugs as well as delivery systems, it is of great importance to know the 'enemies strength'. Taking the different strategies to prolong half-life time discussed within this review into consideration, drug modifications should be based on an exact knowledge of the influence of proteolytic enzymes encountered with systemic circulation as well as the renal clearance of the drug. Within this review, an overview of most important proteolytic enzymes of human blood, liver and kidney as well as their cleavage specificity and inhibitors is provided in order to predict theoretical cleavage of peptide and protein drugs during systemic circulation. Furthermore, methods and strategies discussed within this review should allow well directed peptide/protein drug modification to prolong plasma half life time.

## References

- Adam A, Cugno M, Molinaro G, Perez M, Lepage Y, Agostoni A (2002) Aminopeptidase P in individuals with a history of angio-oedema on ACE inhibitors. *Lancet* 359: 2088–2089
- Ahren B, Simonsson E, Larsson H, Landin-Olsson M, Torgeirsson H, Jansson PA, Sandqvist M, Bavenholm P, Elendic S, Eriksson JW, Dickinson S, Holmes D (2002) Inhibition of dipeptidyl peptidase IV improves metabolic control over a 4-week study period in type 2 diabetes. *Diabetes Care* 25: 869–875
- Amour A, Knight CG, English WR, Webster A, Slocombe PM, Knauper V, Docherty AJ, Becherer JD, Blobel CP, Murphy G (2002) The enzymatic activity of ADAM8 and ADAM9 is not regulated by TIMPs. *FEBS Lett* 524: 154–158

- Anders A, Gilbert S, Garten W, Postina R, Fahrenholz F (2001) Regulation of the alpha-secretase ADAM10 by its prodomain and proprotein convertases. *FASEB J* 15: 1837–1839
- Auricchio S, Greco L, de Vizia B, Buonocore V (1978) Dipeptidylaminopeptidase and carboxypeptidase activities of the brush border of rabbit small intestine. *Gastroenterology* 75: 1073–1079
- Bjerregaard S, Pedersen H, Vedstedsen H, Vermehren C, Soderberg I, Frokjaer S (2001) Parenteral water/oil emulsions containing hydrophilic compounds with enhanced *in vivo* retention: formulation, rheological characterisation and study of *in vivo* fate using whole body gamma-scintigraphy. *Int J Pharmacol* 215: 13–27
- Boulanger L, Roughly P, Gaudreau P (1992) Cathecolin rat growth hormone-releasing factor (1–29) amide in rat serum and liver. *Peptides* 13: 681–689
- Bouma BN, Marx PF, Mosnier LO, Meijers JCTR (2001) Thrombin-activatable fibrinolysis inhibitor (TAFI, plasma procarboxypeptidase B, procarboxypeptidase R, procarboxypeptidase U). *Thromb Res* 101: 329–354
- Boxenbaum H (1982) Interspecies scaling, allometry, physiological time, and the ground plan of pharmacokinetics. *J Pharmacokin Biopharm* 10: 201–227
- Brinkerhoff LH, Kalashnikov V, Thompson LW, Yarnschikov GV, Pierce RA, Galavotti HS, Engelhardt VH, Stangluf CLJ (1999) Terminal modifications inhibit proteolytic degradation of an immunogenic MART-1(27–35) peptide: implications for peptide vaccines. *Int J Cancer* 83: 326–334
- Carter RE, Feldman AR, Coyle JT (1996) Prostate-specific membrane antigen is a hydrolase with substrate and pharmacologic characteristics of a neutrophilicase. *Proc Natl Acad Sci USA* 93: 749–753
- Chaturvedi PR, Decker CJ, Odehns A (2001) Prediction of pharmacokinetic properties using experimental approaches during early drug discovery. *Curr Opin Chem Biol* 5: 452–463
- Chiravuri M, Aggaraberes F, Mathieu SL, Lee H, Huber BT (2000) Vesicular localization and characterization of a novel post-proline-cleaving aminodipeptidase, quiescent cell proline dipeptidase. *J Immunol* 165: 5695–5702
- Cigic B, Pain RH (1999) Competitive inhibition of cathepsin C by guanidinium ions and reexamination of substrate inhibition. *Biochem Biophys Res Commun* 258: 6–10
- Civitelli R, Bacskai BJ, Mahaut-Smith MP, Adams SR, Avioli LV, Tsien RY (1994) Single-cell analysis of cyclic AMP response to parathyroid hormone in osteoblastic cells. *J Bone Miner Res* 9: 1407–1417
- Colciaghi F, Borroni B, Pastorino L, Marcello E, Zimmermann M, Cattanei F, Padovani A, Di Luca M (2002) [alpha]-Secretase ADAM10 as well as [alpha]APPs is reduced in platelets and CSF of Alzheimer disease patients. *Mol Med* 8: 67–74
- Cottrell GS, Hooper NM, Turner AJ (2000) Cloning, expression, and characterization of human cytosolic aminodipeptidase P: a single manganese(II)-dependent enzyme. *Biochemistry* 39: 15121–15128
- Darlak K, Benovic DE, Spatola AF, Gronow Z (1988) Dermorphin analogs: resistance to *in vitro* enzymatic degradation is not always increased by additional D-amino acid substitutions. *Biochem Biophys Res Commun* 156: 125–130
- Dasgupta P, Singh A, Mukherjee R (2002) N-terminal acylation of somatostatin analog with long chain fatty acids enhances its stability and anti-proliferative activity in human breast adenocarcinoma cells. *Biol Pharm Bull* 25: 29–36
- Deacon CF, Hughes TE, Holst JJ (1998) Dipeptidyl peptidase IV inhibition potentiates the insulinotropic effect of glucagon-like peptide 1 in the anesthetized pig. *Diabetes* 47: 764–769
- Deacon CF, Knudsen LB, Madsen K, Wiberg FC, Jacobsen O, Holst JJ (1998) Dipeptidyl peptidase IV resistant analogues of glucagon-like peptide-1 which have extended metabolic stability and improved biological activity. *Diabetologia* 41: 271–278
- Dedrick RL (1973) Animal scale-up. *J Pharmacokin Biopharm* 1: 435–461
- Delgado C, Francis GE, Fisher D (1992) The uses and properties of PEG-linked proteins. *Crit Rev Ther Drug Carrier Syst* 9: 249–304
- Echeteu ZO, Moss DW (1982) Multiple forms of human gamma-glutamyltransferase: preparation and characterization of different molecular weight fractions. *Enzyme* 27: 1–8
- Endo F, Tanoue A, Nakai H, Hata A, Indo Y, Titani K, Matsuda I (1989) Primary structure and gene localization of human prolidase. *J Biol Chem* 264: 4476–4481
- Fernandes AI, Gregoriadis G (1996) Synthesis, characterization and properties of sialylated catalase. *Biochim Biophys Acta* 1293: 90–96
- Fernandes AI, Gregoriadis G (1997) Polysialylated asparaginase: preparation, activity and pharmacokinetics. *Biochim Biophys Acta* 1341: 26–34
- Fluhner R, Capell A, Westmeyer G, Willem M, Hartung B, Condron MM, Teplow DB, Haass C, Walter J (2002) A non-amyloidogenic function of BACE-2 in the secretory pathway. *J Neurochem* 81: 1011–1020
- Fredholt K, Adrian C, Just L, Høj Larsen D, Weng S, Moss B, Juel PG (2000) Chemical and enzymatic stability as well as transport properties of a Leu-enkephalin analogue and ester prodrugs thereof. *J Control Rel* 63: 261–273
- Fuji S, Yokohama T, Ikegaya K, Salo F, Yakoo N (1985) Promoting effect of the new chymotrypsin inhibitor FK-448 on the intestinal absorption of insulin in rats and dogs. *J Pharm Pharmacol* 37: 545–549
- Fujimori A, Cheng SL, Avioli LV, Civitelli R (1992) Structure-function relationship of parathyroid hormone: activation of phospholipase-C, protein kinase-A and -C in osteosarcoma cells. *Endocrinology* 130: 29–36
- Furlan M, Robles R, Lamie B (1996) Partial purification and characterization of a protease from human plasma cleaving von Willebrand factor to fragments produced by *in vivo* proteolysis. *Blood* 87: 4223–4234
- Garcia-Calvo M, Peterson EP, Leiting B, Ruel R, Nicholson DW, Thornberry NA (1998) Inhibition of human caspases by peptide-based and macromolecular inhibitors. *J Biol Chem* 273: 32608–32613
- Green BD, Mooney MH, Gault VA, Irwin N, Bailey CJ, Harriott PBG, O'Harte FP, Platt PR (2004) N-terminal His(7)-modification of glucagon-like peptide-1(7–36) amide generates dipeptidyl peptidase IV-stable analogues with potent antihyperglycaemic activity. *J Endocrinol* 180: 379–388
- Gregorakis AK, Holmes EH, Murphy GP (1998) Prostate-specific membrane antigen: current and future utility. *Semin Urol Oncol* 16: 2–12
- Gregoriadis G, Fernandes A, Mital M, McCormack B (2000) Polysialic acids: potential in improving the stability and pharmacokinetics of proteins and other therapeutics. *Cell Mol Life Sci* 57: 1964–1969
- Gregory JF, Ink SL, Cerda JJ (1987) *Comp Biochem Physiol B Comp Biochem* 88: 1135–1141
- Harris AG (1994) Somatostatin and somatostatin analogues: pharmacokinetics and pharmacodynamic effects. *Gut* 35: 1–4
- Harris JM, Zalipsky S (eds) (1997) Poly(ethylene glycol): chemistry and biological applications. 1997. ACS Books, Washington, DC
- He XH, Shaw PC, Tam SC (1999) Reducing the immunogenicity and improving the *in vivo* activity of trichostatin by site-directed pegylation. *Life Sci* 65: 355–368
- Hernandez-Leckesma B, Davalos A, Bartolome B, Amigo L (2005) Preparation of antioxidant enzymatic hydrolysates from alpha-lactalbumin and beta-lactoglobulin. Identification of active peptides by HPLC-MS/MS. *J Agric Food Chem* 53: 588–593
- Heya T, Mikura Y, Nagai A, Miura Y, Futo T, Tomida Y, Shimizu H, Toguchi H (1994) Controlled release of thyrotropin releasing hormone from microspheres: evaluation of release profiles and pharmacokinetics after subcutaneous administration. *J Pharm Sci* 83: 798–801
- Holland JF, Bast RC, Morton DL (1996) Cancer medicine. Section XVII. Principles of endocrine therapy 1067

- Hooper NM, Keen JN, Turner AJ (1990) Characterization of the glycosyl-phosphatidylinositol-anchored human renal dipeptidase reveals that it is more extensively glycosylated than the pig enzyme. *Biochem J* 265: 429-433
- Hotoda N, Koike H, Sasagawa N, Ishiura S (2002) A secreted form of human ADAM9 has an alpha-secretase activity for APP. *Biochem Biophys Res Commun* 293: 800-805
- Hunfeldt A, Etscheid M, Konig H, Seitz R, Dodi J (1999) Detection of a novel plasma serine protease during purification of vitamin K-dependent coagulation factors. *FEBS Lett* 456: 290-294
- Ikeeda Y, Fujii J, Taniguchi N, Meister A (1995) Expression of an active glycosylated human gamma-glutamyl transpeptidase mutant that lacks a membrane anchor domain. *Proc Natl Acad Sci USA* 92: 126-130
- Irwin N, Green BD, Gault VA, Greer B, Harriott P, Bailey CJ, Flatt PR, O'Harte PP (2005) Degradation, insulin secretion, and antihyperglycemic actions of two palmitate-derived N-terminal pyroglutamate analogues of glucose-dependent insulinotropic polypeptide. *J Med Chem* 48: 1244-1250
- Karn CM, Oglesby TJ, Pangburn MK, Volanakis JE, Powers JC (1992) Substituted isocoumarins as inhibitors of complement serine proteases. *J Immunol* 149: 163-168
- Katre NV, Asherman J, Schaefer H, Hora M (1998) Multivesicular liposome (DepoFoam) technology for the sustained delivery of insulin-like growth factor-I (IGF-I). *J Pharm Sci* 87: 1341-1346
- Kekow J, Ullrichs K, Muller-Ruchholtz W, Gross WL (1988) Measurement of rat insulin. Enzyme-linked immunosorbent assay with increased sensitivity, high accuracy, and greater practicability than established radioimmunoassay. *Diabetes* 37: 321-326
- Khakasa G, D'Souza R, Lewis SNU (2000) Pharmacokinetic study of niosome encapsulated insulin. *Int J Exp Biol* 38: 901-905
- Kim IS, Choi HG, Choi HS, Kim BK, Kim CK (1998) Prolonged systemic delivery of streptokinase using liposome. *Arch Pharm Res* 21: 248-252
- Kim Y-T, Downs D, Wu S, Dashti A, Pan Y, Zhai P, Wang X, Zhang XC, Lin X (2002) Enzymic properties of recombinant BACE2. *Eur J Biochem* 269: 5668-5677
- Klemencic I, Carmona AK, Cezari MH, Juliano MA, Juliano L, Guncar G, Turk D, Krizaj I, Turk V, Turk B (2000) Biochemical characterization of human cathepsin X revealed that the enzyme is an exopeptidase, acting as carboxymonopeptidase or carboxyoligopeptidase. *Eur J Biochem* 267: 5404-5412
- Kohn H, Kanda S, Kanno T (1986) Immunoaffinity purification and characterization of leucine aminopeptidase from human liver. *J Biol Chem* 261: 10744-10748
- Kozlowski A, Harris JM (2001) Improvements in protein PEGylation: pegylated interferons for treatment of hepatitis C. *J Control Rel* 72: 217-224
- Krauland AH, Guggi D, Bernkop-Schnitz A (2004) Oral insulin delivery: the potential of thiolated chitosan-insulin tablets on non-diabetic rats. *J Contr Release* 95: 547-555
- Lampelo S, Vanha-Perttula T (1979) Fractionation and characterization of cystine aminopeptidase (oxycotinase) and arylamidase of the human placenta. *J Reprod Fertil* 56: 285-296
- Langguth P, Bohner V, Biber J, Merkle HP (1994) Metabolism and transport of the pentapeptide metkephamid by brush-border membrane vesicles of rat intestine. *J Pharm Pharmacol* 46: 34-40
- Langguth P, Merkle HP, Amidon G (1994) Oral absorption of peptides: the effect of absorption site and enzyme inhibition on the systemic availability of metkephamid. *Pharm Res* 11: 528-535
- Lavoie A, Tripp E, Hoffbrand AV (1975) Sephadex-gel filtration and heat stability of human jejunal and serum prolylpyroglutamate hydrolase (folate conjugase). Evidence for two different forms. *Biochem Med* 13: 1-6
- Lee H, Jang IH, Ryu SH, Park TG (2003) N-terminal site-specific mono-PEGylation of epidermal growth factor. *Pharm Res* 20: 818-825
- Lee SH, Lee S, Youn YS, Na DH, Chae SY, Byun Y, Lee KC (2005) Synthesis, characterization, and pharmacokinetic studies of PEGylated glucagon-like peptide-1. *Bioconjug Chem* 16: 377-382
- Lees T, Lauffart B, McDermott J, Gibson A, Mantle D (1990) Purification and characterization of tripeptidyl-aminopeptidase from human cerebral cortex. *Biochem Soc Trans* 18: 667
- Lenney JF, George RP, Weiss AM, Kucera CM, Chan PWH, Rinzler GS (1982) Human serum carnosinase: characterization, distinction from cellular carnosinase, and activation by cadmium. *Clin Chim Acta* 123: 221-231
- Lenney JF, Peppers SC, Kucera-Orallo CM, George RP (1985) Characterization of human tissue carnosinase. *Biochem J* 228: 653-660
- Li W, Wang Y, Zhu X, Li M, Su Z (2002) Preparation and characterization of PEGylated adducts of recombinant human tumor necrosis factor- $\alpha$  from *Escherichia coli*. *J Biotechnol* 92: 251-258
- Lin JH (1995) Species similarities and differences in pharmacokinetics. *Drug Metab Dispos* 23: 1008-1021
- Lin JH (1998) Applications and limitations of interspecies scaling and *in vitro* extrapolation in pharmacokinetics. *Drug Metab Dispos* 26: 1202-1212
- Little GH, Starnes WL, Behal FJ (1976) Human liver aminopeptidase. *Methods Enzymol* 45: 495-503
- Mantle D (1991) Characterization of dipeptidyl and tripeptidyl aminopeptidases in human kidney soluble fraction. *Clin Chim Acta* 196: 135-142
- Mantle D, Lauffart B, Gibson A (1991) Purification and characterization of leucyl aminopeptidase and pyroglutamyl aminopeptidase from human skeletal muscle. *Clin Chim Acta* 197: 35-46
- Marastoni M, Salvadori S, Scaranari V, Spisani S, Reali E, Trianello S, Tomatis A (1994) Synthesis and activity of new linear and cyclic peptide T derivatives. *Arzneimittelforschung* 44: 1073-1076
- Marinkovic DV, Marinkovic JN, Erdős EG, Robinson CJG (1977) Purification of carboxypeptidase B from human pancreas. *Biochem J* 163: 253-260
- Marx PF, Havik SR, Marquart JA, Bouma BN, Meijers JC (2004) Generation and characterization of a highly stable form of activated thrombin-activable fibrinolysis inhibitor. *J Biol Chem* 279: 6620-6628
- Masuda S, Watanabe H, Morioka M, Fujita Y, Ageta T, Kodama H (1994) Characteristics of partially purified prolidase and prolidase from the human prostate. *Acta Med Okayama* 48: 173-179
- Matsumoto H, Rogi T, Yamashiro K, Kodama S, Tsuruoka N, Hattori A, Takio K, Mizutani S, Tsujimoto M (2000) Characterization of a recombinant soluble form of human placental leucine aminopeptidase/oxycotinase expressed in Chinese hamster ovary cells. *Eur J Biochem* 267: 46-52
- Matsushima M, Takahashi T, Ichinose M, Miki K, Kurokawa K, Takahashi K (1991) Prolyl aminopeptidases from pig intestinal mucosa and human liver: Purification, characterization and possible identity with leucyl aminopeptidase. *Biomed Res* 23: 323-333
- McClellan JB, Garner CW (1980) Purification and properties of human intestinal alanine aminopeptidase. *Biochim Biophys Acta* 613: 160-167
- Menz GL, McCall MN, Kuchel PW (1989) Characterization of leukocyte enzymes involved in the release of amino acids in incubated blood cell lysates. *J Biol Chem* 264: 2108-2117
- Miller SP, Awasthi YC, Srivastava SK (1976) Studies of human kidney gamma-glutamyl transpeptidase. Purification and structural, kinetic and immunological properties. *J Biol Chem* 251: 2271-2278
- Mohan S, Kutilek S, Zhang C, Shen HG, Kodama Y, Srivastava AK, Wergedal JE, Beamer WG, Baylink DJ (2000) Comparison of bone formation responses to parathyroid hormone (1-34), (1-31), and (2-34) in mice. *Bone* 27: 471-478
- Monfardini C, Schiavon O, Caliceti P, Murguio M, Harris JM, Veronese FM (1995) A branched monomethoxypoly(ethylene glycol) for protein modifica. *Bioconjug Chem* 6: 62-69

- Morishita I, Morishita M, Takayama K, Machida Y, Nagai T (1992) Hypoglycemic effect of novel oral microspheres of insulin with protease inhibitor in normal and diabetic rats. *Int J Pharmacol* 78: 9–16
- Muszynska A, Wolczynski S, Palka J (2001) The mechanism for anthracycline-induced inhibition of collagen biosynthesis. *Eur J Pharmacol* 411: 17–25
- Nagata Y, Mizutani S, Nomura S, Kurauchi O, Kasugai M, Tomoda Y (1991) Purification and properties of human placental aminopeptidase B. *Enzyme* 45: 165–173
- Nagatsu I, Nagatsu T, Yamamoto T, Glenner GG, Mehl JW (1970) Purification of aminopeptidase A in human serum and degradation of angiotensin II by the purified enzyme. *Biochim Biophys Acta* 258: 255–270
- Obach RS, Baxter JG, Liston TE, Silber BM, Jones BC, MacIntyre F, Rance DJ, Wastall P (1997) The prediction of human pharmacokinetic parameters from preclinical and *in vitro* metabolism data. *J Pharmacol Exp Ther* 283: 46–58
- Ody A, Erdős EG (1981) Human polycarboxypeptidase. *Methods Enzymol* 80: 460–466
- Oefner CD, D'Arcy A, Mac Sweeney A, Pierau S, Gardiner R, Dale GE (2003) High-resolution structure of human apo dipeptidyl peptidase IV/CD26 and its complex with 1-[(2-[(5-iodopyridin-2-yl)amino]ethyl)amino]-acetyl]-2-cyano-(S)-pyrrolidine. *Acta Crystallogr Sect D* 59: 1206–1212
- Ohhashi T, Ono T, Arata J, Sugahara K, Kodama H (1990) Characterization of prolidase I and II from erythrocytes of a control, a patient with prolidase deficiency and her mother. *Clin Chim Acta* 187: 1–9
- Ohishi N, Izumi T, Minami M, Kitamura S, Seyama Y, Ohkawa S, Terao S, Yotsumoto H, Takaku F, Shimizu TJ (1987) *J Biol Chem* 262: 10200–10205
- Okada H (1997) One- and three-month release injectable microspheres of the LH-RH superagonist leuprolerin acetate. *Adv Drug Deliv Rev* 28: 43–70
- Okada H, Doken Y, Ogawa Y, Toguchi H (1994) Preparation of three-month depot injectable microspheres of leuprolerin acetate using biodegradable polymers. *Pharm Res* 11: 1143–1147
- Okagawa T, Fujita T, Murakami M, Yamamoto A, Shimura T, Tabata S, Kondo S, Muranishi S (1994) Susceptibility of ebratide to proteolysis in rat intestinal fluid and homogenates and its protection by various protease inhibitors. *Life Sci* 55: 677–683
- Osapay G, Prokai L, Kim HS, Medzhiradzky KF, Coy DH, Liapakis G, Reisine T, Melacini G, Zhu Q, Wang SH, Mattern RH, Goodman M (1997) Lanthionine-somatostatin analogs: synthesis, characterization, biological activity, and enzymatic stability studies. *J Med Chem* 40: 2241–2251
- Parmar H, Phillips RH, Lightman SL, Edwards L, Allen L, Schally AV (1985) Randomised controlled study of orchidectomy vs long-acting D-Trp-6-LHRH microcapsules in advanced prostatic carcinoma. *Lancet* 2: 1201–1205
- Pauly RP, Demuth HU, Rosche F, Schmidt J, White HA, Lynn F, McIntosh CH, Pederson RA (1999) Improved glucose tolerance in rats treated with the dipeptidyl peptidase IV (CD26) inhibitor lile-thiazolidine. *Metabolism* 48: 385–389
- Pauly RP, Rosche F, Wermann M, McIntosh CH, Pederson RA, Demuth HU (1996) Investigation of glucose-dependent insulinotropic polypeptide-(1–42) and glucagon-like peptide-1-(7–36) degradation *in vitro* by dipeptidyl peptidase IV using matrix-assisted laser desorption/ionization-time of flight mass spectrometry. A novel kinetic approach. *J Biol Chem* 271: 23222–23229
- Pelkonen O, Turpeinen M, Uusitalo J, Rautio A, Raunio H (2005) Prediction of drug metabolism and interactions on the basis of *in vitro* investigations. *Basic Clin Pharmacol Toxicol* 96: 167–175
- Pinski J, Schally AV, Yano T, Groot K, Skalošević G, Serfozo P, Reissmann T, Bernd M, Deger W, Kutscher B (1995) Evaluation of the *in vitro* and *in vivo* activity of the L-, D-, and D-Cit6 forms of the LH-RH antagonist Cetrorelix (SB-75). *Int J Pept Protein Res* 45: 410–417
- Powell MF, Grey H, Gaeta F, Sette A, Colon S (1992) Peptide stability in drug development: a comparison of peptide reactivity in different biological media. *J Pharm Sci* 81: 731–735
- Powell MF, Stewart T, Otvos LJ, Urge L, Gaeta FC, Sette A, Arrhenius T, Thomson D, Soda K, Colon SM (1993) Peptide stability in drug development. II. Effect of single amino acid substitution and glycosylation on peptide reactivity in human serum. *Pharm Res* 10: 1268–1273
- Rafferty B, Coy DH, Poole S (1988) Pharmacokinetic evaluation of superactive analogues of growth hormone-releasing factor (1–29)-amide. *Peptides* 9: 207–209
- Ramon J, Saez V, Baez R, Aldana R, Hardy E (2005) PEGylated interferon- $\alpha$ 2b: a branched 40 kDa polyethylene glycol derivative. *Pharm Res* 22: 1375–1387
- Reddy P, Slack JL, Davis R, Cerretti DP, Kozlosky CJ, Blanton RA, Shows D, Peschon JJ, Black RA (2000) Functional analysis of the domain structure of tumor necrosis factor-alpha converting enzyme. *J Biol Chem* 275: 14608–14614
- Reisner AM (1977) Folate conjugates: two separate activities in human jejunum. *Science* 198: 196–197
- Reissmann T, Engel J, Kutscher B (1994) The LHRH antagonist cetrorelix. *Drugs Future* 19: 228–237
- Ritzel U, Leonhardt U, Otteben M, Ruhmann A, Eckart K, Spiess J, Ramadori G (1998) A synthetic glucagon-like peptide-1 analog with improved plasma stability. *J Endocrinol* 159: 93–102
- Rozek A, Powers JP, Friedrich CL, Hancock RE (2003) Structure-based design of an indolipenic peptide analogue with increased protease stability. *Biochemistry* 42: 14130–14138
- Sakai T, Kojima K (1987) Rapid chromatographic purification of dipeptidyl-aminopeptidase II from human kidney. *J Chromatogr* 416: 131–137
- Salhanick AL, Clairmont KB, Buckholz TM, Pellegrino CM, Ha S, Lumb KJ (2005) Contribution of site-specific PEGylation to the dipeptidyl peptidase IV stability of glucose-dependent insulinotropic polypeptide. *Bioorg Med Chem Lett* 15: 4114–4117
- Samuelsson B, Funk CD (1989) Enzymes involved in the biosynthesis of leukotriene B<sub>4</sub>. *J Biol Chem* 264: 19469–19472
- Sawada Y, Hanano M, Sugiyama Y, Iga T (1984) Prediction of the disposition of beta-lactam antibiotics in humans from pharmacokinetic parameters in animals. *J Pharmacokin Pharmacodyn* 12: 241–261
- Schloendorff J, Becherer JD, Blobel CP (2000) Intracellular maturation and localization of the tumor necrosis factor alpha convertase (TACE). *Biochem J* 347: 131–138
- Schwartz WN, Barrett AJ (1980) Human cathepsin H. *Biochem J* 191: 487–497
- Schweissfurth H (1984) Carboxypeptidase N. *Dtsch Med Wochenschr* 109: 254–258
- Seiki M (2003) Membrane-type 1 matrix metalloproteinase: a key enzyme for tumor invasion. *Cancer Lett* 194: 1–11
- Shariat-Madar Z, Mahdi F, Schmaier AH (2004) Recombinant prolysearboxypeptidase activates plasma prekallikrein. *Blood* 15: 4554–4561
- Sharif R, Soloway M (1990) Clinical study of leuprolide depot formulation in the treatment of advanced prostate cancer. The Leuprolide Study Group. *J Urol* 143: 68–71
- Shaw LM (1983) Methods of enzymatic analyses, 3rd ed. Weinheim, pp 349–352
- Shibuya-Saruta H, Kasahara Y, Hashimoto YJCLA (1996) Human serum dipeptidyl peptidase IV (DPP-IV) and its unique properties. *J Clin Lab Anal* 10: 435–440
- Sim RB (1981) The human complement system serine proteases C1bar and C1sbar and their proenzymes. *Methods Enzymol* 80: 26–42
- Sim RB, Porter RR, Reid KBM, Gighi I (1977) The structure and enzymic activities of the C1r and C1s components of C1, the first component of human serum complement. *Biochem J* 163: 219–227
- Song KH, An HM, Kim HJ, Ahn SH, Chung SJ, Shim CK (2002) Simple liquid chromatography-electrospray ionization mass spectrometry

- method for the routine determination of salmon calcitonin in serum. *J Chromatogr B Anal Technol Biomed Sci* 775: 247–255
- Spillatini MG, Sicuteri F, Salmon S, Malfroy B (1990) Characterization of endopeptidase 3.4.24.11 (enkephalinase) activity in human plasma and cerebrospinal fluid. *Biochem Pharmacol* 39: 1353–1356
- Sterchi EE, Green JR, Lentze MJ (1981) The distribution of four peptide hydrolases along the small intestine of the adult human. *Biochem Soc Trans* 9: 130–131
- Sterchi EE, Naim HY, Lentze MJ, Hauri HP, Fransen JAM (1988) N-Benzoyl-L-tyrosyl-p-aminobenzoic acid hydrolase: a metalloendopeptidase of the human intestinal microvillus membrane which degrades biologically active peptides. *Arch Biochem Biophys* 265: 105–118
- Stewart TA, Wear JA, Erdős EG (1981) Human peptidyl dipeptidase (converting enzyme, kininase II). *Methods Enzymol* 80: 450–460
- Stoeckel-Maschek A, Mrestani-Klaus C, Stiebitz B, Demuth HU, Neubert K (2000) Thioxo amino acid pyrrolidines and thiazolidines: new inhibitors of proline specific peptidases. *Biochim Biophys Acta* 1479: 15–31
- Strausberg SL, Ruan B, Fisher KE, Alexander PA, Bryan PN (2005) Directed coevolution of stability and catalytic activity in calcium-free subtilisin. *Biochemistry* 44: 3272–3279
- Su CM, Jensen LR, Heimer EP, Felix AM, Pan YC, Mowles TF (1991) In vitro stability of growth hormone releasing factor (GRF) analogs in porcine plasma. *Horm Metab Res* 23: 15–21
- Sugimoto M, Yamaguchi N, Keliichi K (Characterization of gamma-GTP in a human pancreatic cancer cell line) 1984. *Gastroenterol Jpn* 19: 227–231
- Sugiura M, Ito Y, Hirano K, Sawaki S (1978) Purification and properties of human kidney dipeptidases. *Biochim Biophys Acta* 522: 541–550
- Sumi H, Muramatsu MA (1974) Purification and partial characterization of human C1-esterase. *Agric Biol Chem* 38: 605–611
- Sun X, Yang Z, Li S, Tan Y, Zhang N, Wang X, Yagi S, Yoshioka T, Takimoto A, Mitsushima K, Suganaka A, Frenkel EP, Hoffman RM (2003) In vivo efficacy of recombinant methionine is enhanced by the combination of polyethylene glycol conjugation and pyridoxal 5'-phosphate supplementation. *Cancer Res* 63: 8377–8383
- Sytковский AJ, Lunn ED, Davis KL, Feldman L, Sienkman S (1998) Human erythropoietin dimers with markedly enhanced in vivo activity. *Proc Natl Acad Sci USA* 95: 1184–1188
- Takada Y, Hiwada K, Kokubu T (1981) Isolation and characterization of angiotensin converting enzyme from human kidney. *J Biochem* 90: 1309–1319
- Tokioka-Terao M, Hiwada K, Kokubu T (1984) Purification and characterization of aminopeptidase N from human plasma. *Enzyme* 32: 65–75
- Toth M, Hernandez-Barrantes S, Osenkowski P, Bernardo MM, Gervasi DC, Shimura Y, Meroueh O, Kotra LP, Galvez BG, Arroyo AG, Mobashery S, Fridman R (2002) Complex pattern of membrane type 1 matrix metalloproteinase shedding. Regulation by autocatalytic cells surface inactivation of active enzyme. *J Biol Chem* 277: 26340–26350
- Tsomaia N, Pellegrini M, Hyde K, Gardella TJ, Mierke DF (2004) Toward parathyroid hormone minimization: conformational studies of cyclic PTH(1–14) analogues. *Biochemistry* 43: 690–699
- Uekama K, Arima H, Irie T, Matsubara K, Koniki T (1989) Sustained release of buserelin acetate, a luteinizing hormone-releasing hormone agonist, from an injectable oily preparation utilizing ethylated beta-cyclodextrin. *J Pharm Pharmacol* 41: 874–876
- Uotila L, Koivusalo M (1974) Purification and properties of S-formylglutathione hydrolase from human liver. *J Biol Chem* 249: 7664–7672
- Vincent B, Paiet E, Saftig P, Probert Y, Hartmann D, De Strooper B, Grassi J, Lopez-Perez E, Checler F (2001) The disintegrins ADAM10 and TACE contribute to the constitutive and phorbol ester-regulated normal cleavage of the cellular prion protein. *J Biol Chem* 276: 37743–37746
- Wahlefeld AW, Bergmeyer HU (1983) gamma-Glutamyltransferase. (gamma-Glutamyl)-peptide:amino acid gamma-glutamyltransferase, EC 2.3.2.2. 2. Routine method. *Methods Enzym Anal* 3rd edn., pp 352–356
- Wang TTY, Chandler CJ, Halsted CH (1986) Intracellular pteroylpolyl-glutamate hydrolase from human jejunal mucosa. Isolation and characterization. *J Biol Chem* 261: 13551–13555
- Wang W, Hendricks DF, Scharpe SS (1994) Carboxypeptidase U, a plasma carboxypeptidase with high affinity for plasminogen. *J Biol Chem* 269: 15937–15944
- Werle M, Samhaber A, Bernkop-Schnürch A (2006) Degradation of teriparatide by gastro-intestinal proteolytic enzymes. *J Drug Target* 14: (in press)
- Werle M, Schnitz T, Huang H, Wentzel A, Kolmar H, Bernkop-Schnürch A (2005) The potential of cysteine-knot microproteins as novel pharmacophoric scaffolds in oral peptide drug delivery. *J Drug Target* 14: (in press)
- Wiedeman PE, Trevillian JM (2003) Dipeptidyl peptidase IV inhibitors for the treatment of impaired glucose tolerance and type 2 diabetes. *Curr Opin Investig Drugs* 4: 412–420
- Wong NKH, Kojima M, Dobo J, Ambrus G, Sim RB (1999) Activities of the MBL-associated serine proteases (MASPs) and their regulation by natural inhibitors. *Mol Immunol* 36: 853–861
- Yamaguchi T, Fukase M, Sugimoto T, Kido H, Chihara K (1994) Purification of meprin from human kidney and its role in parathyroid hormone degradation. *Biol Chem Hoppe-Seyler* 375: 821–824
- Yamamoto A, Taniguchi T, Rikyun K, Tsuji T, Fujita T, Murakami M, Muranishi S (1994) Effects of various protease inhibitors on the intestinal absorption and degradation of insulin in rats. *Pharm Res* 11: 1496–1500
- Yousef GM, Kapadia C, Polymeris ME, Borgono C, Hutchinson S, Wasney GA, Soosapillai A, Diamandis EP (2003) The human kallikrein protein 5 (hK5) is enzymatically active, glycosylated and forms complexes with two protease inhibitors in ovarian cancer fluids. *Biochim Biophys Acta* 1628: 88–96
- Yu XP, Chandrasekhar S (1997) Parathyroid hormone (PTH 1–34) regulation of rat osteocalcin gene transcription. *Endocrinology* 138: 3085–3092
- Ziegler R, Raus F (1984) Variations of plasma calcitonin levels measured by radioimmunoassay systems for human calcitonin. *Biomed Pharmacother* 38: 245–251

**Authors' address:** Dr. Andreas Bernkop-Schnürch, Department of Pharmaceutical Technology, Institute of Pharmacy, Leopold-Franzens University Innsbruck, Innrain 52, Josef Möller Haus, 6020 Innsbruck, Austria,  
Fax: +43-512-507-2933, E-mail: andreas.bernkop@uibk.ac.at